

TECHNISCHE UNIVERSITÄT MÜNCHEN
Lehrstuhl für Bodenkunde

Soils of a semiarid shortgrass steppe in Inner Mongolia:
Organic matter composition and distribution as affected by sheep grazing

Markus Steffens

Vollständiger Abdruck der von der Fakultät Wissenschaftszentrum Weihenstephan für Ernährung, Landnutzung und Umwelt der Technischen Universität München zur Erlangung des akademischen Grades eines

Doktors der Naturwissenschaften

genehmigten Dissertation.

Vorsitzender: Univ.-Prof. Dr. K.-J. Hülsbergen

Prüfer der Dissertation: 1. Univ.- Prof. Dr. I. Kögel-Knabner
2. Univ.- Prof. Dr. J. Schnyder
3. Univ.- Prof. Dr. H.-G. Frede
(Justus-Liebig-Universität Giessen)
schriftliche Beurteilung

Die Dissertation wurde am 12.02.2009 bei der Technischen Universität München eingereicht und durch die Fakultät Wissenschaftszentrum Weihenstephan für Ernährung, Landnutzung und Umwelt am 29.04.2009 angenommen.



Summary

The semiarid grasslands of northern China are used for at least two thousand years by nomads and their herds as extensive pastures. They are part of the Eurasian steppe, the largest continuous terrestrial biome in the world. Stocking rates reached a maximum during the last 20 years as a consequence of political decisions in the 1980s. Intensive land use and especially heavy continued grazing resulted in degradation of steppe vegetation associated with changes in the amount and the composition of soil organic matter (SOM). The concurrent degradation of soil structure and destruction of aggregation led to enhanced soil erosion and the formation of dust storms. Nowadays, the most apparent consequences of this overgrazing are wide-spread desertification and a high abundance of severe supra-regional dust storms, impairing not only the local population but also the densely populated coastal regions. Grazed steppe ecosystems are discussed as one of the big global carbon sinks that may have the potential to sequester large amounts of atmospheric CO₂ and mitigate the effects of global change if grazing is abandoned or management improved.

The Sino-German interdisciplinary research group MAGIM was set up to investigate the effects of grazing on semiarid steppe ecosystems and to evaluate the benefits and potentials of grazing management and grazing cessation to mitigate the detrimental effects. This work focussed on changes in the amount, composition and turnover of soil organic matter (SOM) due to continued heavy grazing and grazing cessation and the concurrent degradation of soil structure and aggregation. The central aims were to 1.) investigate the effects of continued heavy grazing and possible benefits of grazing cessation on bulk topsoil parameters using statistical tools; 2.) analyse the impacts of heavy grazing, reduced grazing and time since grazing cessation on the spatial distribution of bulk topsoil parameters and topsoil-vegetation-interactions with univariate and multivariate geostatistical tools; 3.) study the effects of higher OM inputs due to grazing cessation on the amount, composition and turnover of functional SOM fractions and their contribution to aggregate stability in topsoils; and 4.) quantitatively and qualitatively characterise grazing-sensitive SOM fractions in complete soil profiles and reveal the contribution of subsoils to the carbon sequestration and stabilisation potential of steppe soils.

The study area was located approximately 450 km north of Beijing in the autonomous region of Inner Mongolia in northern China. Soils in the study area were characterised as Calcic Chernozems with a sandy texture derived from aeolian deposits above acid volcanic rocks. Climate was classified as middle latitude dry and cold steppe climate with mean annual temperature and precipitation of 0.4 °C and 350 mm. The typical vegetation in this region is dominated by the bunch grasses *Leymus chinensis* and *Stipa grandis*. Herds consisted of 90-70% sheep and 10-30% goats. Five sites with different grazing intensities were selected (ungrazed since 1979 = Ug79, ungrazed since 1999 = Ug99, winter grazing = Wg, continuously grazed = Cg, heavily grazed = Hg). For the statistical and the geostatistical approach topsoils (0-4 cm) of two differently sized regular, orthogonal grids (small grids with 100 sampling points: 15 m spacing, 5 m nested sampling; large grids with 125 sampling points: 50 m spacing, 10 m nested sampling) were sampled. Differently sized grids allowed the exploration of scale effects. Each sample was analysed for bulk density, organic carbon (OC), total N and total S concentration, $\delta^{13}\text{C}$, pH, Ah horizon thickness, vegetation cover and aboveground biomass. The dataset was analysed using general statistics, multivariate explorative statistics, variograms and cross variograms. In each of the five plots representative soil pits were sampled to analyse effects of grazing and grazing cessation on the amount, composition and turnover of SOM in detail. A combined aggregate size, density and particle size fractionation procedure was applied in three horizons of each pit to separate functional SOM fractions and pools. Additionally aggregate stability measurements were done on topsoils.

Statistical analyses showed that bulk density increased significantly with increasing grazing intensity. OC, total N and total S concentrations decreased significantly with increasing grazing intensity. No effect on the pH or C/N ratio was detected. Significant differences in C/S and N/S ratios between differently grazed plots were found. These differences pointed towards a relative accumulation of sulphur in grazed compared to ungrazed areas following an increased organic matter decline or lower inputs of diluting litter. Elemental stocks of the upper 4 cm were calculated for OC, total N and total S using the measured bulk densities. The data revealed significantly lower amounts for all three elements on the heavily grazed site, but no significant differences for the other areas. In addition, elemental stocks were

calculated using an equivalent mass instead of bulk density to take into account changes in bulk density following grazing. This revealed a highly significant decrease for OC, total N and total S with increasing grazing intensity. OC, total N and total S concentrations respond similarly to different grazing intensities, showing highly significant positive correlations. OC concentrations and bulk densities were significantly negatively correlated. Effects of grazing cessation were only found in the long-term, while no ameliorating effects of reduced or excluded grazing could be detected five years after grazing cessation. After 25 years of exclusion, significantly different values were found for all parameters. The statistical approach showed that physical and chemical parameters of steppe topsoils deteriorated significantly following heavy grazing, remained stable if grazing was reduced or excluded for five years and recovered significantly after 25 years of grazing exclusion.

Geostatistical analyses showed that the spatial distribution in small grids changed with grazing intensity. Generally, heterogeneity of topsoil properties increased with decreasing grazing intensity from a homogeneous to a patchy distribution. This is attributed to vegetation recovery/succession and deposition of windblown material in ungrazed areas. Ug99 showed different spatial dependencies than continuously and heavily grazed, but has not yet reached the high variability of Ug79. Large grid sampling did not detect small-scale variability or grazing impacts, but showed spatial dependencies that were attributed to topography or soil erosion/deposition. Low OC concentration and low Ah thickness were associated with hilltop and shoulder positions, resulting in lower OC stocks at these topographic units. The geostatistical approach showed that recovering vegetation and higher deposition of windblown material around recovering plants are crucial processes that initiate the recovery of grazing-degraded areas.

Physical fractionation of topsoils (0-10 cm) showed that greater inputs of organic matter led to larger amounts of OC in coarse aggregate size classes (ASC) and especially in particulate organic matter fractions (POM). No grazing-induced changes of SOM quantity were found in fine ASC and particle size fractions. SOM quality (solid state ^{13}C NMR spectroscopy, neutral sugar analysis) was comparable between different grazing intensities, but ungrazed plots had slightly more decomposed SOM across all fractions. Ug79 showed generally greater radiocarbon concentrations compared with Cg. Aggregate stability, analysed as resistance to

sonication, was greater in Ug79 compared with Cg. Larger litter inputs in grazing enclosures increased POM quantity, led to faster SOM turnover and resulted in the formation and stabilisation of coarse aggregates. Organo-mineral associations turned over faster as indicated by increased radiocarbon concentrations, but the OC content of this pool did not change. The physical fractionation of topsoils showed that additional litter inputs due to grazing cessation were sequestered in the intermediate POM pool and the long-term pool of organo-mineral associations appears to be close to saturation. Aggregate stability and formation in topsoils was increased after grazing cessation.

Higher inputs of organic matter led to higher amounts of OC in coarse ASC and especially in POM fractions across all depth. These processes started in the topsoil and took more than 5 years to reach deeper soil horizons (>10 cm). After 25 years of grazing cessation, subsoils showed clearly higher POM amounts. No grazing-induced changes of SOM quantity were found in fine ASC and particle size fractions. Current carbon loading of fine particle size fractions was similar between differently grazed plots and decreased with depth, pointing towards free sequestration capacities. Despite these free capacities, no increase in current carbon loading after 25 years of grazing exclusion could be detected. It is supposed that either the particle size fractions are already saturated and empirical estimations overestimate sequestration potentials or that the climatic conditions delay the decomposition and incorporation of OM in particle size fractions. POM quality was analysed using solid-state ^{13}C NMR spectroscopy and was comparable between different grazing intensities. POM is decomposed hierarchically from coarse to fine particles in all soil depths and grazing cessation has not affected the OM decomposition processes. The surplus of OM due to grazing cessation was predominately sequestered in readily decomposable POM fractions across all horizons and the long-term stabilisation of OM in these steppe soils is questioned.

Overall, this study statistically substantiates the long process of recovery of physical and chemical soil parameters after grazing cessation. The recovery of degraded areas after grazing cessation starts with the recovery of vegetation. Larger increased litter inputs and larger accumulation of wind-blown materials around individual recovered plants act as nucleus of recovery (islands of fertility). Recovery of topsoils was detectable after 25 years of grazing cessation, but spatial distribution

of vegetation showed first evidence of recovery already after 5 years. In ungrazed topsoils the increased litter inputs were predominately stored in the readily decomposable POM fractions. Abundance and stability of coarse and medium aggregates were increased in ungrazed topsoils as consequence of higher POM amounts. Particle size fractions in topsoils did not change quantitatively after grazing cessation pointing towards saturation of their carbon sequestration potential. Despite saturation higher radiocarbon concentrations of particle size fractions in ungrazed plots show that the generally as stabile assumed pool of organo-mineral associations is taking part in the carbon cycling. Deeper soil horizons received higher OM inputs after 25 years of grazing cessation. But these inputs were also stored in the readily decomposable POM fraction and are therefore not stabilised in the long-term. Finally, grazing reduction and especially grazing cessation can help mitigating the detrimental effects of heavy grazing on semiarid steppe soils when management is controlled for periods longer than 25 years. But if grazed steppe soils can become a carbon sink in the long-term when grazing management is improved or completely stopped has to be questioned.

Zusammenfassung

Die im Norden Chinas gelegenen semiariden Grasländer werden seit mindestens 2000 Jahren von Nomaden als extensives Weideland für vornehmlich Schaf- und Ziegenherden genutzt. Sie sind Teil der eurasischen Steppe, des größten, zusammenhängenden, terrestrischen Ökosystems der Erde und bedecken einen großen Teil der Volksrepublik China (ca. 40% der Staatsfläche). Infolge politischer Entscheidungen stieg die Beweidungsintensität in diesen Regionen seit den 1950er kontinuierlich an und erreichte ein Maximum in den 1990er, das jedoch bis heute andauert. Intensive Landnutzung und insbesondere starke, kontinuierliche Beweidung führten zu einer Degradation der Vegetation mit Auswirkungen auf die Menge und Zusammensetzung der organischen Bodensubstanz (OBS). Damit einher ging eine Verschlechterung der Bodenstruktur sowie eine Zerstörung von Bodenaggregaten und führte zur vermehrten Bodenerosion und zu einem gehäuften Auftreten von Staubstürmen. Die offensichtlichsten Folgen der starken Beweidung sieht man heute in der Desertifikation weiter Landstriche sowie dem häufigen Auftreten von großräumigen Staubstürmen, die nicht nur die lokale Bevölkerung und Landwirtschaft, sondern auch die dicht bevölkerten Küstenregionen beeinträchtigen. Darüber hinaus werden beweidete Grasländer im Allgemeinen und die eurasische Steppe im Speziellen als eine der großen Kohlenstoffsinken betrachtet, die große Mengen an atmosphärischem Kohlendioxid speichern und somit den globalen Klimawandel abmildern könnten, wenn die Nutzung beendet oder zumindest verbessert werden würde.

Im Rahmen der chinesisch-deutschen, interdisziplinären Forschergruppe MAGIM sollten die Auswirkungen einer hohen Beweidungsintensität auf das semiaride Steppen-Ökosystem untersucht und die Folgen und Möglichkeiten der Regeneration durch Beweidungsmanagement und Beendigung der Beweidung betrachtet werden. Die vorliegende Arbeit befasste sich insbesondere mit den Effekten von kontinuierlich starker Beweidung und einem Beweidungstopp auf die Gehalte, chemische Zusammensetzung und Umsatzraten der OBS sowie deren Einfluss auf Bodenstruktur und Aggregation. Die Arbeitsschwerpunkte waren 1.) die statistisch abgesicherte Betrachtung der Effekte kontinuierlich starker Beweidung und eines Beweidungstopps auf bodenphysikalische und –chemische Kenngrößen der oberflächennahen Gesamtböden, 2.) die Analyse der räumlichen Struktur von

Vegetations- und oberflächennahen Gesamtbodeneigenschaften sowie deren Interaktion und Änderung unter starker Beweidung und nach einem Stopp der Beweidung, 3.) die Erfassung der Effekte von höheren Einträgen organischer Substanz infolge eines Beweidungstopps auf die Menge, chemische Zusammensetzung und Umsatzraten funktioneller Fraktionen der OBS sowie deren Einfluß auf die Aggregation von Oberböden und 4.) die quantitative und qualitative Erfassung beweidungssensitiver Fraktionen der OBS über die gesamte Bodentiefe und des Beitrags tieferer Bodenhorizonte zur Kohlenstoffspeicherung sowie der beteiligten Stabilisierungsmechanismen und –potentiale in Graslandböden.

Das Untersuchungsgebiet befindet sich ca. 450 km nördlich von Peking in der autonomen Provinz Innere Mongolei im Norden der Volksrepublik China. Die Böden des Untersuchungsgebiets wurden als sandige Calcic Chernozems klassifiziert, die aus äolischen Sedimenten entstanden, die wiederum auf sauren Vulkangesteinen abgelagert wurden. Ein trocken-kaltes Steppenklima der mittleren Breiten mit einer mittleren, jährlichen Temperatur von 0.4 °C und einem mittleren, jährlichen Niederschlag von 350 mm begünstigt eine typische Steppenvegetation, die hauptsächlich aus dem mehrjährigen Rhizomgras *Leymus Chinensis* und dem mehrjährigen Horstgras *Stipa grandis* besteht. Die Herden im Untersuchungsgebiet setzten sich aus 10-30% Ziegen und 70-90% Schafen zusammen. Zur Bearbeitung der Fragestellung wurden fünf Flächen mit unterschiedlicher Beweidungsintensität ausgewählt (unbeweidet seit 1979: Ug79, unbeweidet seit 1999: Ug99, Winterweide: Wg, kontinuierlich beweidet: Cg, kontinuierlich stark beweidet: Hg). Für die statistische und geostatistische Fragestellung wurden die Oberböden (0-4 cm) der fünf Flächen mit jeweils zwei verschieden großen, regelmäßigen und rechteckigen Rastern beprobt (kleine Raster mit 100 Beprobungspunkten: 15 m Normabstand und 5 m kleinräumige Beprobung; große Raster mit 125 Beprobungspunkten: 50 m Normabstand und 10 m kleinräumige Beprobung). Die unterschiedlichen Beprobungsabstände der beiden Raster ermöglichten die Erfassung von Skaleneffekten. Jede Probe bzw. jeder Beprobungspunkt wurde hinsichtlich Lagerungsdichte, Gehalt an organischem Kohlenstoff, Gesamtstickstoff und Gesamtschwefel, $\delta^{13}\text{C}$, pH-Wert, Mächtigkeit des Ah-Horizontes, Bedeckungsgrad des Bodens mit Vegetation und überirdischer Biomasse untersucht. Der gesamte Datensatz wurde anschließend mithilfe deskriptiver und multivariater explorativer

Statistik sowie uni- und multivariater Geostatistik (Variogramme und Kreuzvariogramme) untersucht. Zur genaueren Betrachtung der beweidungsbedingten Effekte auf die organische Bodensubstanz wurden auf jeder der fünf Flächen zusätzlich repräsentative Profilgruben horizontweise beprobt. Die OBS aus jeweils drei Horizonten wurde anschließend mithilfe einer kombinierten physikalischen Fraktionierung (Aggregatgrößen-, Dichte- und Partikelgrößenfraktionierung) in funktionelle Gruppen und Pools untergliedert. Darüber hinaus wurde die Aggregatstabilität der Oberböden bestimmt.

Die statistische Auswertung der Rasterbeprobung zeigte deutlich die negativen Effekte starker Beweidung auf Oberböden. Die statistischen Analysen zeigen einen signifikanten Anstieg der Lagerungsdichte und eine signifikante Abnahme der organischen Kohlenstoff-, Gesamtstickstoff- und Gesamtschwefelkonzentration mit steigender Beweidungsintensität. Für die Parameter pH-Wert und C/N-Verhältnis konnten keine Effekte, für die Parameter C/S- und N/S-Verhältnis hingegen signifikante Effekte zwischen den verschiedenen Beweidungsintensitäten nachgewiesen werden. Die Unterschiede zwischen den Flächen bezüglich der C/S- und N/S-Verhältnisse deuten auf eine relative Akkumulation von Schwefelverbindungen in beweideten Flächen infolge eines weiter fortgeschrittenem Abbaus der OBS oder eines reduzierten Eintrags von frischem organischen Material (OM) hin. Organische Kohlenstoff-, Gesamtstickstoff- und Gesamtschwefelvorräte für die obersten 4 cm wurden mithilfe der gemessenen Lagerungsdichten bestimmt. Diese Berechnung zeigte signifikant geringere Vorräte auf der kontinuierlich stark beweideten Fläche, während die übrigen Flächen statistisch gleiche Vorräte aufwiesen. Daher wurden die Vorräte zusätzlich unter Zuhilfenahme einer Äquivalenzmasse berechnet, um beweidungsbedingte Änderungen der Lagerungsdichte auszuschließen. Diese Berechnung zeigte nun eine höchst signifikante Abnahme aller Vorräte mit steigender Beweidungsintensität. Des Weiteren waren die Konzentrationen des organischen Kohlenstoffs, Gesamtstickstoffs und Gesamtschwefels über alle Beweidungsstufen hinweg hoch signifikant positiv korreliert. Organischer Kohlenstoff und Lagerungsdichte verhielten sich gegensätzlich und waren hoch signifikant negativ korreliert. Deutliche Verbesserungen der Parameter konnten erst 25 Jahre nach dem Beweidungsstopp eindeutig nachgewiesen werden, während keine Unterschiede innerhalb der ersten

5 Jahre erkennbar waren. Mit dem statistischen Ansatz konnte gezeigt werden, dass sich wichtige physikalische und chemische Oberbodenparameter unter kontinuierlich starker Beweidung signifikant verschlechtern, unter reduzierter Beweidung oder kurz nach einem Beweidungstopp gleich bleiben und 25 nach einem Beweidungstopp signifikant erholen.

Die geostatistische Auswertung der Rasterbeprobung zeigte, dass die räumliche Verteilung in den kleinen Rastern von der Beweidungsintensität beeinflusst wurde. Während die Oberbodenparameter in der kontinuierlich stark beweideten Fläche homogen verteilt waren, wurde die räumliche Verteilung mit abnehmender Beweidungsintensität immer heterogener bis hin zu einer deutlich gemusterten Struktur in Ug79. Dies wird auf den Stopp der Beweidung und die nachfolgende Regeneration und die natürlich einsetzende Sukzession der Vegetation sowie die Ablagerung von windgetragendem Material in den unbeweideten Flächen zurückgeführt. Die Fläche Ug99 zeigte außerdem eine andere räumliche Struktur als die kontinuierlich und die kontinuierlich stark beweidete Fläche, wies aber noch nicht die hohe räumliche Variabilität von Ug79 auf. Die großen Raster zeigten hingegen keine kleinräumige Variabilität oder Beweidungseinflüsse, wiesen dafür aber Strukturen auf, die mit der Topographie sowie Erosions- und Ablagerungsprozessen erklärt werden konnten. Geringe Konzentrationen von organischem Kohlenstoff und geringe Ah-Mächtigkeiten wurden vornehmlich an Kuppen und Oberhängen gefunden und führten zu geringen Vorräten an organischem Kohlenstoff in diesen Landschaftseinheiten. Mithilfe des geostatistischen Ansatzes konnte gezeigt werden, dass die wichtigsten Initialprozesse zur Erholung degradierter Steppenböden eine regenerierende Vegetation und die Ablagerung von windgetragendem Material um diese Pflanzen sind.

Die physikalische Fraktionierung der Oberböden (0-10 cm) zeigte, dass erhöhte Einträge organischer Substanz nach einem Beweidungstopp primär in großen Aggregatgrößenklassen (aggregate size classes: ASC) und darin besonders in Form partikulärer organischer Substanz (particulate organic matter: POM) eingelagert werden. Die OBS in kleinen ASC und Partikelgrößenklassen zeigte hingegen keine quantitativen Änderungen. Die chemische Zusammensetzung der OBS (Festphasen ¹³C NMR Spektroskopie und Neutralzuckeranalyse) war vergleichbar zwischen den verschiedenen beweideten Flächen, wobei die unbeweideten Flächen einen leicht

höheren Abbaugrad aufwiesen. Ug79 hatte zudem höhere Radiokohlenstoffkonzentrationen in allen untersuchten Fraktionen im Vergleich zu Cg. Die Aggregatstabilität wurde mithilfe einer Ultraschallmethode bestimmt und zeigte höhere Stabilitäten in Ug79. Höhere Einträge an organischer Substanz in unbeweideten Flächen erhöhten den Anteil an POM, verkürzten die Umsatzraten der OBS und führten zur Bildung und Stabilisierung von Aggregaten. Der Gehalt an organischem Kohlenstoff in organo-mineralischen Komplexen änderte sich nicht durch die höheren Einträge. Aber höhere Konzentrationen an Radiokohlenstoff deuten darauf hin, dass die Umsatzraten der OBS in diesen Fraktionen durch die höheren Einträge erhöht wurden. Die physikalische Fraktionierung der Oberböden hat gezeigt, dass höhere Einträge an organischer Substanz infolge eines Beweidungsstopps primär in den POM-Fractionen gespeichert werden, die jedoch nur eine mittelfristige Stabilisierung des Materials ermöglichen. Die langzeitstabilen organo-mineralischen Komplexe änderten sich hingegen nicht, was auf eine Sättigung dieses Pools hindeutete. Die Bildung und Stabilisierung von Aggregaten wurde nach einem Beweidungsstopp verbessert.

Die physikalische Fraktionierung aller Horizonte zeigte, dass höhere Einträge an organischer Substanz in allen Horizonten primär in großen ASC und insbesondere in Form von POM gespeichert werden. Diese Anreicherung beginnt im Oberboden (0-10 cm) und benötigt mehr als 5 Jahre um tiefere Horizonte zu erreichen (>10 cm). 25 Jahre nach Beweidungsstopp zeigten alle Horizonte erhöhte Konzentrationen an POM. Im gesamten Profil konnten keine Effekte eines Beweidungsstopps und der nachfolgenden höheren Einträge auf die Menge an OBS in kleinen ASC oder Partikelgrößenfraktionen nachgewiesen werden. Die anhand einer empirischen Gleichung errechnete aktuelle Kohlenstoffbelegung der Partikelgrößenfraktionen war zwischen den verschiedenen Beprobungsflächen gleich und nahm in allen Flächen mit zunehmender Tiefe ab. Dies deutete auf freie Speicherplätze in diesen Partikelgrößenfraktionen hin. Trotz dieser potentiell freien Speicherplätze, konnte auch 25 Jahre nach Beweidungsstopp kein Anstieg der aktuellen Kohlenstoffbelegung gemessen werden. Entweder waren diese Fraktionen bereits gesättigt und die empirische Formel überschätzte die freien Potentiale oder der Eintrag der organischen Substanz in diese Fraktionen war aufgrund von anderen Parametern (bspw. geringe Bodenwassergehalte) verzögert. Die chemische

Zusammensetzung der POM war zwischen den entsprechenden Fraktionen der verschiedenen Beprobungsflächen vergleichbar. Der Abbaugrad der POM nahm mit abnehmender Fraktionsgröße zu und ein Einfluß der Beweidungsintensität auf die Abbauprozesse war nicht festzustellen. Zusammenfassend konnte festgestellt werden, dass höhere Einträge an organischer Substanz infolge eines Beweidungstopps vornehmlich in den nur leicht stabilisierten POM-Fractionen gespeichert werden. Eine langfristige Stabilisierung der zusätzlichen OBS konnte in diesen Böden in den untersuchten Zeiträumen nicht festgestellt werden.

Diese Studie zeigt die Langwierigkeit der Erholung physikalischer und chemischer Bodenfunktionen nach Beendigung der Beweidung von Steppe-Ökosystemen mit höchster statistischer Signifikanz. Die Erholung degradierter Flächen nach einem Stopp der Beweidung beginnt mit der Regeneration der Vegetation. Höhere Einträge an organischem Material durch die Vegetation selbst und die Ablagerung von windgetragenen Material um die Pflanzen herum sind die Ausgangspunkte der Regeneration. Die Erholung der Oberböden war erst 25 Jahre nach dem Beweidungstopp nachweisbar, während die räumliche Verteilung der Vegetation bereits nach 5 Jahren erste Anzeichen einer Regeneration zeigte. Die höheren Einträge an organischer Substanz in den unbeweideten Flächen wurden hauptsächlich in den POM-Fractionen eingelagert und nur kurzfristig stabilisiert. Dies führte zur vermehrten Bildung und Stabilisierung von mittleren und groben Aggregaten, die der starken Erosion in vormals degradierten Flächen entgegenwirken können. Die Partikelgrößenfraktionen der Oberböden haben sich nach dem Beweidungstopp quantitativ nicht verändert, was auf die Sättigung ihrer Kohlenstoffspeicher hindeutet. Aber trotz abgesättigter Kohlenstoffspeicher nahmen die Radiokohlenstoffkonzentrationen in den unbeweideten Flächen zu und deuteten darauf hin, dass auch diese zuvor als relativ stabil angesehenen Fraktionen an dem normalen Umsatz des Kohlenstoffs im Boden teilnehmen und von einer langfristigen Stabilisierung dieser zusätzlichen Einträge nicht ausgegangen werden kann. Die höheren Einträge an organischer Substanz in der Folge des Beweidungstopps erreichten die tieferen Horizonte der Steppeböden erst nach 25 Jahren. Da diese Einträge jedoch auch nur in den relativ labilen POM-Fractionen eingelagert wurden, kann auch für die tieferen Horizonte zunächst keine langfristige Stabilisierung des Kohlenstoffs postuliert werden. Abschließend ist zu bemerken, dass eine

Reduzierung und insbesondere ein kompletter Stopp der Beweidung über längere Zeit die negativen Effekte einer kontinuierlichen Beweidung abmildern können. Ob diese Ökosysteme jedoch durch eine Kontrolle der Nutzung eine der globalen Kohlenstoffsinken werden können, bleibt fraglich.

Table of contents

SUMMARY	I
ZUSAMMENFASSUNG.....	VI
1. INTRODUCTION, AIMS AND STATE OF THE ART	1
1.1 General introduction	1
1.2 Aims and state of the art.....	2
2. MATERIALS AND METHODS	11
2.1 Study area	11
2.1.1 Geology	13
2.1.2 Climate and Hydrology.....	16
2.1.3 Geomorphology.....	20
2.1.4 Vegetation	21
2.1.5 Soils.....	24
2.1.6 Human history	25
2.2 Plot description and sampling design.....	27
2.3 Plot samples.....	31
2.3.1 Determination of bulk density, OC, total N and total S concentrations, pH and $\delta^{13}\text{C}$	31
2.3.2 Stock calculations	31
2.3.3 Statistical analyses.....	32
2.3.4 Geostatistical analyses	34
2.4 Pit samples.....	37
2.4.1 Physical fractionation	37
2.4.2 Particle size distribution	39
2.4.3 Determination of bulk density, OC and total N concentrations and radiocarbon dating	39
2.4.4 Clay mineralogy and selective mineral extraction.....	40
2.4.5 Determination of neutral sugars.....	40
2.4.6 Solid-state ^{13}C NMR spectroscopy.....	41
2.4.7 Aggregate stability.....	42
3. SOIL CLASSIFICATION AND CHARACTERISTICS	43

4.	GRAZING EFFECTS ON CHEMICAL AND PHYSICAL PROPERTIES OF SEMIARID STEPPE SOILS	47
4.1	Results	47
4.1.1	Bulk density, elemental concentrations, ratios and pH	47
4.1.2	OC, N and S stocks.....	49
4.1.3	Minimum detectable differences	51
4.2	Discussion.....	51
4.2.1	Grazing significantly increases bulk density and decreases OC, total N and total S concentrations	51
4.2.2	Sulphur in grazed grassland soils	53
4.2.3	OC, total N, and total S stocks of grazed plots	53
4.2.4	Effects of grazing reduction and enclosure	54
4.3	Conclusion	55
5.	SPATIAL VARIABILITY OF TOPSOILS AND VEGETATION IN GRAZED STEPPE ECOSYSTEMS.....	57
5.1	Results	57
5.1.1	Small grids.....	57
5.1.2	Large grids	62
5.2	Discussion.....	65
5.2.1	Small-scale heterogeneity of topsoils following grazing exclusion	65
5.2.2	Large-scale heterogeneity of topsoils follows geomorphology	68
5.2.3	Detectability of spatial patterns is scale dependent	70
5.3	Conclusion	72
6.	ALTERATION OF SOIL ORGANIC MATTER POOLS AND AGGREGATION IN TOPSOILS AS DRIVEN BY OM INPUT	73
6.1	Results	73
6.1.1	Physical fractionation	73
6.1.1.1	Mass, OC and C to N ratio.....	73
6.1.1.2	Chemical composition of POM and particle size fractions in three ASC.....	76
6.1.2	Aggregate stability.....	81
6.2	Discussion.....	83
6.2.1	Impacts of grazing exclusion on topsoils	83

6.2.1.1	Quantity and distribution of SOM in POM and mineral fractions of steppe topsoils....	83
6.2.1.2	SOM quality in POM and particle size fractions of steppe topsoils	84
6.2.1.3	Stability of different aggregate size classes of steppe topsoils	85
6.2.2	Carbon sequestration in steppe topsoils - effects of grazing cessation.....	86
6.3	Conclusion	87
7.	DISTRIBUTION OF SOIL ORGANIC MATTER BETWEEN FRACTIONS, AGGREGATE SIZE CLASSES AND HORIZONS	89
7.1	Results.....	89
7.1.1	Mass, OC concentration and C-to-N ratio of POM and particle size fractions.....	89
7.1.1.1	POM fractions	89
7.1.1.2	Particle size fractions	93
7.1.1.3	Relative contribution of fractions to total OC	95
7.1.2	Chemical composition of POM fractions	96
7.2	Discussion.....	98
7.2.1	Quantity and distribution of SOM in steppe soils as affected by grazing cessation	98
7.2.1.1	POM fractions	98
7.2.1.2	Mineral fractions.....	100
7.2.2	Effects of grazing cessation on the quality of POM fractions in steppe soils.....	102
7.2.3	Carbon sequestration in steppe soils	105
7.3	Conclusion	107
8.	CONCLUSION.....	108
9.	REFERENCES	110
10.	DANKSAGUNG/ACKNOWLEDGEMENTS	131

List of figures

Figure 1: Location of the experimental area.	11
Figure 2: Digital elevation model of the experimental area	12
Figure 3: Geological map of the experimental area.....	14
Figure 4: Climate at IMGERS	17
Figure 5: Pictures of local precipitation event and gully erosion.....	17
Figure 6: Climate at the experimental sites between 2004 and 2006.....	18
Figure 7: Pictures of a dust devil and a dust storm.....	18
Figure 8: Mean discharge of the Xilin River	19
Figure 9: Typical landforms in the experimental area.....	20
Figure 10: Land use classification of the experimental area	22
Figure 11: Distribution of Kastanozems, Chernozems and Phaeozems in Eurasia	24
Figure 12: Pictures of living conditions in Inner Mongolia	26
Figure 13: Digital elevation model of the experimental sites and sampling grids.....	29
Figure 14: Location of the experimental plots	30
Figure 15: Experimental variogram with fitted variogram model	35
Figure 16: Schematic of conducted fractionation and measurements.....	38
Figure 17: Spectra of soil state ¹³ C NMR experiment with chemical shift regions.	41
Figure 18: Pictures of the five sampled soil pits	43
Figure 19: Boxplots of bulk density and OC concentration.....	47
Figure 20: Correlations between OC, total N and total S concentrations and between bulk density and OC concentration.....	48
Figure 21: Omni-directional semivariograms of bulk density in Ug79 and Hg.....	59
Figure 22: Omni-directional crossvariograms of bulk density, OC, total N and total S concentration (Group 1), vegetation cover and aboveground biomass (Group 2) in Ug79.	61
Figure 23: Omni-directional crossvariograms of OC concentration and δ ¹³ C (representing Group 1), vegetation cover (representing Group 2), pH (representing Group 3), slope angle and altitude in Cg _{large}	64
Figure 24: Map of vegetation cover in Cg _{large}	68
Figure 25: Spatial distribution as affected by sampling scale - omni-directional semivariograms of bulk density in Cg and Cg _{large}	70

Figure 26: ^{13}C CPMAS NMR spectra of POM and selected particle size fractions of cASC in Cg and Ug79	77
Figure 27: Chemical composition of POM and selected particle size fractions of three ASC as analysed by ^{13}C CPMAS NMR spectroscopy.....	78
Figure 28: Radiocarbon concentrations of selected POM and particle size fractions of three ASC in Cg and Ug79	79
Figure 29: Quantity and quality of neutral sugars in selected POM and particle size fractions of three ASC in Cg and Ug79	80
Figure 30: Aggregate stability of three ASC in topsoils of Cg and Ug79 as analysed by sonication	82
Figure 31: Chemical composition (solid state ^{13}C NMR spectroscopy) of POM fractions as affected by aggregate size (A) and sampling depths (B)	103
Figure 32: Chemical composition of POM fractions as analysed by solid state ^{13}C NMR spectroscopy	104

List of tables

Table 1: Characteristics of the three aggregate size classes in the topsoils	37
Table 2: Soil characteristics of experimental plots.....	44
Table 3: Concentrations of Fe, Al and Mn in oxalate and dithionite–citrate–bicarbonate extracts.....	45
Table 4: Cation exchange capacity and exchangeable cations of the experimental plots.	46
Table 5: Clay mineralogy of Ug79.....	46
Table 6: Results of measured and calculated parameters of the upper 4 cm	49
Table 7: MDD for selected topsoil parameters and plots.....	50
Table 8: Mean values of soil characteristics of upper 4 cm	57
Table 9: Nugget, sill and range values derived from fitted variogram models of small grid sampling...	58
Table 10: Mean values and standard deviations for Nu/Nu+Si and range values.....	60
Table 11: Nugget, sill and range values derived from fitted variogram models of large grid sampling.	63
Table 12: Mass distribution, OC concentration and C/N of soil fractions and contribution of OC of a specific fraction to the bulk soil of three aggregate size classes.....	74
Table 13: Soil and vegetation characteristics of upper 10 cm given as arithmetic means and standard deviations of three representative soil pits.	75
Table 14: Mass distribution, OC concentration and C/N of soil fractions and contribution of OC of a specific fraction to the bulk soil of three aggregate size classes as affected by grazing intensity.....	90
Table 15: Relative contribution of POM-OC, sand-OC, silt-OC and clay-OC to ASC-OC and bulk-OC of three horizons	95
Table 16: Chemical composition of POM fractions as analysed by solid state ¹³ C NMR spectroscopy	97

1. Introduction, aims and state of the art

1.1 General introduction

Grasslands cover about 40% of the global terrestrial area, excluding Greenland and Antarctica (Sutie *et al.*, 2005). The Eurasian steppe is one part of these grasslands and represents the largest continuous terrestrial biome in the world. The steppe areas in the autonomous province of Inner Mongolia in northeastern China and especially in the Xilin river basin are representative for semiarid steppe ecosystems in central Asia (Bai *et al.*, 2004). They are used for at least two thousand years by nomads and their herds as extensive pastures. During the last 20 years, stocking rates reached a maximum as a consequence of political decisions. In the 1950s and 1960s, nomads in China were forced to give up their nomadic way of life and had to settle in small villages, hamlets or individual farms. In combination with an increase in number of livestock, this policy led to an increased grazing pressure in the vicinity of the newly established settlements. In the 1980s, a new economic policy allowed individuals to profit directly from the meat or wool production of their herds, once more intensifying the land use. This intensive land use and especially the heavy continued grazing led to a degradation of steppe vegetation associated with changes in the amount and composition of soil organic matter (SOM). The concurrent degradation of soil structure and destruction of aggregation enhanced the erodibility of the soil. Furthermore, most of the grassland carbon is located in the belowground biomass and in the SOM. Hence, increased soil erosion also dislocates large amounts of C and N that were previously stored in the ecosystem. Nowadays, the most apparent consequences are wide-spread desertification and a high abundance of severe supra-regional dust storms impairing not only the local population but also the densely populated coastal regions. China is one of the countries facing the most serious desertification problems in the world. The total area affected by desertification in China is approximately 2.6 million km², covering 27.3% of the total territory (total area of Germany: 357,021 km²). The grasslands of the Xilin river basin also show evidence for degradation due to overgrazing (Tong *et al.*, 2004) and are one source area for dust storms.

Initiatives to mitigate these detrimental effects of the intensive land use were started by the local government but generally missed precise scientific knowledge on sustainable management systems. Moreover, grazed steppe ecosystems are discussed as one of the big global carbon sinks that may have the potential to sequester large amounts of atmospheric CO₂ and mitigate the effects of global climate change if grazing is abandoned or management improved. Therefore, big interest has arisen not only to mitigate the detrimental effects of grazing and intensive land use, but also to increase the carbon sequestration of these ecosystems.

1.2 Aims and state of the art

The sino-german interdisciplinary research group MAGIM was set up to investigate the effects of grazing on semiarid steppe ecosystems and to evaluate the benefits and potentials of grazing management and grazing cessation. This work focussed on changes in the amount, composition and distribution of soil organic matter (SOM) due to continued heavy grazing and grazing cessation and the concurrent degradation of soil structure and aggregation. Therefore, five plots with different grazing intensities and time since grazing cessation were sampled using a regular, orthogonal grid and representative soil pits. While the grid samples were used for detailed statistical analyses of grazing-induced effects on bulk topsoil parameters, samples from representative soil pits were used for studies on the impacts of grazing and grazing cessation on quantity and quality of physical SOM fractions in different soil horizons and aggregate size classes. The four main topics of this study were to...

Research topic I: ...investigate the effects of continued heavy grazing and possible benefits of grazing cessation on bulk topsoil parameters using statistical tools on a large number of samples (Chapter 4).

Land use management has been suggested as a factor that can have a major impact on grassland ecosystems (Conant *et al.*, 2001). Notably, according to

Soussana *et al.* (2004), grassland management strongly affects soil OC stocks. Wu *et al.* (2003) found that the soils of the semiarid to subhumid zone in northeast China, and especially black soils and meadow soils (i.e. Phaeozems), are highly susceptible to OC loss upon management change.

Beside OC, N plays an equally important role in the ecology of grasslands, but few studies have evaluated the impacts of management on soil N (Conant *et al.*, 2005). Generally, changes in soil N stocks after management changes have been closely related to changes in C stocks. Solomon *et al.* (2005) opted to focus on soil S, as this main nutrient may be essential for plant nutrition in sensitive ecosystems such as grasslands. Wang *et al.* (2001b) concluded that sulphur deficiency is widespread in the Inner Mongolia steppe, affecting productivity.

The literature contains contrasting results on the effect of management on C and N concentrations and stocks in grasslands. With increasing grazing intensities, decreasing C stocks (Abril & Bucher, 1999; Neff *et al.*, 2005), as well as unchanged (Berg *et al.*, 1997; Binkley *et al.*, 2003; Barger *et al.*, 2004) and increasing stocks (Reeder & Schuman, 2002; Conant *et al.*, 2005) have all been found. Fewer results are available concerning N in grasslands affected by management, but they also vary. Increasing (Bauer *et al.*, 1987), unchanged (Schuman *et al.*, 1999; Barger *et al.*, 2004) and decreasing (Frank *et al.*, 1995) N concentrations and stocks are described with increasing grazing intensity. Bauer *et al.* (1987) showed negative correlations, while Abril and Bucher (1999) observed positive correlations between OC and N in grazed compared to ungrazed areas. One reason for results showing no or contrasting effects may be the total number of samples. The lower the number of samples, the longer the time and the larger the change until a significant change can be detected (Smith, 2004).

The main objectives of the statistical approach were to i) statistically investigate the effects of continued heavy grazing on bulk density, OC, total N, total S, C/N, C/S, N/S and pH in a steppe ecosystem using a large number of samples; and ii) evaluate possible benefits of grazing cessation.

Research topic II: ...analyse the impacts of heavy grazing, reduced grazing and time since grazing cessation on the spatial distribution of bulk topsoil parameters and topsoil-vegetation-interactions using univariate and multivariate geostatistical tools (Chapter 5).

Soils and vegetation of steppe ecosystems exhibit spatial patterns ranging in extent from landscape to individual plant scale (Ehrenfeld *et al.*, 1997; Rietkerk *et al.*, 2004). Self-organisation of vegetation or inherent soil heterogeneities and intertwined processes such as positive and negative feedbacks between soils and vegetation are discussed as possible reasons for the formation of these patterns (Rietkerk *et al.*, 2002; Wijesinghe *et al.*, 2005; Bestelmeyer *et al.*, 2006). Individual patches in these patterns are not only spots of high floral and faunal biodiversity, but the change of spatial distribution of individual patches and whole patterns is also assumed to be an indicator for changing ecosystems. Schlesinger *et al.* (1996) and Ares *et al.* (2003) suggest the change of spatial distribution of vegetation and topsoil properties following grazing as an early indicator for degradation of arid and semiarid grasslands.

The current literature contains contrasting results on the spatial distribution of topsoil and vegetation properties under herbivory. This complicates the clarification of the present status and the direction in which this ecosystem is going, which makes it difficult to determine how it might best be managed. Adler and Lauenroth (2000) found heterogeneous, patchy distributions of vegetation and soil in ungrazed areas or following grazing exclusion compared to homogeneous spatial distributions in grazed areas. Cui *et al.* (2005) found no change of spatial distribution of soil OC content in grazed compared to ungrazed areas in Inner Mongolia steppe. Su *et al.* (2006) described even increased spatial heterogeneities for particle size fractions, OC and total N concentrations following overgrazing in sandy grasslands in Inner Mongolia.

These contrasting results are mainly the product of two factors biasing the evaluation of spatial distributions of topsoil and vegetation properties. Temporal aspects are crucial as properties take time to change clearly. Cheng *et al.* (2004) found transitions from heterogeneous to homogeneous spatial distributions of soil

elements with successional degraded stages for grasslands in northwestern China. Homogeneous distributions at early stages of degradation were followed by a short interval of increased heterogeneity and a collapse of resource islands at late stages. The sampling scale has to be considered in an inventory of spatial distributions, as all processes take place and are noticeable only on a certain scale. Fuhlendorf and Smeins (1999) showed that the detectability of grazing impacts on vegetation properties changed with the sampled or considered scale of observation. Purtauf *et al.* (2005) and Rietkerk *et al.* (2004) even concluded that there was no correct optimal sampling scale and that studies covering a range of scales were necessary.

The main objectives of the geostatistical approach were i) to analyse the impact of heavy grazing, reduced grazing and time since grazing cessation on the spatial distributions of topsoil (bulk density, OC, total N and total S concentrations, $\delta^{13}\text{C}$, pH and Ah thickness) and vegetation (vegetation cover and aboveground biomass) properties in a semiarid steppe using uni- and multivariate geostatistics; and ii) to evaluate the importance of scale effects on the detectability of grazing induced changes to topsoil and vegetation properties using two different grid sizes.

Research topic III: ...study the effects of higher OM inputs due to grazing cessation on the amount, composition and turnover of functional SOM fractions and their contribution to aggregate stability in topsoils (Chapter 6).

Grassland ecosystems are assumed to have a high capacity to sequester organic carbon in the soil (Cui *et al.*, 2005). Soil organic carbon (SOC) protection mechanisms are intimately tied to the processes of aggregate turnover and stabilisation at multiple scales. The deposition and transformation of organic matter plays a major role in aggregate stabilization and there are strong feedbacks between aggregate turnover and SOC dynamics (von Lützow *et al.*, 2006; Jastrow *et al.*, 2007). Extensive reviews on the relationship between soil organic matter (SOM) and aggregation by Tisdall & Oades (1982) and Loveland & Webb (2003) demonstrated that:

- i) Only part of SOM stabilises aggregates and this is generally the newer or more active material, with a relatively large concentration of mono- or polysaccharides.
- ii) Above a certain SOM concentration, there is no further increase in the stabilising effect.
- iii) There is a large variation in the effectiveness of various organic binding agents, ranging from less effective substances being water-soluble and/or transient to persistent organic bonds.
- iv) Adequate supply of OM is more important for water-stable aggregation than the amount, in that the association of new components with particle surfaces, particularly within aggregates (Puget *et al.*, 1995) is the crucial factor.
- v) Two main classes of aggregates can be defined: microaggregates are stabilized against disruption after rapid wetting and mechanical disturbance through several mechanisms in which organo-mineral complexes play a dominant role. Water stability of macroaggregates depends largely on growing root systems. The stabilization of macroaggregates is controlled by management and is increased under pasture (near continual production of transient mono- and polysaccharides), but decreases rapidly under arable cultivation (Tisdall & Oades, 1982).

Grazing management of grassland ecosystems influences OM input and associated soil properties. Intensive grazing leads to significantly lower SOC concentrations and stocks associated with higher bulk densities in topsoils (Steffens *et al.*, 2008; Steffens *et al.*, 2009a) and additionally to lower mean-weight diameter of water-stable aggregates, lower monosaccharide contents and lower (galactose + mannose)/(xylose + arabinose) ratios (Dormaar & Willms, 1998). These effects were most pronounced at the heavier grazing pressures. Light to moderate grazing intensity does not necessarily lead to a decrease of SOM content and aggregate stability. For example, light grazing pressure for 20 years in the typical steppe of Inner Mongolia caused no significant decrease of SOC content (Cui *et al.*, 2005). Short-duration, low-frequency, intensive grazing systems may have enhanced soil functions by resulting in a more active microbial community, which turned over

organic matter more rapidly and led to higher soil stability and infiltration capacity (Beukes & Cowling, 2003). Franzluebbers *et al.* (2000) found that long-term grazing of pastures with cattle did not adversely affect aggregate distribution and stability compared with haying and concluded that typically grazed pasture management systems have few discernable negative impacts on macroaggregation and aggregate stability.

Physical fractionation procedures by size and density are necessary to determine the effect of grazing management not only for bulk SOM contents, but also for OM contents on the scale of functional SOM fractions. With this approach, Dubeux *et al.* (2006) applied a physical fractionation procedure by size and density to determine the effect of grazing management not only for bulk SOM contents, but also for OM contents on the scale of functional SOM fractions. The study showed that management intensity did not affect C and N concentration in the bulk soil, but did impact C and N concentrations of size fractions of light density SOM. Burke *et al.* (1999) found that over 50 years of heavy grazing by cattle did not have a significant effect on most of the SOM pools and ascribed this to the strong dominance of belowground OM, only minimally influenced by above-ground herbivory. The authors found significant effects of grazing only for coarse particulate organic matter (POM), which had larger contents in ungrazed than in grazed pastures.

Hassink (1995) analysed decomposition rates of physically isolated OM fractions of grassland soils and found decreasing decomposition rate constants in the order light, intermediate and heavy macro-organic matter and lowest values in the microaggregate fractions (<50 μm). Additionally, light and intermediate fractions of the macro-organic matter fraction were found to be much more sensitive to input of organic residues than the other fractions. Therefore, Hassink *et al.* (1997) proposed these fractions as sensitive indicators of changes in SOM.

Very few studies have investigated grazing-induced changes of the composition of SOM on the scale of functional SOM fractions. Ganjegunte *et al.* (2005) studied effects of different grazing management on the amount and composition of topsoil OM. The authors identified an enhanced lignin degradation caused by grazing, but found no significant variation of nuclear magnetic resonance (NMR) spectra of humic and fulvic acids between the grazing treatments.

On the scale of grazing-sensitive aggregate size classes, detailed investigations on the amount, composition and turnover of functional SOM fractions and their contribution to aggregate stabilisation are still lacking. In order to understand the grazing-induced feedbacks between SOM and aggregate stability, this study investigated effects of different organic matter inputs due to different grazing intensities on i) SOC and total N storage in different aggregate size classes of steppe topsoils, ii) changes of the chemical composition, amount and composition of neutral sugars and radiocarbon ages of selected SOC and aggregate size fractions and iii) the formation of stable aggregates and the resultant physical stabilisation of organic matter.

It was hypothesized that i) grazing-sensitive SOM pools can be identified by using physical fractionation according to aggregate size, particle size and density; ii) higher inputs under ungrazed conditions lead to increased SOC and total N storage and greater aggregate formation and stability; iii) higher OC inputs alter biochemical processes as reflected by chemical composition, neutral sugars and radiocarbon ages; and iv) more decomposed or recalcitrant organic matter in small aggregate size classes points towards physical protection and aggregate hierarchy.

Research topic IV: ...quantitatively and qualitatively characterise grazing-sensitive SOM fractions in subsoils and reveal their contribution to the carbon sequestration and stabilisation potential of steppe soils (Chapter 7).

Grazed steppe ecosystems are discussed as one of the big global carbon sinks that may have the potential to sequester large amounts of atmospheric CO₂ and mitigate the effects of global change if grazing is abandoned or management improved. Many studies estimated the effects of grazing cessation on sequestration capacities of steppe soils but disregarded at least two important points. First, many studies compared bulk soil organic carbon (SOC) of differently grazed plots and did not separate between different fractions or pools of SOC (Zhou *et al.*, 2007; Ingram *et al.*, 2008; Wu *et al.*, 2008). Different fractions and pools are not only different in capacity and quality but also in mechanism and temporal scale of OC stabilisation

(von Lützow *et al.*, 2006). Second, most studies based their estimations on data from topsoils, as the upper cm of the soil are taken as most sensitive to management changes. Don *et al.* (2008), Rumpel *et al.* (2002) and Jobbagy and Jackson (2000) suggest deeper soil layers to be important for the sequestration of OC in soils as large amounts may be stored in deeper soil layers.

Von Lützow *et al.* (von Lützow *et al.*, 2006) reviewed the literature with focus on OM stabilisation mechanisms. They propose three main mechanisms of OM stabilisation with relevance varying between soil types and horizons and time-scales in which these mechanisms can stabilise the OM - 1.) selective preservation due to recalcitrance, 2.) stabilisation by spatial inaccessibility of OM for microorganisms and enzymes and 3.) stabilisation by interaction with surfaces and metal ions. Many studies discuss sequestration capacities or stabilisation mechanisms and conclude that the potential C sequestration of soils and their according stabilisation mechanisms are limited (Hassink, 1997; Chung *et al.*, 2008; Gulde *et al.*, 2008). Kölbl and Kögel-Knabner (2004) propose an upper limit of occluded POM and explain this with the limited capacity of soils to form aggregates. Kleber *et al.* (2005) suggest a finite stabilisation capacity of soil minerals for organic matter, limited by the area density of reactive surface sites. Recent studies describe clay fraction OC not to be as stable as expected. Kadono *et al.* (2008) describe a labile clay-associated OM fraction and derive their results from incubation studies.

In a previous study, we analysed the grazing-induced feedbacks between SOM and aggregate stability in grazed semiarid steppe soils (Steffens *et al.*, 2009b). This investigation was conducted in topsoils (0-10 cm) of four differently grazed plots, because several authors showed that grazing cessation first affected topsoils. The most interesting result of our study was that fine particle size fractions in topsoils were obviously saturated and additional OM inputs due to grazing cessation were predominately stored in readily decomposable POM fractions. In the same plots, Gao *et al.* (2008a) describe changing species compositions and functional groups as a consequence of grazing cessation, with especially higher abundances of deep rooting perennial forbs, shrubs and semishrubs in long-term ungrazed areas. Gao (2007) found higher belowground biomass and cumulated root lengths in deeper soil horizons of ungrazed plots compared grazed plots. Taking this into account, deeper

soil horizons may be affected by higher inputs of OM following grazing cessation and may have great importance for the sequestration of C in grazed steppe soils.

The main questions were: i) Is it possible to separate grazing-sensitive SOM pools using a physical fractionation procedure for the complete soil profile when considering aggregate size, particle size and density?; ii) Are subsoil SOC pools quantitatively and/or qualitatively affected by grazing cessation? Is it possible to detect effects already 5 years after grazing cessation? and iii) Which stabilisation mechanisms are responsible for the sequestration of OC in subsoils of grazed steppe ecosystems?

2. Materials and methods

2.1 Study area

The study area is located in the northeastern part of the Peoples Republic of China in the autonomous province Inner Mongolia (Figure 1). Situated 60 km southeast of Xilinhot and 450 km north of Beijing, it belongs to the administrative district of the Xilin Gol League named after the Xilin River, close to the town of Tuanbu. The whole region is part of the UNESCO Biosphere Reserve Xilin Gol, designated by

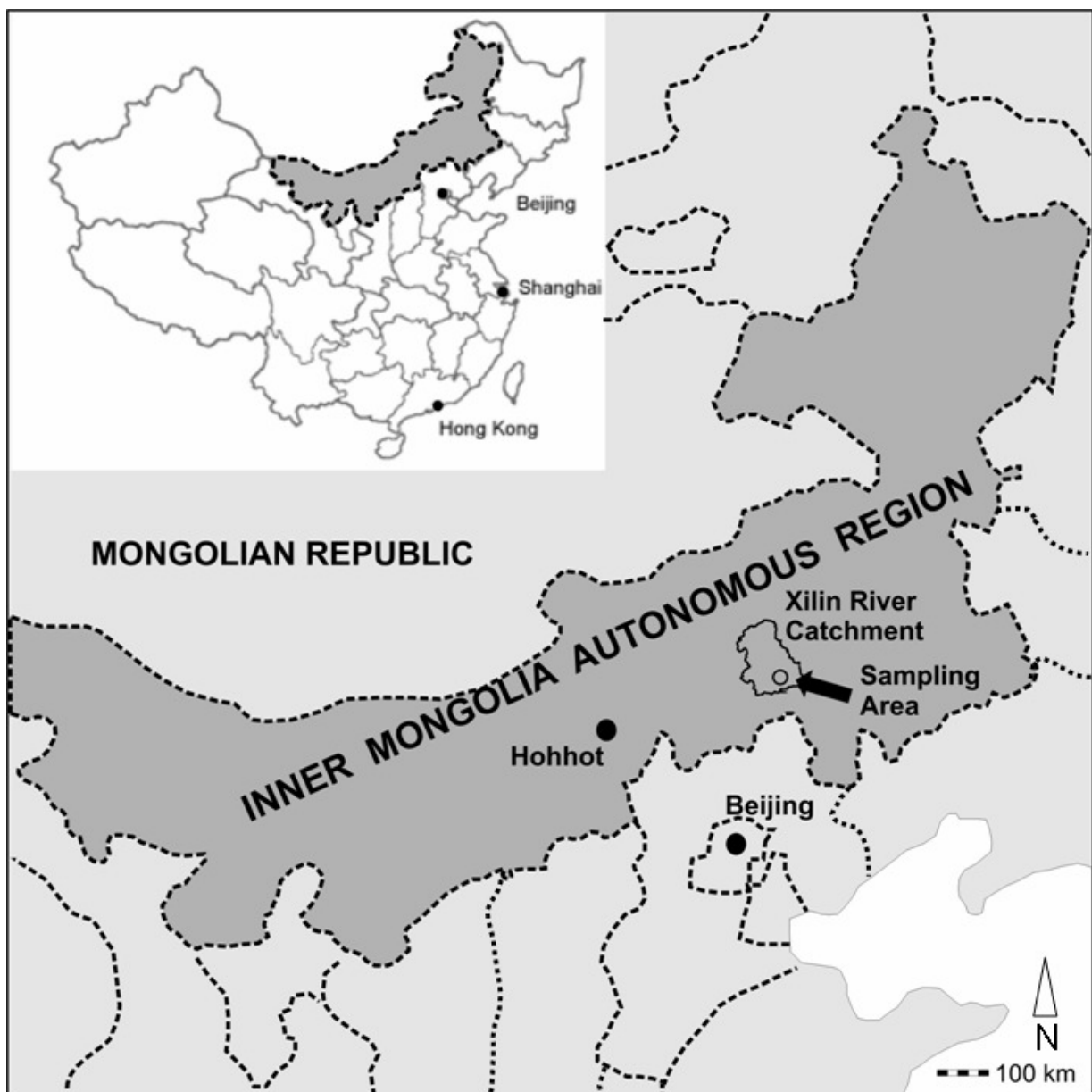


Figure 1: Location of the experimental area.

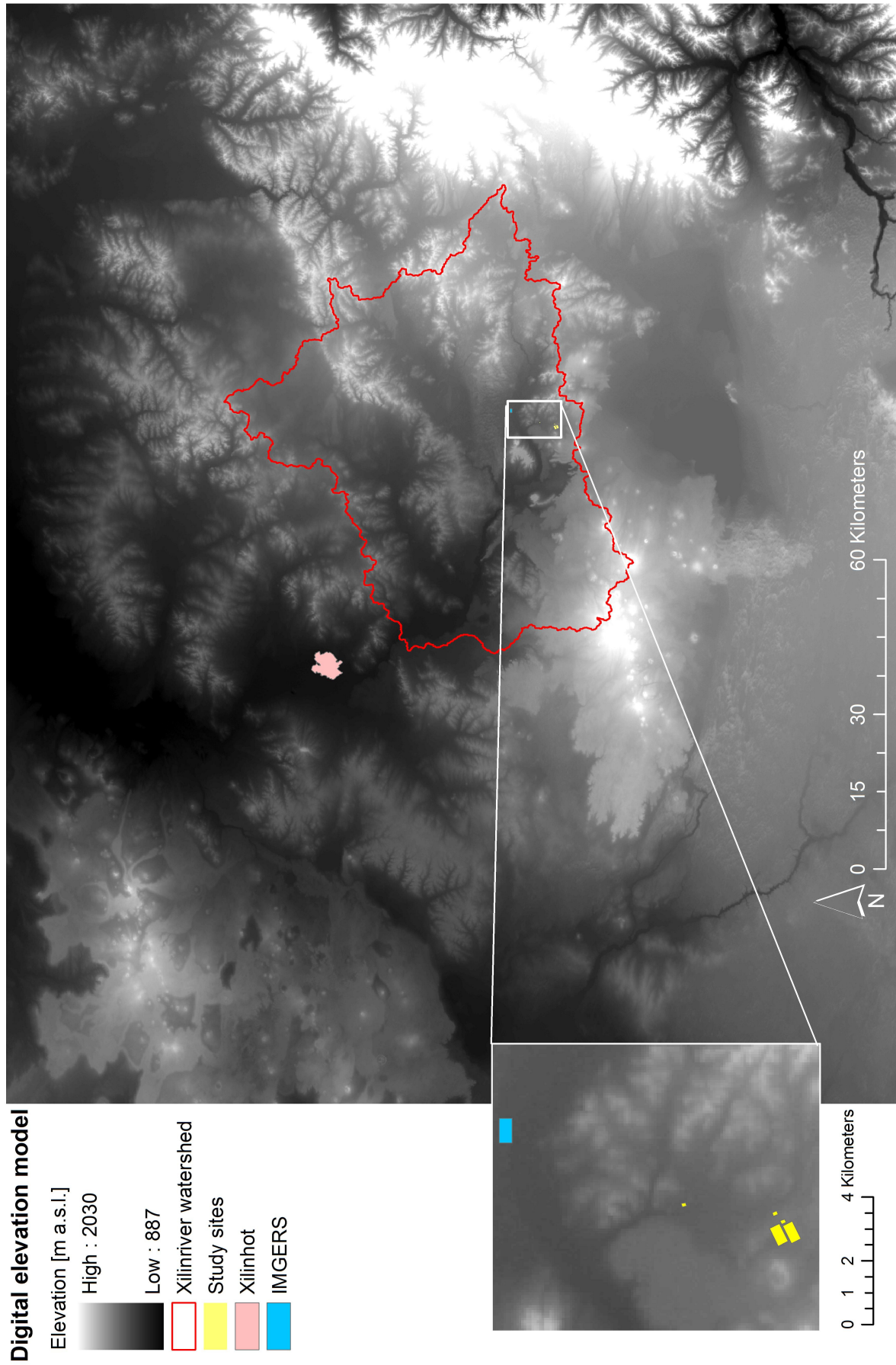


Figure 2: Digital elevation model of the experimental area (calculated using the SRTM dataset).

the United Nations' Man and Biosphere Programme (UNESCO/MAB), and belongs to the Xilin River watershed (Figure 2). The experimental area lies 15 km southwest of the Inner Mongolia Grassland Ecosystem Research Station (IMGERS), which is administered by the Institute of Botany at the Chinese Academy of Sciences (43°33'06" N, 116°40'12" E).

2.1.1 Geology

The geological evolution of the Xilin River catchment started in the Proterozoic when the Archaean Cratons North China and Siberia (Angara) were separated by the Palaeoasian or Turkestan Ocean (Kusky *et al.*, 2007). During the Palaeozoic both cratons moved towards each other, amalgamating island arcs and microcontinents to their active margins in an oceanic setting, each forming an accretionary wedge (Tang & Yan, 1993; Xiao *et al.*, 2003; Kusky *et al.*, 2007; Windley *et al.*, 2007) as part of the variscan orogeny. The North China Craton mainly accumulated ordovician and silurian arc materials (Shi *et al.*, 2003), while Siberia collected precambrian terranes, devonian and carboniferous island arcs and ophiolite complexes (Chen *et al.*, 2000). Relicts were found in the northern Xilin River catchment in form of paleozoic schists (Pz1wn; Figure 3) and upper carboniferous sandstones (C3l), belonging to the Wenduermiao formation and the Linxi sub-province. Shi *et al.* (Shi *et al.*, 2003) sampled zircons in the metamorphic rocks of the Xilin Gol complex 20 km to the southeast of Xilinhot and measured ages between 437 and 316 Ma (most likely Pz1wn). Since the Permian most of the oceanic crust was subducted and Andean-type magmatic margins established along the subduction zones of both cratons. The eastern and western part of the Xilin River catchment contains many relicts of these times with detrital, volcanic and plutonic rocks, formed in lower to middle Permian times (Wang *et al.*, 2004a; P1z1, P1z2, P1z3, dv43(2), d43(2), do43(1)b, Yd43(1), Yd43(1)b, Yd43(1)c, Yo43(1)b, Y52(1), Y52(1)a, Y52(1)b, Y52(1)c and Y52(1)y). Shi *et al.* (2004) determined the exact emplacement age of the acid plutonic rocks 10 km to the south of Xilinhot to be 276 Ma (Y52(1)). With final subduction of the intervening ocean in the late Permian, the two opposing continental margins collided and completed the formation of the supercontinent Pangäa (Sengör & Natal'in, 1996; Robinson *et al.*, 1999; Xiao *et al.*, 2003). This collision gave rise to the Solonker suture, the eastern segment of the Central Asian Orogenetic Belt (Altaid Tectonic Collage; Chen *et al.*, 2000; Liu *et al.*, 2005), spanning from the Ural to the Pacific

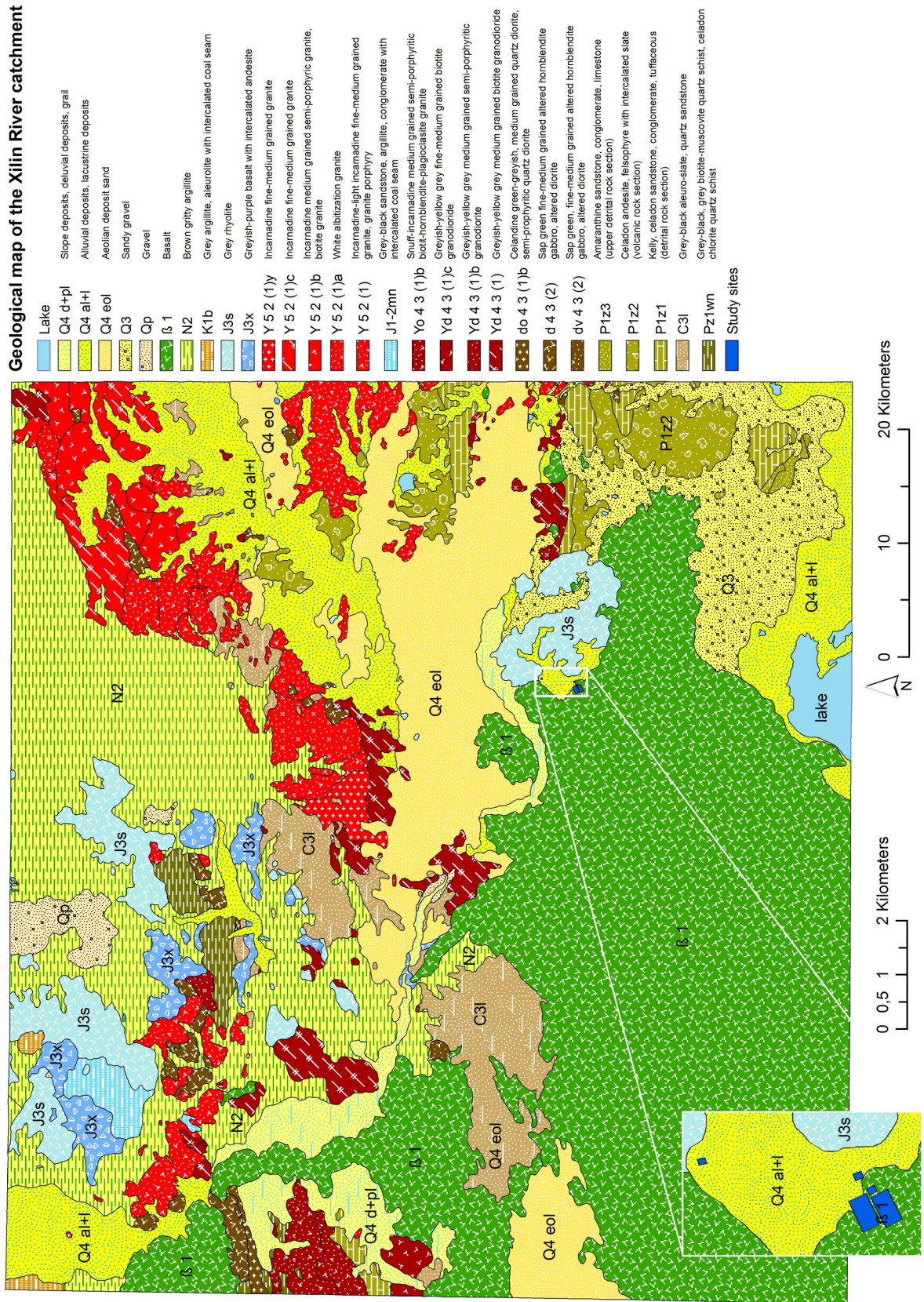


Figure 3: Geological map of the experimental area.

Ocean. The northern accretionary zone, between Siberia and the Solonker suture is called Altaids and the southern accretionary zone between the North China and the Solonker suture is called Manchurides or Xingmeng (Liu *et al.*, 2005).

In the Triassic, the continental crusts collided and under predominant northward subduction during final formation of the suture gave rise to a large-scale, south directed thrust and fold belt of Himalayan proportions (Xiao *et al.*, 2004; Windley *et al.*, 2007). This period was marked by an absence of sedimentation following the consequent uplift and formation a high-standing plateau (Meng, 2003), accompanied by the large scale continental crustal growth (Hong *et al.*, 2004) and the emplacement of immense volumes of crustal melt granitic magmas (Jahn *et al.*, 2000). Since early Jurassic, terrestrial sediments were deposited across the suture and the entire orogen (J1-2mn; Xiao *et al.*, 2003; Wang *et al.*, 2004c; Liu *et al.*, 2005) implying the erosion of the formerly high-standing plateau. Late Jurassic voluminous plutonism (J3s and J3x) mark the starting point of an intracontinental rifting as the result of the beginning interactions between the Eurasian, Indian and Pacific plate (Ren *et al.*, 2002). The following crustal extension, an asthenospheric upwelling and the gravitational collapse of the overthickened crust resulted in the formation of the northeast Asian Basin and Range type fault basin system in the Cretaceous (Meng, 2003; Meng *et al.*, 2003). Xilingol was situated in the southeast of the Erlian Basin structure, which was filled with different sediments, volcanics and intercalated coal measures. The deposition into this basin system already stopped in upper cretaceous when the structure was lifted and eroded (Ren *et al.*, 1998; Meng, 2003). Last remnants were found in the northern part of Xilingol in form of argillites with intercalated coal measures (K1b; Meng *et al.*, 2003). At the end of the Mesozoic, the amalgamation of Siberia and North China was completed (Zheng *et al.*, 1991).

The cenozoic era was controlled by the alpidian orogeny when the Indian and Japanese plates collided with Siberia and led to the uplift of the Mongolian plateau. No sediments were deposited, but most of the materials in the Erlian basin were eroded. Only few sediments of the Pliocene were conserved in the area (N2). Since the Neogene, volcanism occurred mainly along old craton boundaries and marked the reactivation following an upwelling plume (Ren *et al.*, 2002). Three episodes of eruption south and west of Xilinhot between Pliocene and Pleistocene (Ren *et al.*, 2002; Zheng *et al.*, 2002; Wang *et al.*, 2003) were the product of these reactivation of

old craton boundaries. Wang and Mo (1995) assume these volcanos to denote continental rifting with a low spreading rate. In the southwest of the Xilingol basaltic lavae were extruded in the early Pleistocene ($\beta 1$). Further remnants of the ice ages are present as coarse sediments in the north and south of the experimental area (Q3, Qp and Q4d+pl).

Quaternary sand lands are ascribed to deposition of long-distance transported aeolian materials from deserts and sandy lands lying further north and northwest by winds (Q4eol; Li *et al.*, 1990; Wang *et al.*, 2001a; cited in:). Alternatively, in situ accumulation of loose lacustrine sediment particles exposed and reworked locally by aeolian activities after the lakes diminished or desiccated may also be the cause of its formation (Q4al+l; Yang & Song, 1992; cited in:; Wang *et al.*, 2004b). Yang *et al.* (2004) assume the present sandy lands to originate as mobile dunes of the last glacial.

2.1.2 Climate and Hydrology

The study area is situated at the northwestern limit of the Pacific monsoon, where the climate changes from semihumid to semiarid (Wang *et al.*, 2004b). The climate was classified as a dry and cold middle latitude steppe climate or BSk following the classification of Köppen and Geiger (Figure 4). This climate evolved during the Holocene and Liu *et al.* (2002) distinguished four stages for the Dali Nor area: cold and humid during early Holocene (about 10,000-8,000 ^{14}C yr B.P.), warm and humid between 8,000 and 5,900 B.P., followed by a warm and dry stage between 5,900 and 2,900 B.P. and cool and dry during the late Holocene (2,900 ^{14}C yr B.P. to the present). Following their results, aeolian activities and desertification began around 5,900 ^{14}C yr B.P. with the weakening of the summer monsoon and increasing winter temperatures (Liu *et al.*, 2002).

Between 1982 and 2003, mean annual temperature at IMGERS was slightly above zero (0.7 ± 0.9 °C), with January as the coldest (mean -21 ± 4 °C) and July as the warmest month (mean 19 ± 2 °C). The frost-free period lasts from 120 to 140 days (Jianguo & Loucks, 1992). The mean annual precipitation at IMGERS was 343.4 ± 65.8 mm between 1982 and 2003. 66% of the annual precipitation fell between June and August, which is in good accordance to Chen (1988) who reported 60-80% of the annual precipitation in the same period. During this annual maximum,

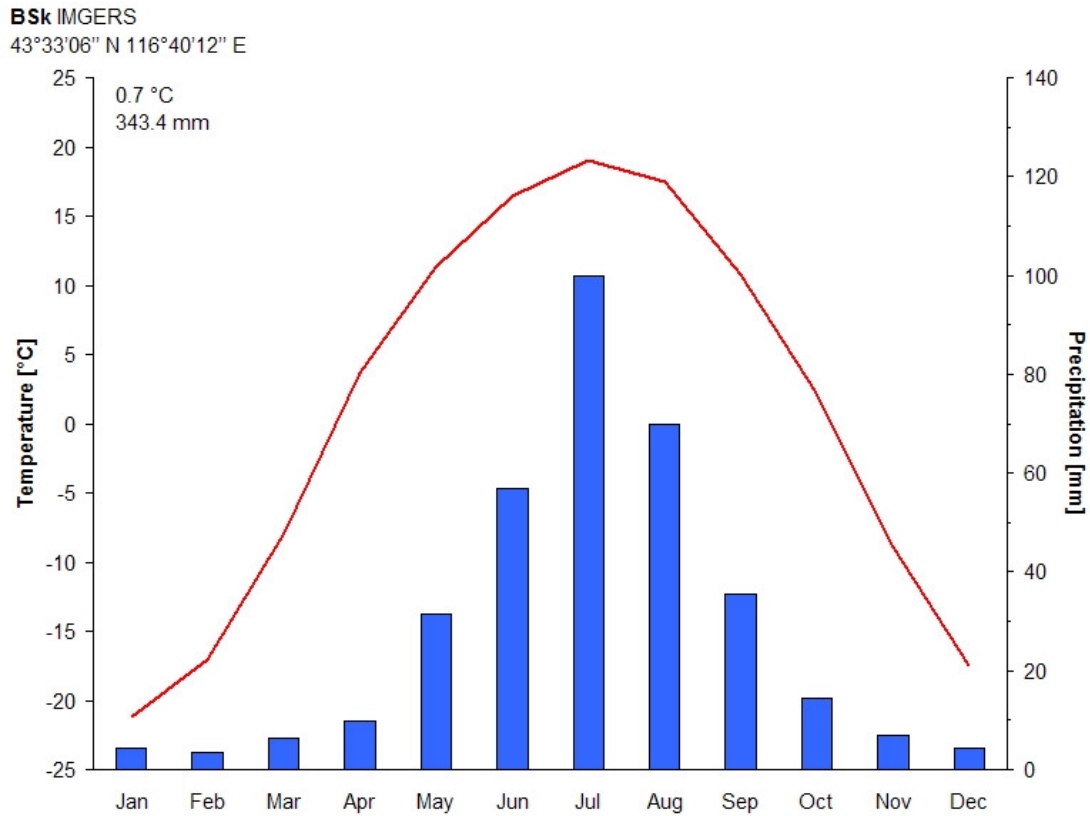


Figure 4: Climate at IMGERS (calculated using the monthly means of the years 1982-2003).

precipitation mainly falls from local convective clouds, showing large spatial heterogeneities (Figure 5). These single events were temporally and spatially restrained and delivered large proportions of the annual precipitation. Up to 61 mm were measured during single events (11.08.2004), which resulted in the formation and expansion of gullies (Figure 5). Beside the spatial heterogeneities, large annual fluctuations of annual precipitation occur as a consequence of the varying distances



Figure 5: Pictures of local precipitation event and gully erosion.

of the northwestern movement of the southeastern monsoon cyclones. Xiao *et al.* (Xiao *et al.*, 1995) found coefficients of variation of approximately 50% for the summer months (Figure 6). The potential annual evaporation (~1,700 mm) highly exceeds the annual precipitation (180–500 mm) (Liang *et al.*, 2003). Annual fluctuations of precipitation were intensified by the spatial heterogeneous accumulation of snow. Areas with higher groundcover accumulated more snow than bare soil (Holst *et al.*, 2008).

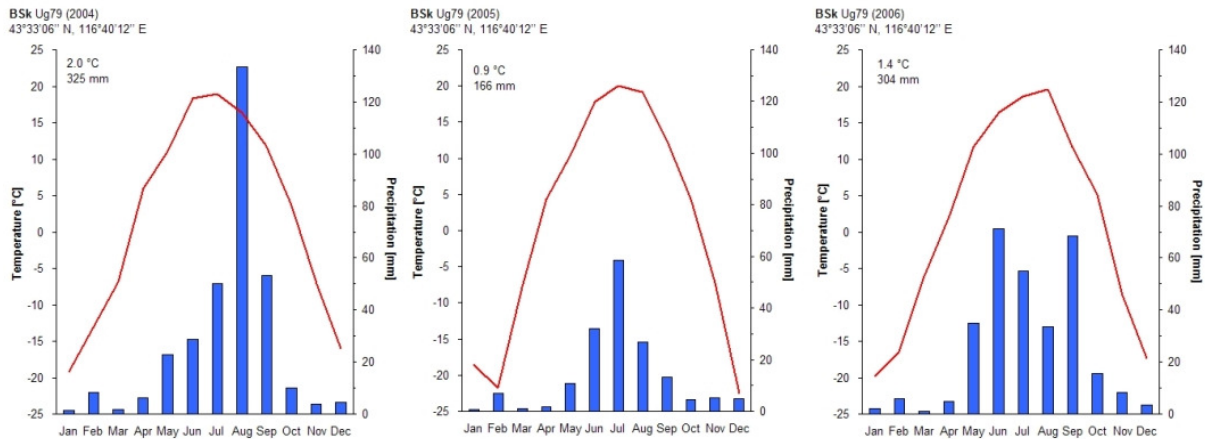


Figure 6: Climate at the experimental sites between 2004 and 2006 (data provided by Bettina Ketzler).

Between 2004 and 2006, main wind direction was west to northwest (Hoffmann *et al.*, 2007). Cold and dry NW winds in winter and more humid SE winds in summer are a result of the seasonal change between the brumal Mongolian anticyclone and the summer thermal depression over Central Asia (Ripley, 1992; Zhu, 1993). After the cold and dry winter numerous strong storms result from high air pressure



Figure 7: Pictures of a dust devil and a dust storm (Pictures taken by Carsten Hoffmann).

gradients between the Siberian mainland and East Asia (Hoffmann *et al.*, 2008). Especially in spring between March and May local (dust devils), regional and supra-regional dust storms occur frequently (Figure 7). During these events dust emission as well as accumulation occurs. Source areas are the drylands in the West and Northwest, which are up to several hundreds kilometers apart from the experimental site (Hoffmann *et al.*, 2008).

MAGIM's study area in the Xilin river catchment comprises an area of 3,650 km² with an elevation between 900 m and 1,400 m a.s.l. (Liang *et al.*, 2003). The river itself has its source at the western spurs of the Greater Chingan. From its source, the endorheic river flows approximately 80 km in western direction, turns to the northwest and drains away north of Xilinhot. Mean annual discharge was measured near IMGERS between 2004 and 2006 and was below 1 m³ s⁻¹ (Figure 8). Peak discharge was measured between April and May and was attributed to snowmelt and thawing of the ice along the banks of the Xilin River. Summer precipitation had no significant impact on the discharge.

**Mean discharge Xilin River
(1957-2004)**

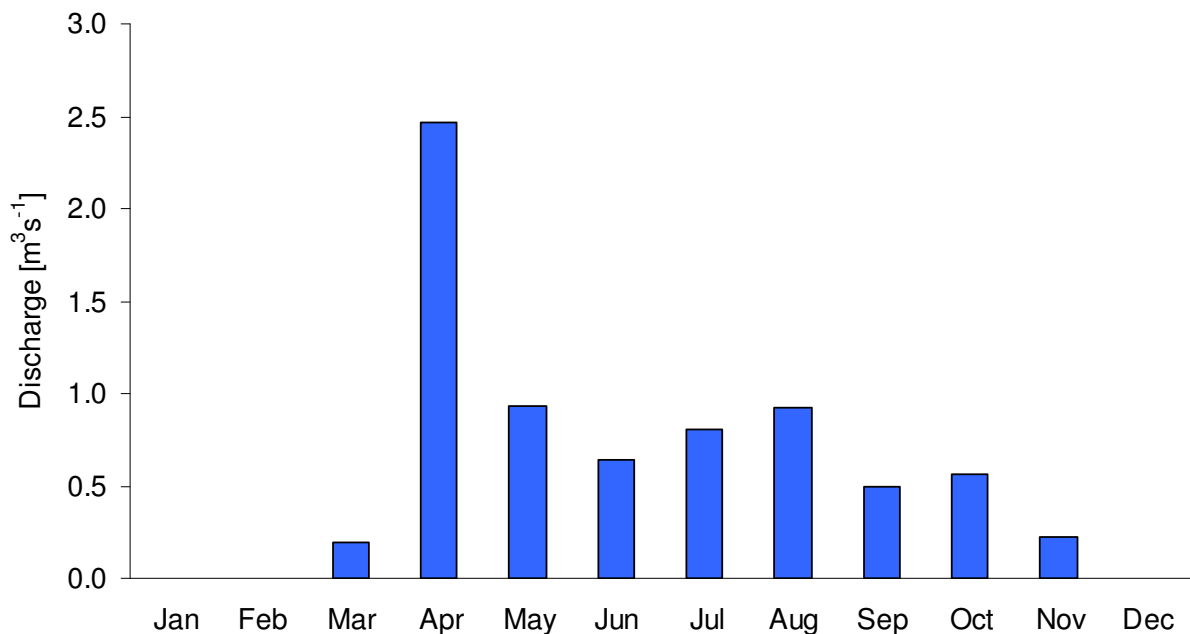


Figure 8: Mean discharge of the Xilin River (data provided by Katrin Schneider).

2.1.3 Geomorphology

The study area is located on the high-standing Mongolian plateau in a diverse geological setting. The complete Xilin river catchment covers about 10,700 km² in area and the landforms in the basin can be divided into several types: lava tablelands, low mountains, hills, high plateaus, and sandy lands (Figure 9). Large areas of lava tablelands exist in the southern part of the basin, whereas low mountains, hills and high plateaus are found in the middle and lower reaches of the



Figure 9: Typical landforms in the experimental area

Xilin River in the northern part of the basin. Between the two regions there are stretches of sandy lands. (Tong *et al.*, 2004). MAGIM's study area (Figure 2) is situated in the southern part of the catchment and comprises an area of 3,650 km² with an elevation between 900 m in the lower reaches of the Xilin river in the northwest and 1,400 m a.s.l. atop the Daxinganling Mountains in the east (Liang *et al.*, 2003). Most noticeable in this area are high-standing, plain plateaus of basaltic lava and volcanic domes of different magmatic origin. Weathering processes of these prominent landforms together with wind erosion and deposition of windblown materials produced a gently rolling landscape. North of IMGERS a branch of the Hunshandake sandy land is situated. During strong, single precipitation events surface flow leads to gully erosion (Figure 5).

2.1.4 Vegetation

The study area is part of the Central Asian subregion of the temperate Eurasian steppe belt (Lavrenko & Karamysheva, 1993), located where the temperate broad-leaved forest is gradually replaced by the typical steppe (Wang *et al.*, 2004b). The current vegetation established in middle Holocene as a consequence of the weakening of the summer monsoon (Figure 10). Plant-available water, as consequence of generally low and annually and spatially highly fluctuating precipitation in combination with a generally high evapotranspiration, is the most limiting factor of plant growth in steppe ecosystems. Additional factors limiting the performance of vegetation are the short growing season of approximately 150 days, a short frost-free period of less than 150 days and generally low mean monthly temperatures between October and March. Growing season in the Xilin River basin starts at early April, reaches peak biomass around mid of august and ends at late September for perennial plant species, whereas annual plant species usually germinate in early July following the main precipitation events (Bai *et al.*, 2004); Figure 4). They concluded that January-July precipitation is the primary climatic factor causing large fluctuations in annual biomass production.

The vegetation of the Xilin River catchment is classified as a *Stipa grandis* and *Leymus chinensis* dominated grass steppe (Giese, 2007). The predominant species are the perennial rhizome grass *Leymus chinensis*, dominating

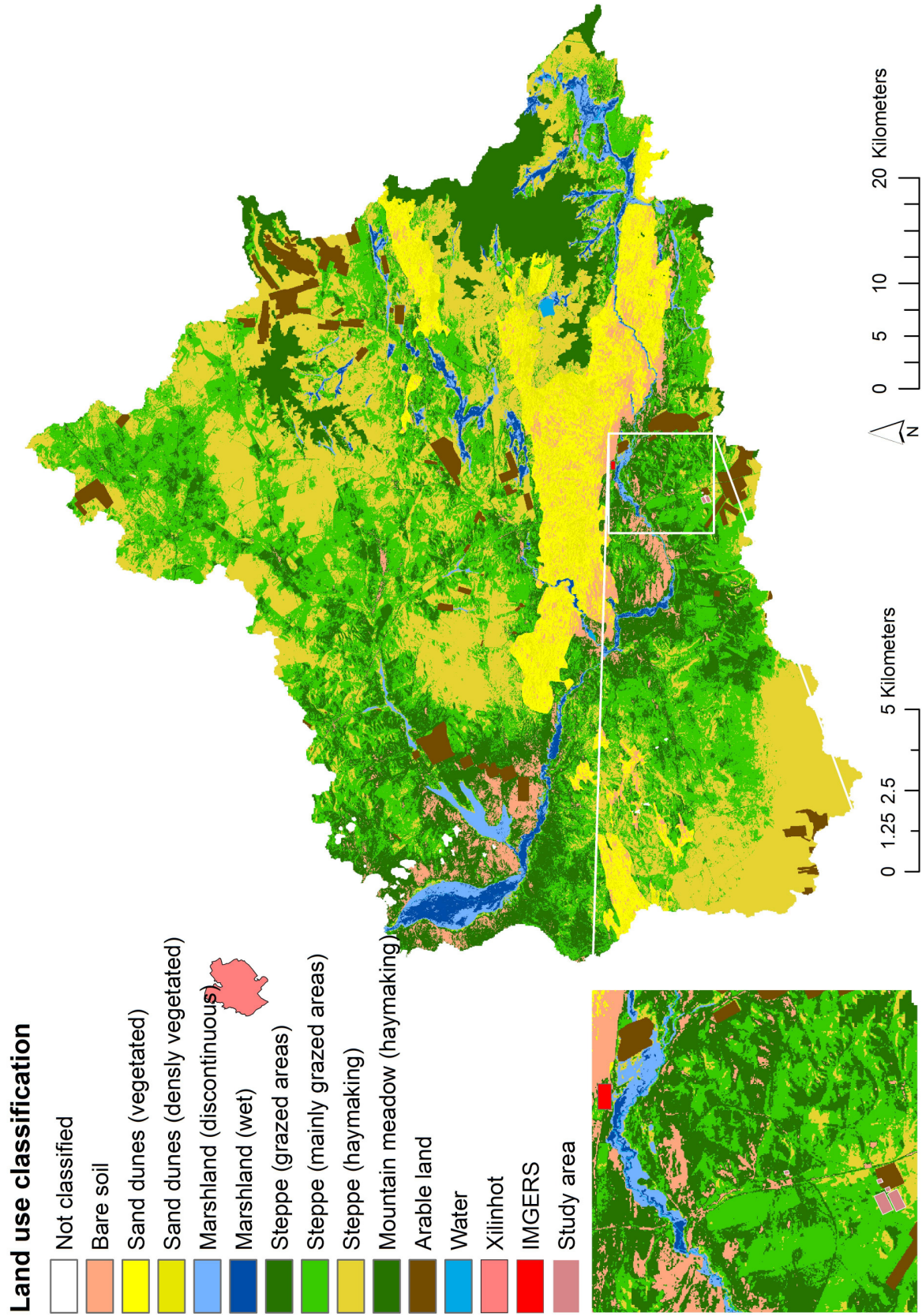


Figure 10: Land use classification of the experimental area (map compiled by Lia Fan).

in areas with a relatively higher water availability and the perennial bunchgrass *Stipa grandis* in drier areas. Most of the species are perennials with their persistent organs directly at the soil surface (*Hemicryptophytes*) or well protected within the topsoil (*Cryptophytes*). A few exceptions are semi-shrubs as *Caragana microphylla* and dwarf-shrubs (*Chameaphytes*), mainly represented by *Artemisia* species. Annual species are minor within the plant community, but opportunistically some (mainly *Chenopodiaceae*) can appear widespread if growing conditions are favourable. Beside the shrubs, the aboveground parts of the vegetation die at the end of the growing season in August and September. The average vegetation ground cover depends on the soil conditions and topographical position in general, but is highly variable due to precipitation amount and distribution and land-use. At peak biomass time in 2004 (mid of August) plant cover at the experimental sites was between 77% and 60% (green parts). The total aboveground biomass increased with decreasing grazing intensity (Table 13). Impact of grazing on the heavily grazed site is indicated by a shift in vegetation composition towards herbaceous species such as *Artemisia frigida* and *Potentilla acaulis* (Giese, personal communication). Tong *et al.* (2004) reported that herbaceous species, such as *Artemisia frigida*, *Cleistogenes squarrosa* and *Potentilla acaulis* are indicators for overgrazing. The plant composition in each treatment was homogenous, except for Ug79. Here, the vegetation was patchier with a mix of *Stipa grandis*, *Leymus chinensis* and *Caragana microphylla* bushes. When litter material was considered, Hg had the lowest and Ug79 the highest soil cover. Hg was the only treatment where bare soil was visible, while the soil of all other treatments was covered by vegetation or litter material.

Regarding plant productivity, these semiarid grasslands are less productive ecosystems when compared to other pastures throughout the world. Ug79 showed the highest aboveground net primary productivity (ANPP) in 2004 with approximately 200 g dry matter m⁻²a⁻¹ (Giese, 2007). However, above ground biomass varies greatly between years caused by variations in annual precipitation. European pastures produce up to 2000 g dry matter m⁻²a⁻¹ and North American long grass steppes are taken as the most productive natural semiarid grasslands with ANPP of 700 g dry matter m⁻²a⁻¹. But it is also notable, that North American short grass steppes showed clearly lower ANPP of 100 g dry matter m⁻²a⁻¹ (Giese, 2007). Nevertheless many authors showed that in semi-arid grasslands belowground

productivity weight out the aboveground productivity by far (Milchunas & Lauenroth, 2001). The belowground net primary productivity (BNPP) is much more difficult to measure and reliable data from semiarid ecosystems is rare. Estimates reach up to more than 90% of carbon that is allocated to belowground plant organs. Gao (2007) estimated a belowground allocation for carbon in the studied area of approximately 60%.

2.1.5 Soils

Aeolian sediments in semiarid climates, covered by grassland vegetation form typical steppe soils, all characterised by a mollic horizon. This diagnostic horizon of the WRB (IUSS Working Group WRB, 2006) is defined as a well-structured, dark-coloured surface horizon with a high base saturation and a moderate to high content of organic matter. Typical soil types of steppe ecosystems are Phaeozems, Chernozems and Kastanozems, ordered with decreasing precipitation and soil water content.

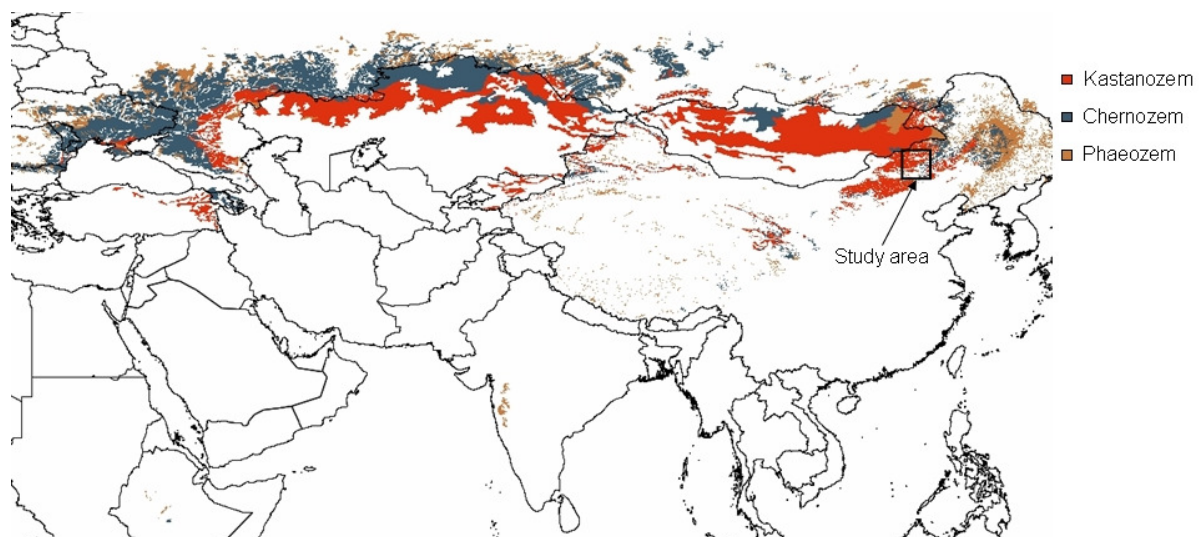


Figure 11: Distribution of Kastanozems, Chernozems and Phaeozems in Eurasia.

Phaeozems (*phaios*, greek: dusky; *zemlja*, russian: earth or land) are the soils of the wetter grasslands (predominately tall-grass steppe) and forest regions (Figure 11). The moderate continental climate is humid enough that there is, in most years, some percolation through the soil, but also with periods in which the soil dries out. Phaeozems are characterised by dark and humus-rich surface horizons. As a consequence of the higher precipitation and water content, these soils are leached

more intensively leading to lower base saturation and may not have secondary carbonates.

Chernozem (*chernij*, russian: black; *zemlja*, russian: earth or land) is the typical soil type in the drier climate, south of the Phaeozems (Figure 11). The tall-grass steppe regions are characterised by a continental climate with cold winters and hot summers, which are dry at least in the late summer. Chernozems show a thick black surface layer that is rich in organic matter and secondary carbonates in the subsoil.

Kastanozems (*kashtan*, russian, *castanea*, latin: chestnut; *zemlja*, russian: earth or land) are typical for dry grasslands and short-grass steppes south of the Eurasian tall-grass steppe belt with Chernozems (Figure 11). As a consequence of the dry climate, the profile of Kastanozems has a thinner humus-rich surface horizon, which is not as dark as Chernozems. Less percolation leads to a more prominent accumulation of secondary carbonates and in some cases also secondary gypsum in Kastanozems.

2.1.6 Human history

Located in the middle of central asia, the Mongolian plateau has been home to many tribes mainly living of extensive nomadic pastoralism and livestock breeding (Neupert, 1999). In the 4th century, Chinese historians describe the tribes of the Xianbei and the Kitan to live in the northeastern areas as nomads travelling with herds of camels, cattle, horses, sheep and goats (Priewe, 2007). This traditional nomadic live form was adapted to the limited availability of natural resources. It was sustainable due to small livestock densities and the permanent movement of the herds around large areas. Hay making did not play a significant role and the grazing stress on the grazed pastures was low. This Mongolian way of life was normal until 1911 when during the Chinese revolution the northern part claimed independence, which was ultimately attained in 1921, and the southern part, including the studied areas, became part of China. Starting from this time, many Han farmers migrated to the extensively populated areas. In contrast to the nomadic life of the Mongolians, the Han lived in villages and introduced a completely sedentary agriculture and pasture system with public or collective land. Not only the way of steppe management changed, but also the number of inhabitants increased significantly. In 1947 the area became the Inner Mongolia Autonomous Region. When Mao Tse-tung

became the leader of the Peoples Republic of China in 1949, the government even stimulated the migration of Han farmers to the region. During the Great Leap Forward (1958-1960), the policy was to expand the cultivation of the grassland and Mongolian nomadic herders were sedentarised (Gernet, 1997) as nomadism was considered a backward activity (Neupert, 1999); Figure 12. The consequence was that only the areas close to the settlements were used for grazing and the remote areas were used for hay making. Thus, the grazing stress on the grazed areas increased, whereas no nutrient recycling occurred in the hay areas. Another important factor was that the grasslands were public or collective land and therefore a free and uncontrolled resource. No attempts of local and central government were made to equate the intensification by technological inputs, e.g. additional nutritional inputs, establishment of artificial pastures with improved pasture species or enforce scientifically estimated stocking levels. Additionally, the number of animals in Inner Mongolia nearly tripled between 1952 and 1988, from 26 million to more than 72 million (Neupert, 1999). Economic reforms in the early 1980s amplified this increase. In particular the



Figure 12: Pictures of living conditions in Inner Mongolia. Typical farm house with a sheep pen (left picture). The heavily grazed site is located directly in front of the farm. Sheep and goats on the way to the pasture (right picture).

“household responsibility” system, transferring animals from collectives to private households. This was followed by the “double responsibility”, which not only distributed animals to individual households but also leased the land. In exchange, the herders are required to sell at fixed prices to the state live animals and animal products in quantities stipulated in the contracts that give them control over these assets. After providing to the state the contracted quotas, herders are free to sell

surplus meat and animal products on the open market (Gernet, 1997; Neupert, 1999). This situation greatly stimulated herdsmen once more to increase animal numbers. Additionally, the government remains the owner of the land, but the farmers are free to decide how it is used. The negotiations between farmers and the local governments are only valid for a few years. This means in practice that the farmer strives for a short term maximal economic output. The long term view, which would require a sustainable use of the grassland, is not the main interest of the farmers, because they are not certain to keep the land for more than a few years. In the course of this development, the average Inner Mongolian grassland area per sheep unit decreased from 5 hectares in the late 1950s to less than 1 hectare at the end of the last century. The strong increase in livestock numbers within the last decades resulted in vast degraded areas (Tong *et al.*, 2004), which mainly can be found in plains around hamlets and villages (Holst *et al.*, 2007).

Corresponding to large parts of the Inner Mongolian steppe the Xilin River Basins has severe ecological problems caused by overgrazing. According to Kawamura *et al.* (2005) livestock number of the Bainyinxile Livestock Farm, which covers approximately 33% of the central Xilin River Basin, increased from 1950 to 2001. In December 2001 the total livestock number of the Bayinxile livestock farm was 252,700 sheep units. Thus, the average stocking rate was 0.76 sheep units per ha, including mowing land. Tong *et al.* (2004) examined the steppe degradation in the Xilin River basin and showed that the total area of degraded steppe increased from 7191 km² in 1985 to 7689 km² in 1999, which means 67% and 72% of the total basin, respectively.

2.2 Plot description and sampling design

The whole area is grazed by herds that are composed of 70 - 90 % sheep and 10 - 30 % goats. Before 1979, the whole experimental area was grazed at low intensity. In 1979, one plot (24 ha) was fenced and excluded from grazing (Ug79). After 1979, the grazing intensity in the region increased to a moderate level. In 1999, two plots were fenced. One was completely excluded from grazing (25 ha; Ug99), the other is still grazed during winter (34 ha; winter grazing = Wg), equivalent to a grazing intensity of 0.5 sheep units ha⁻¹ yr⁻¹ (1 sheep unit = 1 ewe and 1 lamb). Plot 4 (24 ha) is grazed during the whole year, with the highest intensity during summer

(continuously grazed = Cg), equivalent to a grazing intensity of 1.2 sheep units $\text{ha}^{-1} \text{yr}^{-1}$. The heavily grazed plot has been grazed every day for the past 30 years (100 ha; heavily grazed = Hg), representing a grazing intensity of 2.0 sheep units $\text{ha}^{-1} \text{yr}^{-1}$. During the night, herds are put into pens outside the plots, so that the input of organic material by faeces to grazed plots is reduced. There was no application of fertilisers to any of the four plots.

From June to August 2004, 650 points were sampled in five plots using regular, orthogonal grids (Figure 13 and Figure 14). On Cg and Wg, large grids (300 m to 550 m; further denominated with the index large as Cg_{large} and Wg_{large}) and on Hg, Cg, Ug99 and Ug79, small grids (105 m to 135 m) were sampled. The large grids consisted of 125 sampling points with a spacing of 50 m and the small grids contained 100 sampling points with 15 m spacing. The exact position of each point was measured with a Real Time Kinematic Differential GPS (Hoffmann *et al.*, 2007). Small-scale variability was considered through additional sampling nests with spacing of 10 m and 5 m within large and small grids. Vegetation was obtained at 550 sampling points (Ug79, Ug99, Hg, Wg_{large} and Cg_{large}) by subproject P2, using the non destructive method based on the Braun-Blanquet system (Braun-Blanquet, 1964). Vegetation cover was determined in 1 m^2 sized subplots. Aboveground biomass was harvested at peak time (August 2004) at all sampling points by cutting a 0.25 m x 0.25 m square at 1 cm height. Prior to soil sampling, vegetation cover was removed and the upper 4 cm of soil were taken in triplicate with a stainless steel cylinder (100 cm^3) and bulked to obtain a composite sample at each of 650 points. Thickness of the Ah horizon (Ah thickness) was determined with a soil auger at every other sampling position and when topography changed at every position (387 points).

Ug79, Ug99, Cg and Hg are flat areas with no particular topography (Figure 13). The maximum vertical difference in the small plots is below 10 m. In contrast, Cg_{large} and Wg_{large} showed significant topographic features and vertical differences with more than 20 m. Cg_{large} is divided into three topographic areas - a backslope and summit in the eastern and a flat area with a longish depression in the western part. Wg_{large} is characterised by three mounds and small depressions between the mounds.

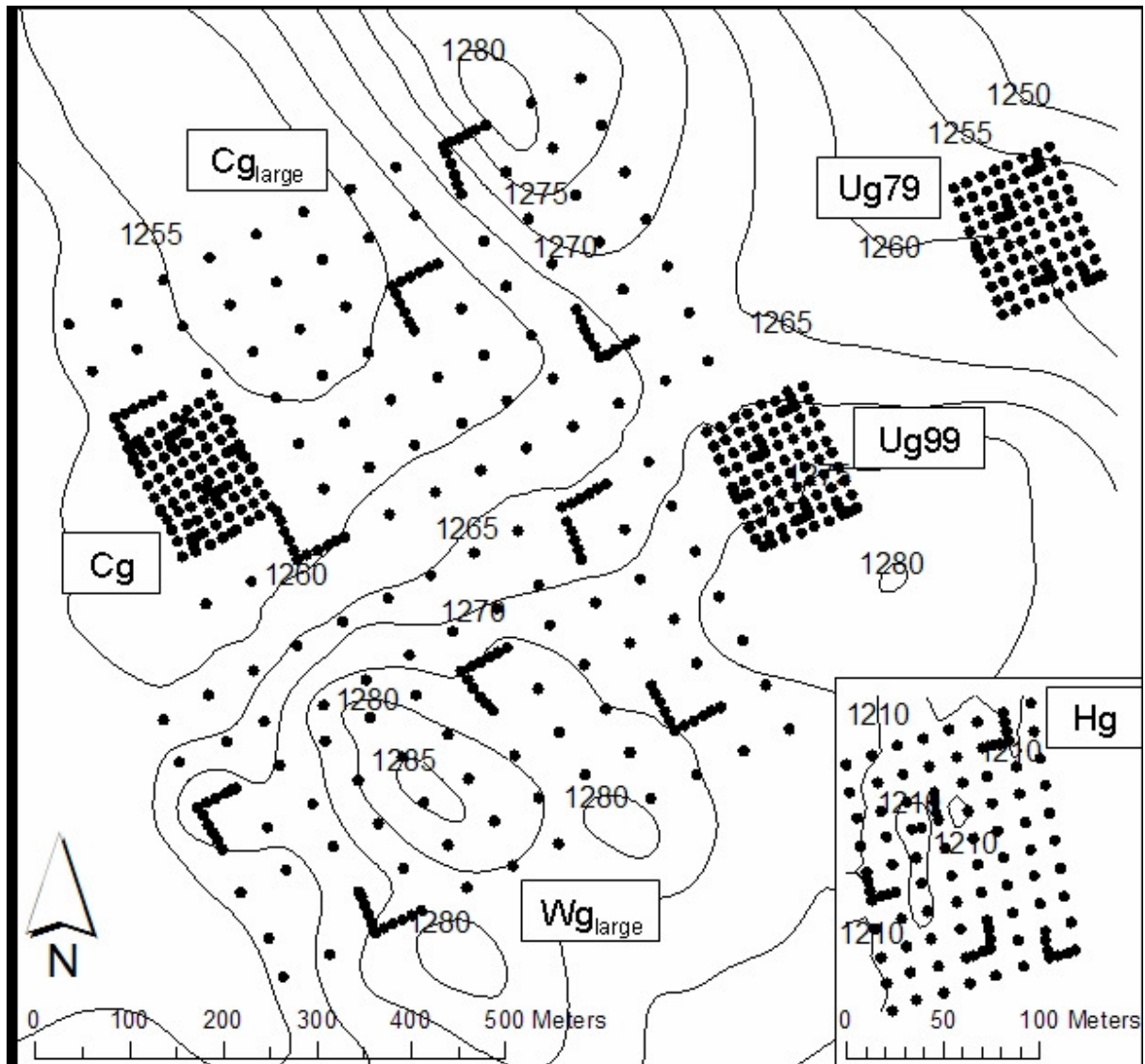


Figure 13: Digital elevation model of the experimental sites and sampling grids.

Three representative soil pits were sampled on each of the five plots to characterise the soils. In each plot the upper 10 cm of one pit were taken as mixed samples. One representative soil pit was selected in each plot based on extensive statistical and geostatistical analyses (Steffens *et al.*, 2008; Steffens *et al.*, 2009a). Three horizons were sampled as mixed samples in each of the soil pits - upper 10 cm, from 10 cm to carbonate boundary and from carbonate boundary to the parent material (Chapter 3).



Figure 14: Location of the experimental plots (Ug79 = ungrazed since 1979, Ug99 = ungrazed since 1999, Wg = wintergrazing, Cg = continuously grazed, Hg = heavily grazed). Pictures were taken from the top of a volcano with the upper picture facing ESE and the lower picture facing NNE.

2.3 Plot samples

2.3.1 Determination of bulk density, OC, total N and total S concentrations, pH and $\delta^{13}\text{C}$

Each soil sample was analysed for bulk density, total C, total N, total S concentration and pH (650 points). Bulk density of the soil was calculated with the mass of the oven-dry soil (105° C) divided by the core volume (Hartge & Horn, 1992). Prior to chemical analyses, samples were sieved to <2 mm. Total C, total N and total S concentrations were determined in duplicate by dry combustion on a Vario Max CNS elemental analyser (Elementar Analysensysteme GmbH, Hanau). All samples were free of carbonate so that the total C concentration equalled the organic carbon (OC) concentration. Soil pH was determined in a 1:2.5 soil to 0.01 M CaCl₂ solution. $\delta^{13}\text{C}$ was analysed for 245 points in $W_{\text{g}_{\text{large}}}$ and $C_{\text{g}_{\text{large}}}$ with a Carlo-Erba 1108 elemental analyser coupled via a Conflo II Interface to a Finnigan Delta C mass spectrometer (Thermo-Finnigan, Bremen).

2.3.2 Stock calculations

OC, total N, and total S stocks [kg m^{-2}] of the upper four centimetres were calculated using elemental concentration and bulk density (Eq. 1), referred to as the “conventional stock calculation” below.

$$ES = BD \times EC \times a \times 10^{-6} \quad (1)$$

ES = Elemental stock [kg m^{-2}]

BD = Bulk density [g cm^{-3}]

EC = Elemental concentration [mg g^{-1}]

a = Area multiplier (4 cm depth \times 10,000 $\text{cm}^2 = 40,000 \text{ cm}^3 \text{ m}^{-2}$)

Grazing may significantly influence bulk densities and consequently affect the stock calculations. Therefore, stocks were calculated using a normalised soil mass (Eq. 2) as described by Ellert and Bettany (1995) and Veldkamp (1994). This is

referred to as the “equivalent stock calculation” below and yields OC*, total N* and total S* stocks.

$$ES^* = EM \times EC \times 10^{-3} \quad (2)$$

ES^* = Elemental stock [kg m⁻²]

EM = Equivalent mass (37.7033 kg m⁻²)

EC = Elemental concentration [g kg⁻¹]

Plot Ug79 was used as a reference. Hence, the mean soil mass of one square metre down to a depth of four centimetres was calculated for Ug79 and used as normalised mass (37.7033 kg m⁻²). This mass equals a sampling depth of 3.47 cm on Ug99, 3.45 cm on Wg, 3.23 cm on Cg, and 2.98 cm on Hg.

2.3.3 Statistical analyses

All statistical analyses were conducted using SPSS 13.0.1 for Windows (SPSS Inc., Chicago). All data sets were described by ordinary statistics including mean, median, mode, standard deviation, skewness, kurtosis, variance and coefficient of variation. In all exploratory statistics, a critical significance level of $p = 0.01$ was used. Normal distribution and homogeneity of variances for each collective were tested using the Kolmogoroff-Smirnoff test and the Levené test. The effect of grazing intensity on analysed parameters for normally distributed collectives was tested with a one-way analysis of variance (ANOVA). Tukey and Scheffé and least significant difference (LSD) tests were used as post hoc tests with increasing conservativeness. When the assumption of equal variances was violated, the Tanham test was used. Correlations among different analysed parameters for normally distributed data sets were tested using Pearson’s correlation coefficient. For non-normal distributed data sets, the effect of the stocking rate was analysed with the nonparametric Kruskal-Wallis test. As a post hoc test, the Wilcoxon-Mann-Whitney U-test with the Shaffer-correction was calculated to compare all possible combinations. The nonparametric Spearman-Rho was used for non-normally distributed collectives to test correlations among the analysed parameters.

The minimum detectable difference (MDD) gives the smallest difference between means that is detectable with a given number of samples (Zar, 1999). MDD is a parametric quantity and can only be used for normally distributed data sets. The MDD was calculated for all suitable data collectives, dealing with bulk density, elemental concentrations and elemental stocks using (Eq. 3). A statistical power of 0.90 and a significance level of 0.01 were used. In 90 % of the trials, a difference between two sample collectives will be detected with a significance level of 99 %.

$$MDD = \sqrt{\frac{s^2}{n}} (t_{\alpha,v} + t_{\beta(1),v}) \quad (3)$$

MDD = Minimum detectable difference

s^2 = variance

n = number of samples

$t_{\alpha,v}$ = significance level, critical value of the t-distribution

$t_{\beta(1),v}$ = statistical power (1- β), critical value of the t-distribution

To compare MDD for different plots, the relative MDD was calculated (Eq. 4). Therefore, the MDD of each plot was standardised using the mean of the analysed parameter in each plot.

$$MDD_{rel.} = \frac{MDD}{\bar{x}} \times 100 \% \quad (4)$$

$MDD_{rel.}$ = relative minimum detectable difference

MDD = Minimum detectable difference

\bar{x} = Mean of analysed variable and plot

2.3.4 Geostatistical analyses

Statistical analyses were carried out using SPSS 14.0 (SPSS Inc., Chicago) and geostatistical analyses using R 2.0.1 (RDevelopmentCoreTeam, 2004) in combination with the g-stat 2.4.0 package (Pebesma, 2004). Prior to geostatistical analysis, each parameter in each plot was tested for normal distribution using the Kolmogoroff-Smirnoff test. The spatial behaviour of all properties was analysed using experimental variograms. These tools are based on the theory of regionalised variables and describe the degree of spatial variability of a parameter by analysing changes in space as a function of distance between sampling points (Webster & Oliver, 2001). Equation 5 gives the calculation of the semivariance which describes the average change of a given parameter at a distinct distance for all possible paired points:

$$\gamma(h) = \frac{1}{2N(h)} \sum_{i=1}^{N(h)} [A_i(x_i) - A_i(x_i + h)]^2 \quad (5)$$

$\gamma(h)$ = semivariance for lag vector h

$N(h)$ = number of pairs of data points separated by lag vector h

$A_i(x_i)$ and $A_i(x_i+h)$ = actual values of the measured parameter A at the certain positions (x_i) separated by h

All possible distances in one diagram produce an experimental variogram of a given parameter (Figure 15). All experimental variograms were calculated for a maximum distance (lag vector) of 100 m for the small grids and 550 m for the large grids, corresponding to at least 100 point pairs. But all distances with more than 50 point pairs were considered for visual control, corresponding to 150 m in the small grids and 650 m in the large grids. Distances between sampling points were grouped into distance classes which cover 5 m in small grids and 10 m in large grids. Each parameter in each plot was tested for anisotropy and trends using directional variograms before calculating omnidirectional variograms. Experimental variograms can be described with variogram models, generally based on three parameters - nugget, sill and range. Most variograms start with a y-offset, which is called nugget

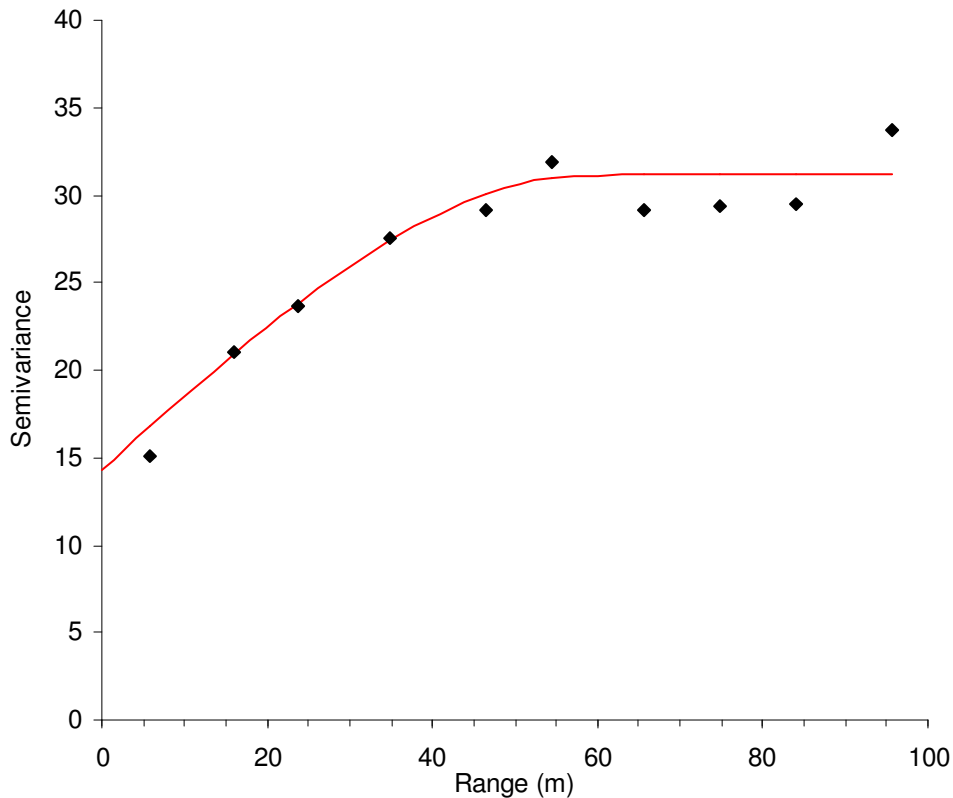


Figure 15: Experimental variogram with fitted variogram model

and gives the variation of the analysed parameter at distances smaller than the shortest considered distance. This variability results from small-scale variability and measuring uncertainties. The maximum value that is reached by the experimental variogram is referred to as sill variance. For stationary variables, this value usually equals the statistical variance of the whole plot. The range gives the distance where the experimental variogram reaches the sill and defines the distance of spatial dependencies for this specific parameter in this plot. An appropriate model variogram was fitted to each experimental variogram using the gstat fitting routine (Pebesma & Wesseling, 1998), based on the reweighted least squares estimation of variogram model parameters (Cressie, 1985). Five different weighting methods were compared and the one with the best fit, decided by the parameter sum of squared errors and by visual control, was used. The relative percental contribution of nugget to total variance (nugget+sill) was calculated (referred to as $Nu/Nu+Si$ below) as an indicator for spatial distribution. Low ratios point towards a low relative nugget effect and lead to the assumption of a stronger spatial dependency and a more homogeneous distribution of the analysed parameter in space for the tested sampling distance. Large values indicate that a large portion of the variance takes place at small scales.

This shows a more heterogeneous, patchy distribution and leads to the assumption that small-scale processes control the spatial distribution of this parameter.

To simplify the analysis, the properties of each plot showing comparable range values were merged in two conceptual groups (topsoil and vegetation parameters). Two groups were used for the small grids (Group 1: bulk density, OC, total N and total S concentration; Group 2: vegetation cover and aboveground biomass). In the large grids, the additional parameters pH and Ah thickness showed clearly different range values than the other topsoil parameters and were merged in a third group (Group I: bulk density, OC, total N, total S concentration and $\delta^{13}\text{C}$; Group II: vegetation cover and aboveground biomass; Group III: pH and Ah thickness). For each plot and each group mean values and standard deviations of $\text{Nu}/\text{Nu}+\text{Si}$ and range values were calculated (e.g. mean range of Group 1 in Ug79 is the sum of the four ranges of bulk density, OC, total N and total S divided by four).

Multivariate geostatistics analyses analyse spatial correlations of two or more variables. The spatial correspondence of two or more properties in space is described using experimental crossvariograms (Wackernagel, 1998). Experimental crossvariograms are calculated using Equation 6 and are described by the same properties as variograms:

$$\Gamma(h) = \frac{1}{2N(h)} \sum_{i=1}^{N(h)} [A_i(x_i) - A_i(x_i + h)] \times [(B_i(x_i) - B_i(x_i + h))] \quad (6)$$

$\Gamma(h)$ = crossvariance for lag vector h

$N(h)$ = number of pairs of data points separated by lag vector h

$A_i(x_i)$ and $A_i(x_i+h)$ = actual values of measured parameter A at certain positions (x_i) separated by h

$B_i(x_i)$ and $B_i(x_i+h)$ = actual values of measured parameter B at certain positions (x_i) separated by h

For properties that are positively related in space, positive crossvariances are calculated that increase with increasing distance between the sampling points. Negative crossvariance values are found if variables are inversely related in space.

While for semivariograms the semivariance can be taken as an indicator for the dimension of difference between the values in space, cross variograms do not supply this information.

2.4 Pit samples

2.4.1 Physical fractionation

The air-dried soil (see 2.2) was dry sieved gently by hand to three aggregate size classes (ASC): 2000-6300 μm , 630-2000 μm and <630 μm (referred to as coarse ASC = cASC, medium ASC = mASC and fine ASC = fASC). Aggregate size distribution was similar between all four plots (Table 1). It is assumed that physical effects such as soil compaction or destruction of aggregates by trampling by grazing sheep are of minor importance when sampling the upper 10 cm. These effects will be amplified when shallower layers are the focus of research.

Table 1: Characteristics of the three aggregate size classes in the topsoils (cASC = 2000-6300 μm , mASC = 630-2000 μm , fASC = <630 μm ; Cg = continuously grazed, Wg = winter grazing, Ug99 = ungrazed since 1999, Ug79 = ungrazed since 1979) given as arithmetic means and standard deviations of three replicates.

Plot	ASC	Contribution [%]	OC [mg g^{-1}]	Total N [mg g^{-1}]	C/N
Cg	cASC	11.3 \pm 3.6	20.4 \pm 1.9	2.1 \pm 0.2	9.8
	mASC	8.5 \pm 2.0	32.1 \pm 9.0	2.8 \pm 0.5	11.4
	fASC	80.2 \pm 5.6	18.2 \pm 0.9	2.0 \pm 0.1	9.1
Wg	cASC	13.6 \pm 2.0	21.0 \pm 2.4	2.1 \pm 0.2	10.0
	mASC	10.9 \pm 0.2	27.9 \pm 5.1	2.5 \pm 0.4	11.0
	fASC	75.5 \pm 2.2	19.5 \pm 1.2	2.1 \pm 0.1	9.2
Ug99	cASC	10.4 \pm 2.3	24.7 \pm 5.6	2.3 \pm 0.4	10.6
	mASC	10.8 \pm 1.8	34.0 \pm 7.6	3.0 \pm 0.6	11.3
	fASC	78.8 \pm 4.0	24.0 \pm 4.3	2.5 \pm 0.4	9.7
Ug79	cASC	7.6 \pm 3.0	19.3 \pm 1.1	2.0 \pm 0.1	9.8
	mASC	9.5 \pm 1.5	29.8 \pm 4.3	2.6 \pm 0.2	11.6
	fASC	82.9 \pm 4.4	19.4 \pm 0.7	2.1 \pm 0.1	9.3

A physical fractionation procedure was conducted in duplicate for all three aggregate size classes (Kölbl & Kögel-Knabner, 2004; Figure 16). Briefly, the free particulate organic matter (referred to as fPOM) was separated using a Na-polytungstate solution ($\rho = 1.8 \text{ g cm}^{-3}$). To obtain the POM occluded in aggregates (referred to as oPOM), the subsequent heavy fraction ($>1.8 \text{ g cm}^{-3}$) was treated by

ultrasound. An energy input of 150 J ml^{-1} (constant energy output of 75 W , treatment times were adjusted to sample volume, approximately 10 min) was used to disrupt all macroaggregates and to obtain highest similarity of clay yields compared to standard particle size analysis, but to minimise the production of artefacts following heavy ultrasonication (Schmidt *et al.*, 1999). With a subsequent density fractionation step (Na-polytungstate solution, $\rho = 1.8 \text{ g cm}^{-3}$), the occluded POM floating on the

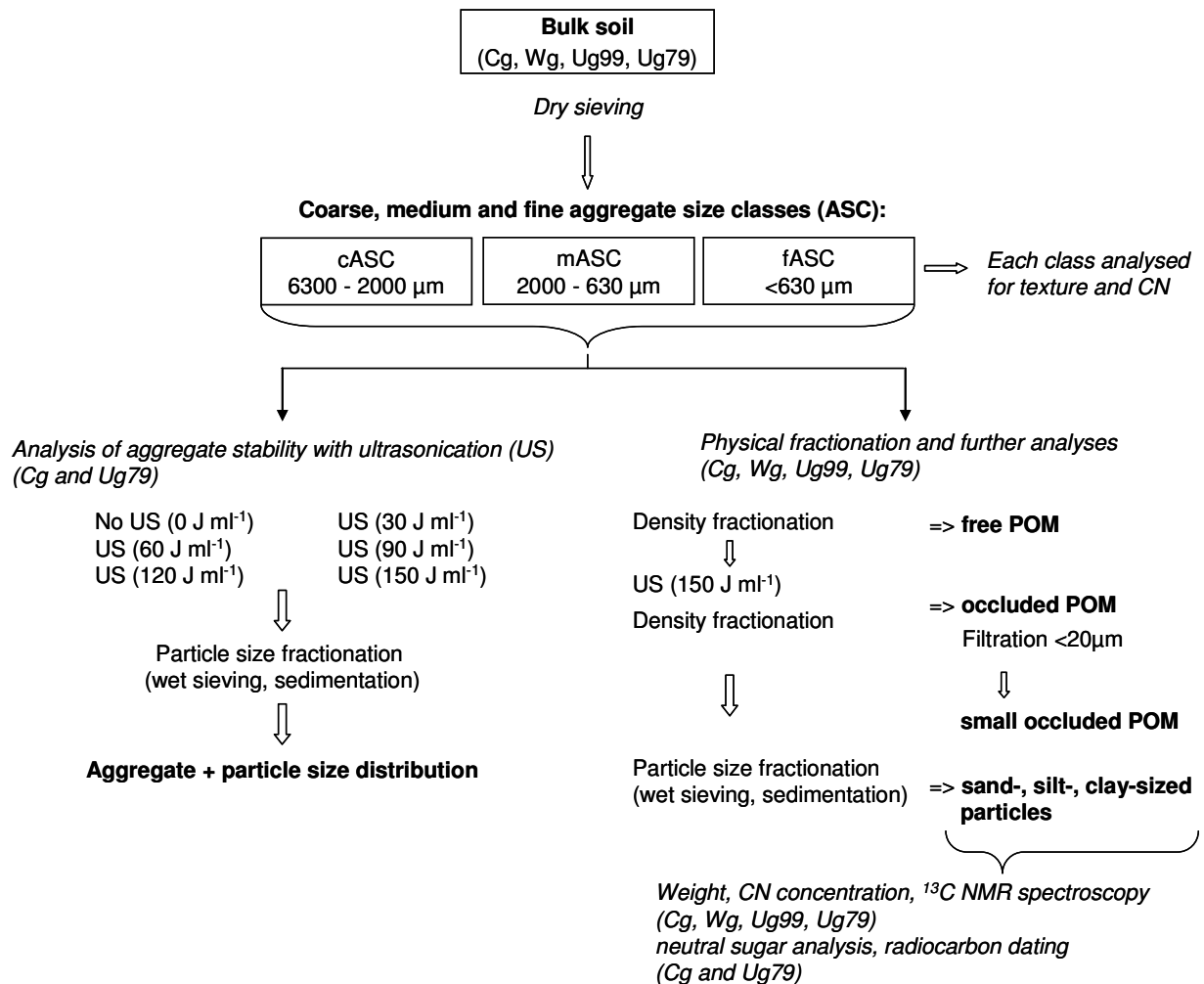


Figure 16: Schematic of conducted fractionation and measurements (Cg = continuously grazed, Wg = winter grazing, Ug99 = ungrazed since 1999, Ug79 = ungrazed since 1979).

suspension was obtained after centrifugation (10 min at $3500 \text{ rev min}^{-1}$). This fraction was sieved at $20 \mu\text{m}$ (referred to as oPOM) and the remaining solution subsequently filtered to $0.22 \mu\text{m}$ (referred to as oPOM_{small}). The residue of the density fractionation procedure - mineral particles and organo-mineral associations - was sieved at $200 \mu\text{m}$, $63 \mu\text{m}$ and $20 \mu\text{m}$ to obtain the coarse, medium and fine sand and the coarse silt fraction (cS, fS, cSi). Finer particles were separated by sedimentation into medium silt ($20\text{-}6.3 \mu\text{m}$; mSi), fine silt ($6.3\text{-}2.0 \mu\text{m}$; fSi), coarse and medium clay (0.2-

2.0 μm ; cC) and by centrifugation into fine clay (<0.2 μm ; fC). All particle size fractions were washed with bi-distilled water, freeze-dried, weighed and ground for further analyses.

2.4.2 Particle size distribution

Particle size distribution was determined after H_2O_2 treatment to remove the coagulating organic matter. The proportion of the sand fraction (63-2000 μm) and the coarse silt fraction (20-63 μm) were identified by wet sieving. The relative amounts of the medium (6.3-20 μm) and fine silt (2.0-6.3 μm) and the clay (<2 μm) fractions were measured by sedimentation with a SediGraph 5100 (Micrometrics). The SediGraph 5100 system uses particle sedimentation rates in combination with X-ray absorption for particle size analyses. This method provides a total of 90 data points (cumulative mass percentage) that enables the calculation of the grain size ranges.

2.4.3 Determination of bulk density, OC and total N concentrations and radiocarbon dating

Bulk soil material, POM and particle size fractions were analysed in duplicate for total carbon and nitrogen (N_{tot}) concentrations by dry combustion at 950 $^\circ\text{C}$ on a Vario EL elemental analyser (Elementar Analysensysteme, Hanau, Germany). All samples were free of carbonates so that the total carbon concentration was taken as the organic carbon (OC) concentration. The potential C-loading of particles <20 μm was calculated using the empirical formula of Hassink (1997) to consider differences in texture (Eq. 7).

$$C_{\text{pot}} = a + b \times \text{particles}_{<20\mu\text{m}} \quad (7)$$

C_{pot} is the potential C saturation of particles <20 μm [mg g^{-1} fraction], a and b are empirically determined constants ($a = 4.09$ and $b = 0.37$) and $\text{particles}_{<20\mu\text{m}}$ is the concentration of soil particles <20 μm [%]. The current C-saturation was calculated as the sum of the measured OC concentration of particles <20 μm .

The radiocarbon concentration was determined for bulk soil samples as well as for selected POM and particle size fractions at the Leibniz AMS lab in Kiel, Germany.

For the measurement, CO₂ was produced from solid samples by combustion at 900 °C and reduced to graphite. The measured radiocarbon concentration was corrected for isotope fractionation and is given in % modern carbon (pMC). Conventional radiocarbon ages in years before 1950 (years BP) were calculated according to Stuiver & Polach (1977).

2.4.4 Clay mineralogy and selective mineral extraction

Clay mineralogy was assessed for all horizons of Ug79 by X-ray diffraction (XRD) after Moore and Reynolds (1989). The samples were preliminary treated with hydrogen peroxide to remove organic matter (H₂O₂). XRD was performed on random powder samples and on oriented samples (Co-K α ; Philips diffractometer PW 1830) after saturation with Ca²⁺ and glycerol (room temperature) and K⁺ (room temperature and stepwise heated to 560°).

Quantity and quality of Fe and Al species were analysed on bulk soils <2 mm. Iron and aluminium from poorly crystalline Fe oxides and Al-phases were extracted with 0.2 M NH₄-oxalate (at pH3) by the method of Schwertmann (1964). Total iron oxides were estimated by the DCB-method (Mehra & Jackson, 1960). Since partial dissolution of other minerals may also take place, Fe and Al in the extracts were measured by inductively coupled plasma optical emission spectroscopy (Vista Pro CCD Simultaneous, Varian, Darmstadt).

2.4.5 Determination of neutral sugars

Selected POM and particle size fractions were analysed for seven neutral sugars (rhamnose, fucose, arabinose, xylose, manose, galactose and glucose) from non-cellulosic carbohydrates according to Spielvogel *et al.* (2007). Basically, the analysis was carried out in three steps: (1) Hydrolysis of samples with 4M trifluoroacetic acid according to Amelung *et al.* (1996), (2) acetate alditol derivatisation according to Black & Fox (1996), modified by Rumpel & Dignac (2006) and subsequent (3) GC-FID analysis of the extracted monomers. Recoveries were reduced below 30% when dealing with iron-containing samples, as the solution became viscous after the addition of ammonium. The recovery was increased by adding ethylenediamine tetraacetic acid (EDTA) as a chelating agent. The mean

recovery of the sum of neutral sugars was $77\pm 15\%$ for fPOMs, $82\pm 13\%$ for oPOMs and $93\pm 8\%$ for particle size fractions.

2.4.6 Solid-state ^{13}C NMR spectroscopy

All POM and selected particle size fractions were analysed by solid-state ^{13}C NMR spectroscopy (Bruker DSX 200 NMR spectrometer, Bruker, Karlsruhe, Germany). Particle size fractions were treated with HF (Eusterhues *et al.*, 2007) prior to the measurement to reduce interfering impacts of iron-containing silica minerals. Carbon losses through HF-treatment increased from $10\pm 2\%$ for mSi, $10\pm 1\%$ for fSi, $16\pm 2\%$ for cC and $45\pm 9\%$ for fC.

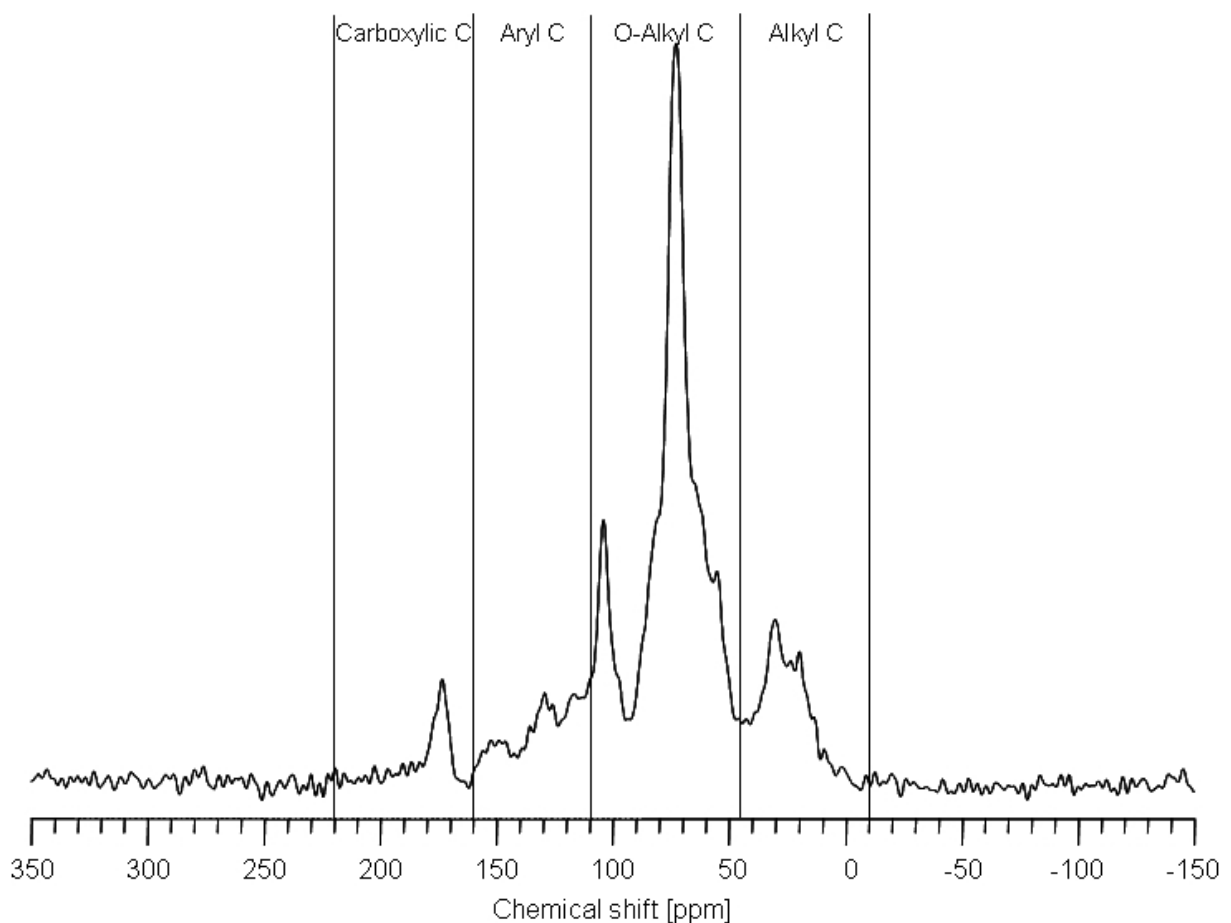


Figure 17: Spectra of solid state ^{13}C NMR experiment with chemical shift regions.

The cross-polarization magic angle spinning (CP MAS) technique with a ^{13}C -resonance frequency of 50.32 MHz and a spinning speed of 6.8 kHz was applied. A ramped ^1H -pulse starting at 100% to 50% of the initial power was used during a contact time of 0.2 ms in order to circumvent spin modulation during the Hartmann-Hahn contact. Pulse delays between 200 and 600 ms were used for all spectra. Pre-

experiments confirmed that the pulse delays were long enough to avoid saturation. Depending on the C contents of the samples, between 2000 and 250,000 scans were accumulated and a line broadening between 0 and 50 Hz was applied. The ^{13}C chemical shifts were calibrated relative to tetramethylsilane (0 ppm). The relative contributions of the various C groups were determined by integration of the signal intensity in their respective chemical shift regions according to Knicker *et al.* (2005; Figure 17). The region from 220 to 160 ppm was assigned to carbonyl (aldehyde and ketone) and carboxyl/amide C. Olefinic and aromatic C were detected between 160 and 110 ppm. O-alkyl and N-alkyl-C signals were found from 110 to 60 ppm and from 60 to 45 ppm. Resonances of alkyl C were assigned to the region 45 to -10 ppm.

2.4.7 Aggregate stability

All three aggregate size classes (cASC, mASC, fASC) of Cg and Ug79 were analyzed for aggregate stability using ultrasonic dispersion, followed by wet sieving and a standard particle size analysis to obtain sand-, silt- and clay-sized particles (Pipette-method according to Köhn). 15 g of the sieved aggregates were immersed in deionised water and floating organic matter was removed. The probe tip of the ultrasonic device (Branson Sonifier 250, Branson, CT, USA) was immersed 15 mm into the suspension. The temperature of the suspension was kept below 30°C using a water cooling jacket. The sonifier operated at a constant energy output of 75 W. The energy E (J ml^{-1}) dissipated into the suspension was calculated using Equation 8,

$$E = \frac{P \times t}{V} \quad (8)$$

where P is the power output (W), t the sonication time (s) and V the volume of the suspension (ml). The latter was calculated using an average particle density of 2.65 g cm^{-3} and a water density of 1.0 g cm^{-3} . The power output of the sonifier was calibrated calorimetrically with demineralised water (North, 1976; Schmidt *et al.*, 1999). For different inputs of dispersing energy, the ultrasonication time was increased. Treatment times varied between 1 and 10 min to produce a range of energies between 15 and 150 J ml^{-1} .

3. Soil classification and characteristics

All five sampled profiles showed a similar sequence of horizons (Figure 18) - a 43 cm to 76 cm thick, yellowish-red, well structured, dark and humic Ah-horizon above the sandy parent material. The Ah-horizon was divided in the upper 30 cm



Figure 18: Pictures of the five sampled soil pits (from upper left to lower right: Hg, Cg, Wg, Ug99 and Ug79).

which were carbonate-free and a lower horizon with secondary carbonates. The parent material was characterised as aeolian sediment above weathered acid volcanic rocks. Mean thickness of Ah was 77 ± 10 cm (Hg: 104 ± 2 cm, Cg: 99 ± 7 cm, Cg_{large}: 81 ± 22 cm, Wg_{large}: 63 ± 22 cm, Ug99: 77 ± 15 cm, Ug79: 86 ± 11 cm), measured at 407 positions using a soil auger. In a depth of approximately 30 cm secondary carbonates became abundant. Evidences for bioturbation by macrofauna were found in all pits and all horizons. All further analyses of pit samples were conducted only for

Table 2: Soil characteristics of experimental plots (Cg = continuously grazed, Wg = winter grazing, Ug99 = ungrazed since 1999, Ug79 = ungrazed since 1979).

Plot	Horizon	Depth [cm]	Sand [mg g ⁻¹]	Silt [mg g ⁻¹]	Clay [mg g ⁻¹]	Munsell colour (dry)	C _{tot}	N _{tot}	C _{min} [mg g ⁻¹]	N _{min}	OC	C/N	¹⁴ C concentration [pMC]	Conventional age	pH
Hg	Ah1	0-10	662	158	180	n.d.	16.5	1.6	0.1	0.0	16.4	10.6	107.8	>1954 AD	n.d.
	Ah2	10-26	758	107	135	n.d.	9.8	0.9	0.1	0.0	9.7	11.0	98.5	125 BP	n.d.
	Ah3	26-76	779	95	126	n.d.	5.7	0.5	0.2	0.0	5.4	10.9	81.2	1675 BP	n.d.
Cg	C	>76	850	62	88	n.d.	1.4	0.1	0.0	0.0	1.4	12.8	73.8	2435 BP	n.d.
	Ah1	0-10	548	211	242	10 YR 3/3	19.4	2.1	1.3	0.4	18.1	9.3	105.1	>1954 AD	6.9
	Ah2	10-30	558	192	250	10 YR 3/3	12.8	1.5	1.1	0.4	11.7	8.7	88.3	1000 BP	7.2
Wg	Ah3	30-68	608	173	219	10 YR 3/3	12.0	1.3	2.1	0.3	9.9	9.5	84.0	1405 BP	7.4
	C	>68	462	236	302	10 YR 5/3	10.7	0.6	7.5	0.2	3.2	18.8	63.0	3710 BP	7.3
	Ah1	0-10	549	182	270	10 YR 3/3	18.0	1.9	0.6	0.6	17.4	9.3	100.0	5 BP	6.8
Ug99	Ah2	10-31	532	229	239	10 YR 3/3	11.8	1.7	0.6	0.2	11.2	7.0	91.9	680 BP	7.1
	Ah3	31-58	439	326	235	10 YR 3/3	11.8	1.0	2.8	0.2	8.9	11.7	76.6	2145 BP	7.2
	C	>58	621	148	231	10 YR 6/4	8.2	0.4	6.4	0.1	1.8	20.0	70.2	2840 BP	7.4
Ug79	Ah1	0-10	483	258	259	10 YR 3/2	21.7	2.3	2.1	0.3	19.6	9.3	109.2	>1954 AD	7.1
	Ah2	10-34	606	169	225	10 YR 3/2	16.6	1.9	0.9	0.3	15.7	8.6	99.5	40 BP	7.2
	Ah3	34-60	543	208	249	10 YR 3/4	15.2	0.9	9.0	0.2	6.2	16.4	85.8	1230 BP	7.4
Ug79	C	>60	688	136	176	10 YR 5/4	6.1	0.3	4.9	0.2	1.2	19.1	76.5	2150 BP	7.3
	Ah1	0-10	642	135	223	10 YR 3/3	19.9	2.0	1.9	0.6	18.0	10.0	112.2	>1954 AD	6.8
	Ah2	10-25	748	100	152	10 YR 3/3	9.2	1.0	1.1	0.4	8.2	9.1	100.9	>1954 AD	7.1
Ug79	Ah3	25-43	739	113	148	10 YR 3/4	5.9	0.7	0.7	0.2	5.3	8.7	92.3	645 BP	7.0
	C	>43	742	102	156	10 YR 5/3	6.9	0.4	3.8	0.2	3.0	16.7	85.6	1250 BP	7.3

Cg, Wg, Ug99 and Ug79. Hg was not included in these analyses because the soil showed different horizon thicknesses and parent material. The plot was situated at a clearly different position in landscape and it is assumed to affect water content at least in subsoils and deposition of topsoil material that was eroded by water at higher positions.

The Ah-horizons of Cg, Wg, Ug99 and Ug79 had a loamy texture with 583 ± 93 mg sand g soil⁻¹, 191 ± 63 mg silt g soil⁻¹ and 226 ± 36 mg clay g soil⁻¹ (Table 2). With exception of Wg, contribution of sand increased, contribution of silt decreased and contribution of clay remained similar with depth. In Wg, proportion of sand decreased and of silt increased with depth. Total C, OC, total N and N_{min} concentrations were comparable between the plots and decreased with depth (mean OC concentration in Ah1: 18.3 ± 0.9 mg g⁻¹, Ah2: 11.7 ± 3.1 mg g⁻¹ and Ah3: 7.6 ± 2.2 mg g⁻¹). C/N ratio was similar across all plots and horizons with a mean of 9.8 ± 2.3 . pH increased with depth and C_{min} was significantly higher in Ah3 both due to secondary carbonates. Radiocarbon concentrations generally decreased in the order Ah1>Ah2>Ah3. Ungrazed plots and especially Ug79 had generally higher radiocarbon concentrations compared to the grazed plots Wg and Cg. Concentrations of Fe_{DCB} and Fe_{Ox} were generally low in all plots and slightly decreased with depth (Table 3). Potential cation exchange capacity was comparable

Table 3: Concentrations of Fe, Al and Mn in oxalate and dithionite–citrate–bicarbonate extracts.

Plot	Horizon	Depth [cm]	Al _{DCB}	Al _{Ox}	[mg g ⁻¹]			
					Fe _{DCB}	Fe _{Ox}	Mn _{DCB}	Mn _{Ox}
Cg	Ah1	0-10	0.3	1.6	3.1	1.1	0.2	0.5
	Ah2	10-30	0.5	2.0	4.5	1.4	0.2	0.4
	Ah3	30-68	0.3	1.8	2.4	1.1	0.1	0.4
	C	>68	0.2	1.3	2.2	0.8	0.1	0.4
Wg	Ah1	0-10	0.3	1.8	3.0	1.4	0.2	0.5
	Ah2	10-31	0.3	2.0	2.5	1.3	0.1	0.4
	Ah3	30-58	0.2	1.8	2.4	1.1	0.1	0.4
	C	>58	0.2	0.8	1.8	0.5	0.1	0.2
Ug99	Ah1	0-10	0.2	1.6	2.6	1.0	0.1	0.4
	Ah2	10-34	0.4	1.7	4.3	1.1	0.2	0.5
	Ah3	34-60	0.2	1.3	1.7	0.6	0.1	0.3
	C	>60	0.2	0.8	1.7	0.5	0.1	0.2
Ug79	Ah1	0-10	0.2	1.3	1.9	1.2	0.1	0.4
	Ah2	10-25	0.2	1.2	1.7	0.8	0.1	0.3
	Ah3	25-43	0.2	1.0	1.3	0.6	0.1	0.2
	C	>43	0.2	0.8	1.4	0.5	0.1	0.2

between the different plots and decreased with depth from $161 \pm 20 \text{ mmol}_c \text{ kg}^{-1}$ in Ah1 to $149 \pm 29 \text{ mmol}_c \text{ kg}^{-1}$ in Ah2 and $98 \pm 22 \text{ mmol}_c \text{ kg}^{-1}$ in Ah3. Base saturation was at least 100%, but contribution of Ca was overestimated as a consequence of secondary carbonates (Table 4). Following the WRB (2006) these horizons are classified as mollic horizons and the soils are classified as Calcic Chernozems.

Table 4: Cation exchange capacity and exchangeable cations of the experimental plots.

Plot	Horizon	Depth [cm]	CEC _{pot}	Ca	Mg	K	Na	Base saturation [%]
Cg	Ah1	0-10	183.9	159.7	19.7	7.0	2.4	103
	Ah2	10-30	166.3	162.2	21.6	2.7	3.2	114
	Ah3	30-68	108.4	195.9	22.0	2.6	1.5	205
	C	>68	174.5	144.7	47.5	3.1	3.6	114
Wg	Ah1	0-10	146.3	147.2	23.7	4.7	1.1	121
	Ah2	10-31	121.3	146.0	32.5	2.5	1.4	150
	Ah3	30-58	85.8	190.9	28.4	2.8	2.7	262
	C	>58	84.5	108.4	23.7	2.2	1.7	161
Ug99	Ah1	0-10	171.9	180.9	12.3	7.0	1.1	117
	Ah2	10-34	181.4	154.7	16.5	3.2	1.4	97
	Ah3	34-60	122.2	169.7	20.6	1.9	1.1	158
	C	>60	77.7	109.8	20.6	1.9	12.4	186
Ug79	Ah1	0-10	142.9	133.5	20.2	6.3	1.1	113
	Ah2	10-25	128.2	95.6	18.3	2.4	1.2	92
	Ah3	25-43	74.5	83.6	15.2	2.1	8.7	147
	C	>43	62.1	114.6	13.0	1.7	1.1	210

Illite was most abundant in all horizons of Ug79 and decreased from 700 mg g^{-1} in Ah1 to 470 mg g^{-1} in Ah3 (Table 5). Smectite minerals (Illite contribution of less than 50%) doubled from 160 mg g^{-1} in Ah1 to 320 mg g^{-1} in Ah3. Kaolinite, Vermiculite and Smectite minerals (Illite contribution of more than 50%) were less abundant and their sum increased from 140 mg g^{-1} in Ah1 to 210 mg g^{-1} in Ah3.

Table 5: Clay mineralogy of Ug79.

Horizon	Kaolinite	Illite	Illite/Smectite (Illite <50%)	Illite/Smectite (Illite >50%)	Vermiculite
	[mg g ⁻¹]	[mg g ⁻¹]	[mg g ⁻¹]	[mg g ⁻¹]	[mg g ⁻¹]
Ah1	50	700	160	30	60
Ah2	30	650	200	50	70
Ah3	40	590	240	60	70
C	80	470	320	50	80

4. Grazing effects on chemical and physical properties of semiarid steppe soils

4.1 Results

4.1.1 Bulk density, elemental concentrations, ratios and pH

Plots with lower grazing intensities showed significantly ($p < 0.01$) lower bulk densities compared to more heavily grazed plots (Figure 19). The highest mean bulk density of 1.28 g cm^{-3} was measured in the heavily grazed plot (Hg). This plot also

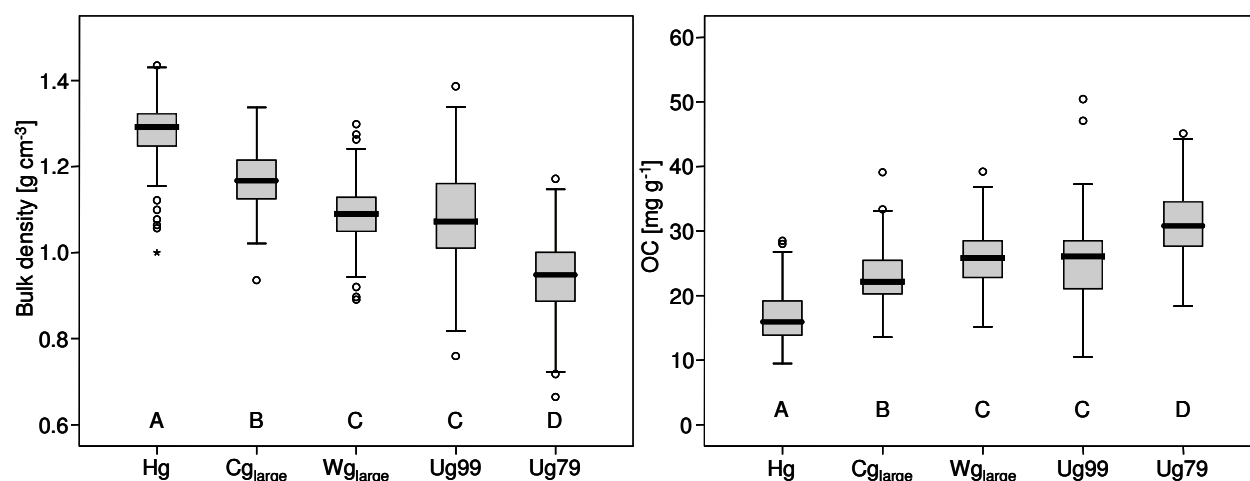


Figure 19: Boxplots of bulk density and OC concentration.

contained the highest single value of 1.44 g cm^{-3} . Mean bulk densities of Cg_{large}, Wg_{large} and Ug99 follow in decreasing order. Only Wg_{large} and Ug99 showed similar mean values and no significant differences. Ug79 showed the lowest bulk densities, with a 26 % lower mean of 0.94 g cm^{-3} and 0.66 g cm^{-3} as the lowest detected value. Bulk density showed a highly significant negative correlation to the OC concentration (Figure 20).

OC, total N and total S concentrations increased significantly ($p < 0.01$) with decreasing grazing intensity (Figure 19). All three elemental concentrations were positively correlated at the highest level of significance (Figure 20). The lowest mean concentrations were determined in Hg, containing 17.0 mg g^{-1} C, 1.74 mg g^{-1} N and 0.026 mg g^{-1} S. Cg_{large}, Wg_{large} and Ug99 showed increasing elemental concentrations with decreasing grazing intensities. Highest mean values were measured in Ug79, containing on average 82% higher OC, 81% higher total N and

60% higher total S concentrations than Hg. Only Wg_{large} and Ug99 had similar means, whereas the other plots were significantly different at the highest level.

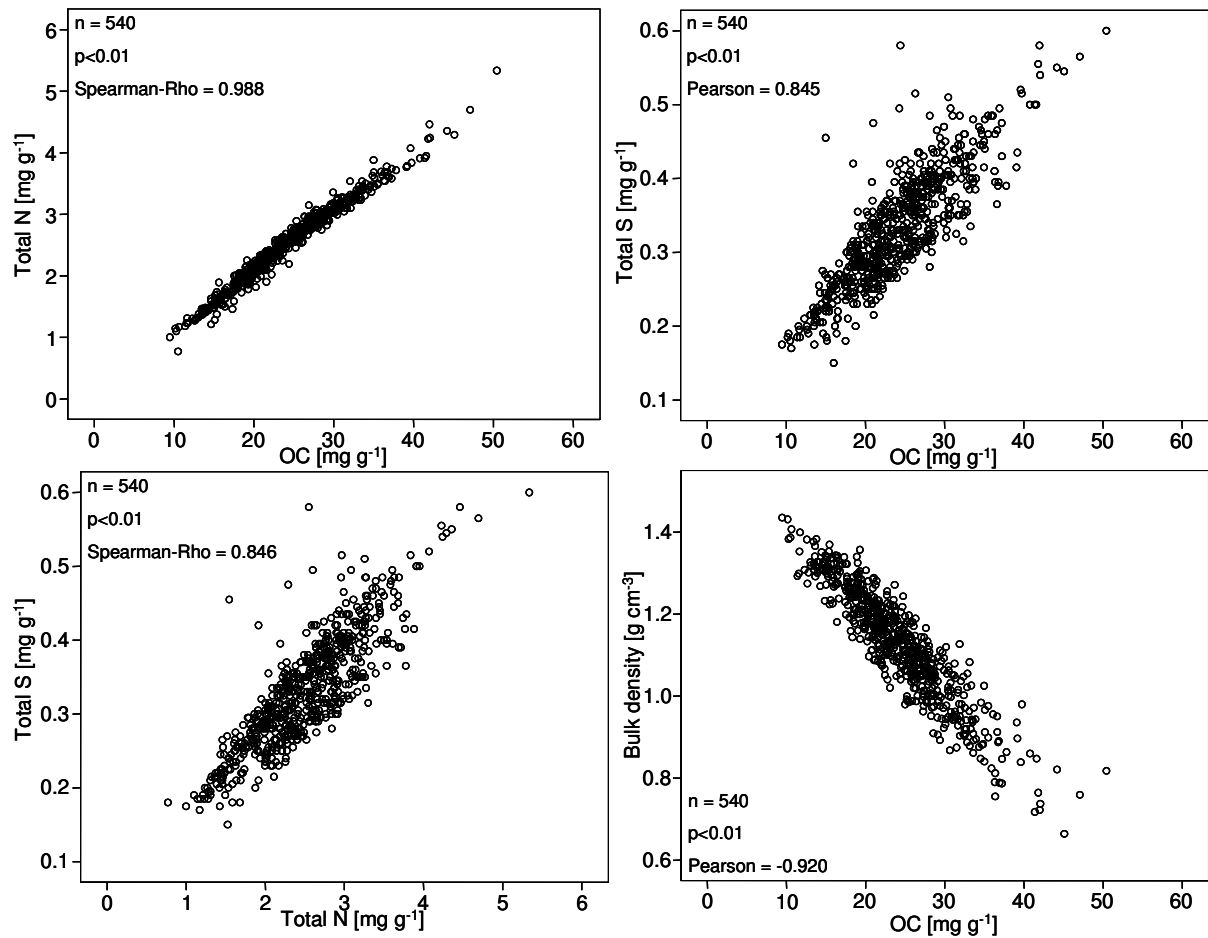


Figure 20: Correlations between OC, total N and total S concentrations and between bulk density and OC concentration.

The pH values of the five plots varied between 6.6 and 6.8 and exhibited significant differences ($p < 0.01$). Mean pH-values of 6.6 were calculated for Hg, Cg_{large} and Ug79 (Table 6) and significantly different values of 6.7 and 6.8 for Wg_{large} and Ug99, but overall differences between the plots were small.

Significant differences were found ($p < 0.01$), but no perceptible effect of pasture management on the C/N ratio. Only a narrow range between a maximum mean of 9.8 for Ug79 and a minimum mean of 9.5 for Wg was found. Ug99, Hg and Cg_{large} varied between these values, showing no significant differences. Narrower C/S and N/S ratios, with 65.1 and 6.7 were found in Hg compared to the other plots (Table 6), pointing towards effects of heavy grazing on total S. Cg_{large} showed the widest ratios with 79.0 for C/S and 8.3 for N/S. Wg_{large}, Ug79 and Ug99 varied between these extremes and were closer to Cg_{large}.

Table 6: Results of measured and calculated parameters of the upper 4 cm in five plots with different grazing intensities (mean in bold letters and standard deviation below). Different letters give significant differences ($p = 0.01$). Latin letters give results of Kruskal-Wallis tests, greek letters results of ANOVA. Conventional elemental stocks (ES) were calculated using Eq. 1 and equivalent elemental stocks (ES*) using Eq. 2 (Hg = heavily grazed, Cg_{large} = continuously grazed, Wg_{large} = winter grazing, Ug99 = ungrazed since 1999, Ug79 = ungrazed since 1979).

	Hg		Cg _{large}		Wg _{large}		Ug99		Ug79	
n	98		123		122		99		98	
Bulk density [g cm ⁻³]	1.28 0.08	A	1.17 0.07	B	1.09 0.08	C	1.09 0.12	C	0.94 0.10	D
OC [mg g ⁻¹]	17.0 4.2	A	23.0 4.1	B	25.9 4.5	C	25.5 6.3	C	31.0 5.5	D
Total N [mg g ⁻¹]	1.74 0.39	α	2.40 0.40	β	2.72 0.44	γ	2.65 0.67	γ	3.15 0.50	δ
Total S [mg g ⁻¹]	0.26 0.05	A	0.29 0.05	B	0.34 0.06	C	0.34 0.08	C	0.42 0.06	D
OC/N	9.7 0.4	A	9.6 0.4	B	9.5 0.4	B	9.7 0.7	CBA	9.8 0.3	DA
OC/S	65.1 6.2	A	79.0 6.5	BC	76.5 10.7	C	74.8 10.9	DC	74.4 7.7	DC
N/S	6.7 0.5	A	8.3 0.7	B	8.0 1.1	BC	7.7 1.1	C	7.6 0.7	DC
OC stock [kg m ⁻²]	0.86 0.16	α	1.06 0.14	β	1.12 0.14	βγ	1.08 0.16	β	1.15 0.11	γ
N stock [kg m ⁻²]	0.09 0.01	A	0.11 0.01	B	0.12 0.01	C	0.11 0.02	CB	0.12 0.01	C
S stock [kg m ⁻²]	0.013 0.002	α	0.014 0.002	α	0.015 0.002	β	0.015 0.002	β	0.016 0.002	γ
OC* stock [kg m ⁻²]	0.64 0.16	A	0.87 0.16	B	0.98 0.17	C	0.96 0.24	C	1.17 0.21	D
N* stock [kg m ⁻²]	0.06 0.01	α	0.09 0.02	β	0.10 0.02	γ	0.10 0.03	γ	0.12 0.02	δ
S* stock [kg m ⁻²]	0.010 0.002	A	0.011 0.002	B	0.013 0.002	C	0.013 0.003	C	0.016 0.002	C
pH	6.6 0.25	A	6.6 0.35	A	6.7 0.29	AB	6.8 0.27	B	6.6 0.24	A

4.1.2 OC, N and S stocks

Conventional stocks of OC, total N and total S were calculated using the bulk densities and the elemental concentrations for each sampling point (Eq. 1). For all three elements, the lowest means were calculated in Hg (Table 6). The lowest single values for OC stocks (0.54 kg m⁻²) and N stocks (0.04 kg m⁻²) were also found in Hg. Significant differences were calculated between all five plots and for all three elemental stocks. But absolute mean values of Cg_{large}, Wg_{large}, Ug99 and Ug79 showed only small differences. Cg_{large} has a 24%, Wg 31%, Ug99 26% and Ug79

34% higher OC stock than Hg. To summarise, only Hg showed significantly lower values of OC, total N and total S stocks when using the conventional calculation.

The alternative equivalent mass calculation of stocks (Eq. 2) showed different results compared to the conventional calculation using bulk densities (Table 6). The equivalent mass calculation revealed a significant loss of OC, total N and total S per unit soil mass with increasing grazing intensity over the complete range of grazing intensities. Hg accounted for the lowest means of all analysed elements, containing 0.64 kg C m⁻², 0.06 kg N m⁻² and 0.01 kg S m⁻². Significantly higher stocks were calculated for Cg_{large}, containing 35% more OC, 38% more N and 12% more S than Hg. No significant differences were found between Wg_{large} and Ug99, but both showed significantly higher values than Cg_{large} and significantly lower values than Ug79. The highest means for all three elements were calculated in Ug79, with 82% higher OC, 81% higher N, and 60% higher S stocks than Hg.

Table 7: MDD for selected topsoil parameters and plots (minimum detectable difference, Eq. 3; statistical power = 0.90, significance level = 0.01; MDD in bold letters, MDD_{rel} (relative minimum detectable difference, Eq. 4) given below; n.n. = not normal distributed; Hg = heavily grazed, Cg_{large} = continuously grazed, Wg_{large} = winter grazing, Ug99 = ungrazed since 1999, Ug79 = ungrazed since 1979).

	Hg	Cg_{large}	Wg_{large}	Ug99	Ug79
Bulk density [g cm ⁻³]	0.029 2.3 (n.n.)	0.022 1.9	0.025 2.3	0.043 4.0	0.036 3.8
OC [mg g ⁻¹]	1.541 9.1 (n.n.)	1.357 5.9	1.479 5.7	2.325 9.1	2.034 6.6
Total N [mg g ⁻¹]	0.143 8.2	0.131 5.5	0.145 5.3	0.247 9.3	0.186 5.9
Total S [mg g ⁻¹]	0.020 7.7 (n.n.)	0.016 5.6 (n.n.)	0.020 5.8	0.029 8.4	0.022 5.3
OC stock [kg m ⁻²]	0.058 6.8	0.045 4.2	0.045 4.0	0.059 5.4	0.041 3.6
N stock [kg m ⁻²]	0.0054 6.1	0.0044 3.9	0.0045 3.8	0.0067 6.0 (n.n.)	0.0036 3.1
S stock [kg m ⁻²]	0.0008 6.1	0.0006 4.4	0.0007 5.0	0.0009 6.0	0.0006 3.6
OC/N	0.137 1.4	0.142 1.5 (n.n.)	0.122 1.3	0.243 2.5 (n.n.)	0.112 1.1
OC/S	2.284 3.5 (n.n.)	2.150 2.7	3.576 4.7	4.005 5.4 (n.n.)	2.856 3.8 (n.n.)
N/S	0.201 3.0 (n.n.)	0.217 2.6	0.358 4.4	0.404 5.2 (n.n.)	0.253 3.3 (n.n.)

4.1.3 Minimum detectable differences

All data collectives and plots showed a $MDD_{rel} < 10\%$ (Table 7). For many parameters and plots, even $MDD_{rel} < 5\%$ were calculated. $C_{g\text{large}}$ and Ug79 accounted for the lowest MDD_{rel} of all analysed parameters. The reasons were a large number of samples for $C_{g\text{large}}$ and low variances for Ug79. With this dataset, it was possible to detect a change in the mean value of a parameter of less than 5% with a statistical power of 90% and a level of significance of 0.01.

4.2 Discussion

4.2.1 Grazing significantly increases bulk density and decreases OC, total N and total S concentrations

The results show significantly higher bulk densities and significantly lower OC, total N and total S concentrations in areas with higher grazing intensities compared to ungrazed areas (Table 6 and Figure 19). Increasing grazing intensity leads to a reduction in the number of plants, plant basal area, and amount of deposited dead plant material that acts as a protective mulch (da Silva *et al.*, 2003). In addition, animal trampling has a severe effect on soil compaction (Hamza & Anderson, 2005), and at the same time may stimulate organic matter decomposition, due to the destruction of soil aggregates by mechanical stress. Vegetation grows better, produces more root exudates and develops a wider ramified root system in ungrazed areas compared to grazed plots (Su *et al.*, 2004; Wang, 2004). Kelly *et al.* (1996) report lower total soil C and N concentrations due to reduced plant inputs following exclusion of vegetation. Thus, data has to be discussed in the light of this complex web of interrelated phenomena that result from intensive grazing, i.e. direct impact of animal trampling, reduced above- and belowground organic matter input and erosion.

Higher bulk densities as a consequence of increased animal trampling have been observed for different grazing animals and different grassland ecosystems (Wang & Ripley, 1997; Brevik *et al.*, 2002; Daniel *et al.*, 2002; Binkley *et al.*, 2003). Willat and Pullar (1984) measured hoof pressures up to 200 kPa for running sheep and postulate structural damage associated with increased bulk density and a decrease in total pore volume.

Figure 20 shows a highly significant negative correlation between OC and bulk density. Organic matter is a binding force between particles and within aggregates and thus affects soil compactability (Soane, (1990). Living roots, and to a lesser extent also dead roots, provide a filamentous network which resists compactive loads (Soane, 1990). Imhoff *et al.* (2000) found significantly lower bulk densities under plants compared to places between plants and ascribe this to a greater root production directly below plants. A part of the organic matter is known to be occluded in aggregates, mostly inaccessible to microbes and therefore protected against microbial decomposition (Jastrow *et al.*, 1996). Through aggregate disruption, this occluded organic matter may become accessible to microbial decomposition (Balesdent *et al.*, 2000; Solomon *et al.*, 2005). Lavee *et al.* (1996) found a correlation between aggregate stability and soil organic matter content for a Terra Rossa and a Lithosol in Israel and postulated that grazing and human activities interfere with the development of aggregate stability. Following this scenario, ungrazed areas will exhibit lower bulk densities and higher soil organic matter concentrations.

Higher bulk densities and lower elemental concentrations in heavily grazed areas may also be caused by erosion. Heavily grazed steppe areas in regions of Inner Mongolia with lower vegetation height and lower vegetation cover are characterised by higher wind speeds (Li *et al.*, 2000), conditions favourable for soil erosion. When the topsoil, with the highest concentrations of organic matter of the whole profile (Woods, 1989; Deen & Katakai, 2003), is eroded in heavily grazed areas (Gregorich *et al.*, 1998; Li *et al.*, 2005), deeper horizons with lower elemental concentrations and higher bulk densities will be exposed. Wind erosion leads to a preferential loss of fine, C- and N-rich particles and a relative accumulation of coarse soil particles (Lobe *et al.*, 2001; Li *et al.*, 2004; Neff *et al.*, 2005; Su *et al.*, 2005; Wang *et al.*, 2006); Table 8). Eroded fine material will be deposited in ungrazed areas or around individual plants and increase the C and N concentrations and decrease bulk densities of the uppermost soil layers (Hook *et al.*, 1991; Su *et al.*, 2004).

It is considered that increased bulk densities and decreased OC, total N and total S concentrations in grazed areas are a combined effect of loss of organic matter following animal trampling, lower above- and belowground organic matter input as a

4.2.2 Sulphur in grazed grassland soils

Total S concentrations decrease significantly with increasing grazing intensities (Table 6) and are positively correlated to OC and total N (Figure 20). This indicates that S in these grassland soils is mainly bound in organic matter. But a small portion of total S is bound as inorganic S and is most probably not affected by grazing. This can be seen in lower coefficients of correlation between OC and total S, and total N and total S. In contrast to the C/N ratio, C/S and N/S ratios showed significantly lower values for Hg compared to the other plots. This is attributed to a relative accumulation of S-rich organic matter and lower litter inputs in Hg. S-rich components of the organic matter seem to be more resistant to mineralisation than OC or N and tend to accumulate in the remaining organic matter (McLaren & Swift, 1977). Hg or generally grazed plots have less diluting fresh litter material and thus a higher proportion of decomposed organic matter. This leads to a relatively higher total S concentration and lower C/S and N/S ratios. Solomon *et al.* (2005) describe narrower C/S and N/S ratios in cultivated compared to native grasslands of South Africa. They ascribed this to an increased mineralisation of organic matter that was physically protected in aggregates before cultivation.

Narrower C/S and N/S ratios in heavily grazed areas point towards a relative or absolute accumulation of S. This is assumed to be the result of selective mineralisation of S-depleted organic matter and lower input of organic matter in heavily grazed areas.

4.2.3 OC, total N, and total S stocks of grazed plots

OC and total N stocks of the upper 4 cm vary around 1 kg C m^{-2} and 0.1 kg N m^{-2} (Table 6). Conventional OC, total N and total S stocks of the upper 4 cm reflect the findings of decreasing elemental concentrations in heavily grazed areas (Table 6). But whereas Hg exhibits significantly lower OC, total N and total S stocks compared to ungrazed areas, the lower grazing intensities showed no significant differences for elemental stocks compared to the ungrazed areas. This discrepancy is the direct consequence of stock calculations using bulk densities. As elemental concentrations in grazed areas decrease, bulk densities increase, compensating for the lower concentrations in the computation of stocks (Figure 20). This is a consequence of the compaction of topsoils in grazed areas and sampling to a

constant depth. Similar results are reported by Mikhailova *et al.* (2000) and Osher *et al.* (2003), who found changing bulk densities as a consequence of grazing, interfering with conventional stock calculations. Decreasing Ah horizon thicknesses due to increased bulk densities as a consequence of grazing pressure have been reported by Dormaar and Willms (1998). If sampling is done to a constant depth, additional soil masses are sampled in heavily grazed areas, which lead to an overestimation of elemental stocks for grazed compared to ungrazed areas. In addition, grazed areas may suffer an additional loss of OC- and N-rich topsoil material through wind erosion, which is not included in the calculation either. Errors in stock calculations as a result of these processes can be avoided if the sampling depth is corrected (Berg *et al.*, 1997; Gifford & Roderick, 2003) or stocks are calculated with a normalised mass. Veldkamp (1994) and Ellert and Bettany (1995) describe the equivalent mass approach to compare elemental stocks of areas with differing management, which has been tested by several authors for different forms of management and environments (Mikhailova *et al.*, 2000; Malhi *et al.*, 2002; VandenBygaart & Kay, 2004). This alternative elemental stock calculation was also used for the upper 4 cm and showed significantly lower stocks for all elements in all grazing intensities compared to Ug79 (Table 6). Compared to the conventional calculation, these results indicate that grazing at all intensities reduces stocks, and not just heavy grazing. Future studies should survey not only elemental concentrations and bulk densities, but also changing horizontal thicknesses as a consequence of wind erosion and compaction due to management.

4.2.4 Effects of grazing reduction and enclosure

Ameliorating effects of reduced and excluded grazing on physical and chemical topsoil parameters have been shown in a number of studies (Braunack & Walker, 1985; Abril & Bucher, 1999; Su *et al.*, 2004; Su *et al.*, 2005; Drewry, 2006). How much time these processes take to affect topsoil parameters is not clear (Drewry, 2006). Cg_{large}, Wg_{large} and Ug99 were grazed with the same intensity until 1999, when grazing in Wg_{large} was reduced and in Ug99 completely excluded. This chronosequence enables the analysis of short-term effects of grazing reduction and exclusion on the analysed topsoil parameters. Significant differences for all analysed parameters were recorded between Cg_{large} and Wg_{large} and Cg_{large} and Ug99 (Table 6, Figure 19). These results confirm the detrimental effects of continued grazing even

after periods as short as five years. No significant differences were detected between Ug99 and Wg_{large}. Either no ameliorative processes occurred and only Cg_{large} deteriorated, or both plots ameliorated to the same degree. The period between grazing cessation and sampling may also have been too short to detect significant effects. Holt (1997) also found no significant changes in total C concentration 6 to 8 years after grazing cessation in semi-arid grasslands in Australia. In contrast, several authors found significant ameliorations of topsoil parameters after five years or less of reduced or excluded grazing (Orr, 1975; Su *et al.*, 2004; Su *et al.*, 2005). Spatial factors may also obstruct the detection of ameliorative processes, increasing elemental concentrations and reducing bulk density. Higher litter inputs and increased deposition of windblown fine materials will at first take place around individual plants or small patches of plants, so-called “islands of fertility” (Hook *et al.*, 1991; Burke *et al.*, 1998). With time, these patches will spread and change the mean values of the whole plot. But in the first years after changed management, these changes will be detected only by sampling at selected positions.

To summarise, continued grazing for five years caused a significant deterioration in physical and chemical topsoil parameters compared to reduced and excluded grazing. Ameliorative processes in the first five years are assumed but could not be verified for reduced grazing and grazing exclusion. Reducing the grazing intensity seems to preserve the status quo and is therefore recommended as a conservative form of grazing management for this shortgrass steppe ecosystem in Inner Mongolia.

4.3 Conclusion

The statistical approach revealed a significant deterioration of physical and chemical topsoil parameters as a consequence of sheep grazing in a *Leymus chinensis/Stipa grandis* dominated shortgrass steppe in Inner Mongolia. Five plots with different grazing intensities were analysed at 540 sampling points. Significantly higher bulk densities and lower OC, total N and total S concentrations were found in grazed areas compared to ungrazed areas. This is attributed to the combined effect of animal trampling, reduced above- and belowground organic matter input and root growth and erosion as a consequence of grazing. Elemental stocks, calculated using bulk densities as well as an equivalent mass to take into account changing bulk

densities following grazing, showed a significant decrease for OC, total N and total S in grazed areas. Highest losses were calculated for heavily grazed areas. Whereas C/N remained constant in all analysed plots, C/S and N/S ratios showed narrower values in heavily grazed areas. This points towards a selective mineralisation of S-depleted organic matter and lower organic matter inputs in grazed areas. Despite low MDD values resulting from the large number of samples and low variances, no ameliorating effects of reduced or excluded grazing could be verified five years after land use change. Long-term effects are presumed, as 25 years of exclusion showed significantly different values. Sheep grazing at reduced intensities is considered to be a conservative form of grassland management, as no detrimental effects were detected during the first five years.

5. Spatial variability of topsoils and vegetation in grazed steppe ecosystems

5.1 Results

5.1.1 Small grids

All properties in all plots were normally distributed. Directional variograms of small grids showed isotropic behaviour of all analysed properties underlining the stationarity of the data collectives. Only Cg showed a significant trend in north-south direction for all topsoil properties, which was modelled using a first-order regression between each soil variable and the geographic coordinates. Variables were detrended by subtracting soil variables from linear model calculations, as the residuals were considered to be closer to stationary (Iqbal *et al.*, 2005). Quality of the trend removal is shown in Table 9, with Cg_{trend} giving the variogram properties of the uncleared model and Cg the properties of the detrended collective. All further analyses were conducted using the detrended collective Cg. Spatial behaviour of all properties in all plots was analysed using omnidirectional variograms. In most cases, best fits to experimental variograms were obtained with spherical models. The aboveground biomass in Ug99 was not spatially structured, manifested in a pure nugget effect.

Table 8: Mean values of soil characteristics of upper 4 cm (Ug79 = ungrazed since 1979, Ug99 = ungrazed since 1999, Cg = continuously grazed, Hg = heavily grazed, Wg_{large} = large grid winter grazing, Cg_{large} = large grid continuously grazed).

Plot	N	Grazing intensity	Sand	Silt	Clay	OC	Total N	Total S	pH
		[sheep units ha ⁻¹ yr ⁻¹]	[mg g ⁻¹]	(CaCl ₂)					
Ug79	98	0	491	349	160	31.0	3.15	0.42	6.6
Ug99	99	0	467	370	163	25.5	2.65	0.34	6.8
Cg	88	1.2	511	321	168	22.2	2.36	0.35	6.6
Hg	98	2.0	681	209	110	17.0	1.74	0.26	6.6
Wg _{large}	122	0.5	439	378	183	25.9	2.72	0.34	6.7
Cg _{large}	123	1.2	494	335	171	23.0	2.40	0.29	6.6

Spatial distributions of bulk density, OC, total N and total S concentrations were comparable within each plot (Table 9), but different between the four plots. Spatial heterogeneity of topsoil properties increased in the order Hg, Cg, Ug99 and Ug79 from a homogeneous to a pure nugget or patchy distribution (Table 10). These

Table 9: Nugget, sill and range values derived from fitted variogram models of small grid sampling (Sph = spherical model, Gau = gaussian model, Nug = nugget model; Ug79 = ungrazed since 1979, Ug99 = ungrazed since 1999, Cg = continuously grazed detrended, Cg_{trend} = continuously grazed not detrended, Hg = heavily grazed). Nu/Nu+Si is the percental contribution of nugget to total variance (nugget + sill). Variance gives the calculated statistical variance of each parameter in each plot. Several parameters were merged in two conceptual groups, based on comparable range values (Group1 and Group 2). Note that Nu/Nu+Si is not comparable between spherical and gaussian models, as gaussian models do not reach a definite maximum of variance.

Group	Parameter	Plot	Nugget	Sill	Range [m]	Variance	Nu/Nu+Si [%]	Method
Group 1	Bulk density	Ug79	0.0050	0.0043	40.6	0.010	53.9	Sph
		Ug99	0.0045	0.0113	80.3	0.014	28.5	Sph
		Cg	0.0004	0.0031	70.0	0.005	11.4	Sph
		Cg _{trend}	0.0009	0.0061	128.2	0.005	12.5	Sph
		Hg	0.0010	0.0057	47.0	0.006	15.2	Sph
	OC	Ug79	14.3	16.9	59.9	30.4	45.9	Sph
		Ug99	5.6	40.5	79.8	40.1	12.2	Sph
		Cg	3.5	7.0	85.0	13.9	33.3	Sph
		Cg _{trend}	3.0	16.0	130.0	13.9	15.8	Sph
		Hg	4.1	15.9	81.5	17.4	20.4	Sph
	Total N	Ug79	0.13	0.12	50.8	0.25	51.7	Sph
		Ug99	0.12	0.40	79.9	0.45	23.3	Sph
		Cg	0.04	0.07	60.0	0.16	36.4	Sph
		Cg _{trend}	0.03	0.23	140.0	0.16	11.5	Sph
		Hg	0.03	0.14	79.1	0.15	17.3	Sph
	Total S	Ug79	0.0019	0.0018	34.8	0.004	51.4	Sph
		Ug99	0.0018	0.0048	61.9	0.006	27.6	Sph
		Cg	0.0008	0.0012	40.0	0.003	41.0	Sph
		Cg _{trend}	0.0014	0.0044	93.8	0.003	8.5	Gau
		Hg	0.0002	0.0029	41.0	0.003	5.0	Sph
Group 2	Vegetation cover	Ug79	48.6	30.9	21.7	78.1	61.2	Sph
		Ug99	25.0	34.0	55.0	59.3	42.4	Sph
		Cg				no data		
		Hg	76.5	68.7	66.2	134.3	52.7	Sph
	Aboveground biomass	Ug79	3028.8	3280.7	25.3	5956.8	48.0	Sph
		Ug99	4590.7	0.0	0.0	4952.4	100.0	Nug
		Cg				no data		
		Hg	710.0	1100.0	65.0	1727.4	39.2	Sph

findings are most noticeable for $Nu/Nu+Si$ which increased from a mean for all four properties of 15% ($\pm 7\%$) in Hg to 51% ($\pm 3\%$) in Ug79. The maximum distance covered by spatial dependencies is described by the range, with the highest mean value of 76 m (± 5 m) found in Ug99. Cg had the second highest (64 m, ± 19 m), Hg the third highest (62 m, ± 21 m) and Ug79 the shortest spatial dependencies (47 m, ± 11 m). Values for total variance, a first indicator for the amplitude of spatial variation, were highest in Ug99, second in Ug79 and Cg and Hg showed similar low values. Nugget values, representing the small-scale heterogeneity, were highest in Ug79, followed by Ug99, Cg and Hg. Sill values describe the extent of spatial dependencies and were highest in Ug99, followed by Hg, Ug79 and Cg. It is notable that total S concentration exhibited similar spatial distributions to OC, total N and bulk density, but showed at least 20% shorter ranges. To summarise, topsoil properties showed increasing homogeneity and extent of patches in the order Ug79, Ug99, and Cg/Hg (Figure 21). While Ug79 was characterised by heterogeneously distributed and defined small patches, Cg/Hg were characterised by a few merging, homogeneous large patch.

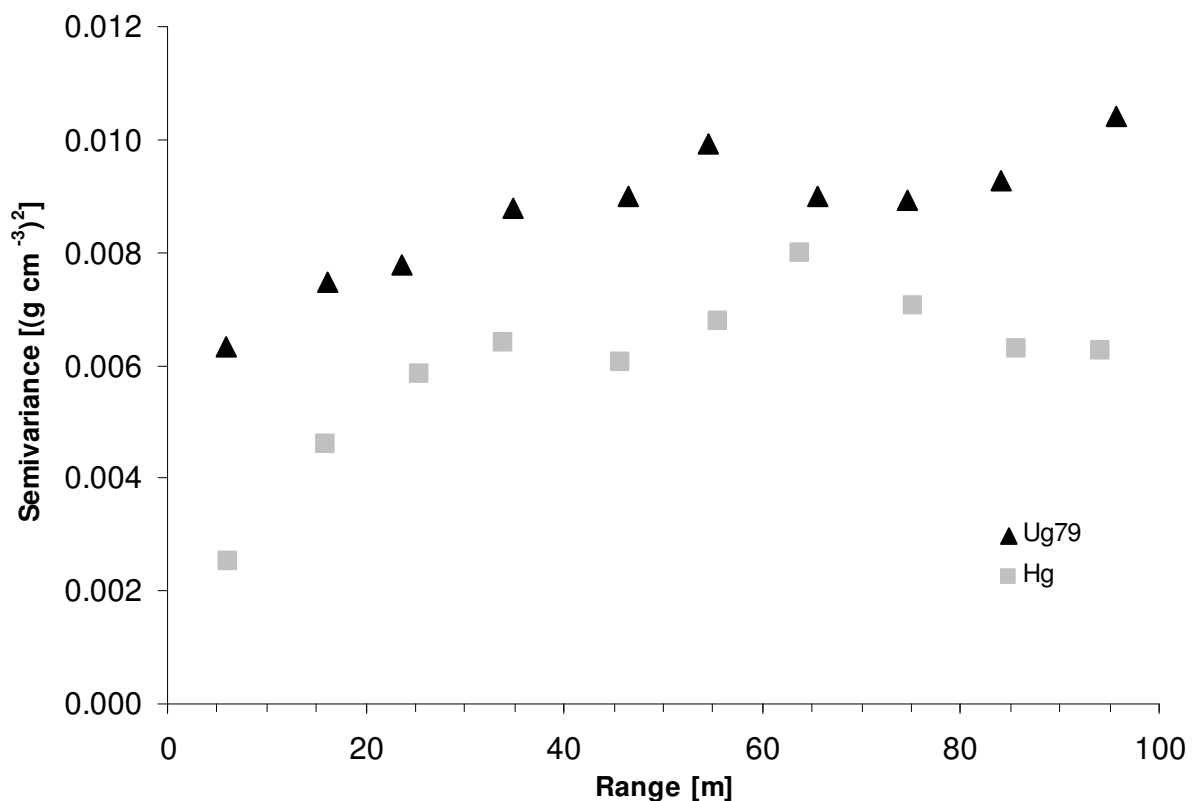


Figure 21: Omni-directional semivariograms of bulk density in Ug79 and Hg.

Vegetation cover and biomass were measured for Ug79, Ug99 and Hg. Both properties showed equal spatial behaviours in Ug79 and Hg, but contrasting spatial behaviour in Ug99 (Table 9). Ug79 revealed a heterogeneous distribution of vegetation, expressed by the highest mean Nu/Nu+Si ratio of 55% ($\pm 9\%$) and the shortest mean range of 24 m (± 3 m). Hg was characterised by a more homogeneously distributed vegetation, displayed by the lowest mean Nu/Nu+Si (46%, $\pm 10\%$) and the widest mean range (66 m, ± 1 m). Ug99 had medium mean Nu/Nu+Si and range values, but extreme single values. For vegetation cover, Ug99 showed values close to Hg and for aboveground biomass results close to Ug79. Generally, heterogeneity of vegetation increased from Hg to Ug79 and Ug99 seemed to be a transition between the two states. Hg was characterised by a homogeneously distributed and productive vegetation, comparable to grazing lawns and Ug79 by a heterogeneously distributed vegetation consisting of many small patches, clearly differing in biomass production, comparable to islands or niches.

Table 10: Mean values and standard deviations for Nu/Nu+Si and range values of Group 1 (bulk density, OC, total N and total S concentration) and Group 2 (vegetation cover and aboveground biomass) for small grids (Ug79 = ungrazed since 1979, Ug99 = ungrazed since 1999, Cg = continuously grazed, Hg = heavily grazed) and Group I (bulk density, OC, total N, total S concentration and $\delta^{13}\text{C}$), Group II (vegetation cover and aboveground biomass) and Group III (pH and Ah thickness) for large grids (Wg_{large} = winter grazing, Cg_{large} = continuously grazed).

Grid	Group	Plot	Mean Nu/Nu+Si [%]	Mean range [m]
Small grid (15 m standard distance, 5 minimum distance)	Group 1	Ug79	50.7 \pm 3.4	46.5 \pm 11.1
		Ug99	22.9 \pm 7.5	75.5 \pm 9.1
		Cg	30.5 \pm 13.1	63.8 \pm 18.9
		Hg	14.5 \pm 6.7	62.2 \pm 21.1
	Group 2	Ug79	54.6 \pm 9.3	23.5 \pm 2.5
		Ug99	71.2 \pm 40.7	27.5 \pm 38.9
		Cg	no data	
		Hg	46.0 \pm 9.5	65.6 \pm 0.9
Large grid (50 m standard distance, 10 m minimum distance)	Group I	Wg _{large}	41 \pm 6	83 \pm 10
		Cg _{large}	72 \pm 3	174 \pm 38
	Group II	Wg _{large}	50 \pm 14	83 \pm 18
		Cg _{large}	26 \pm 0.1	234 \pm 23
	Group III	Wg _{large}	51 \pm 1.3	132 \pm 1.3
		Cg _{large}	49 \pm 7	385 \pm 7

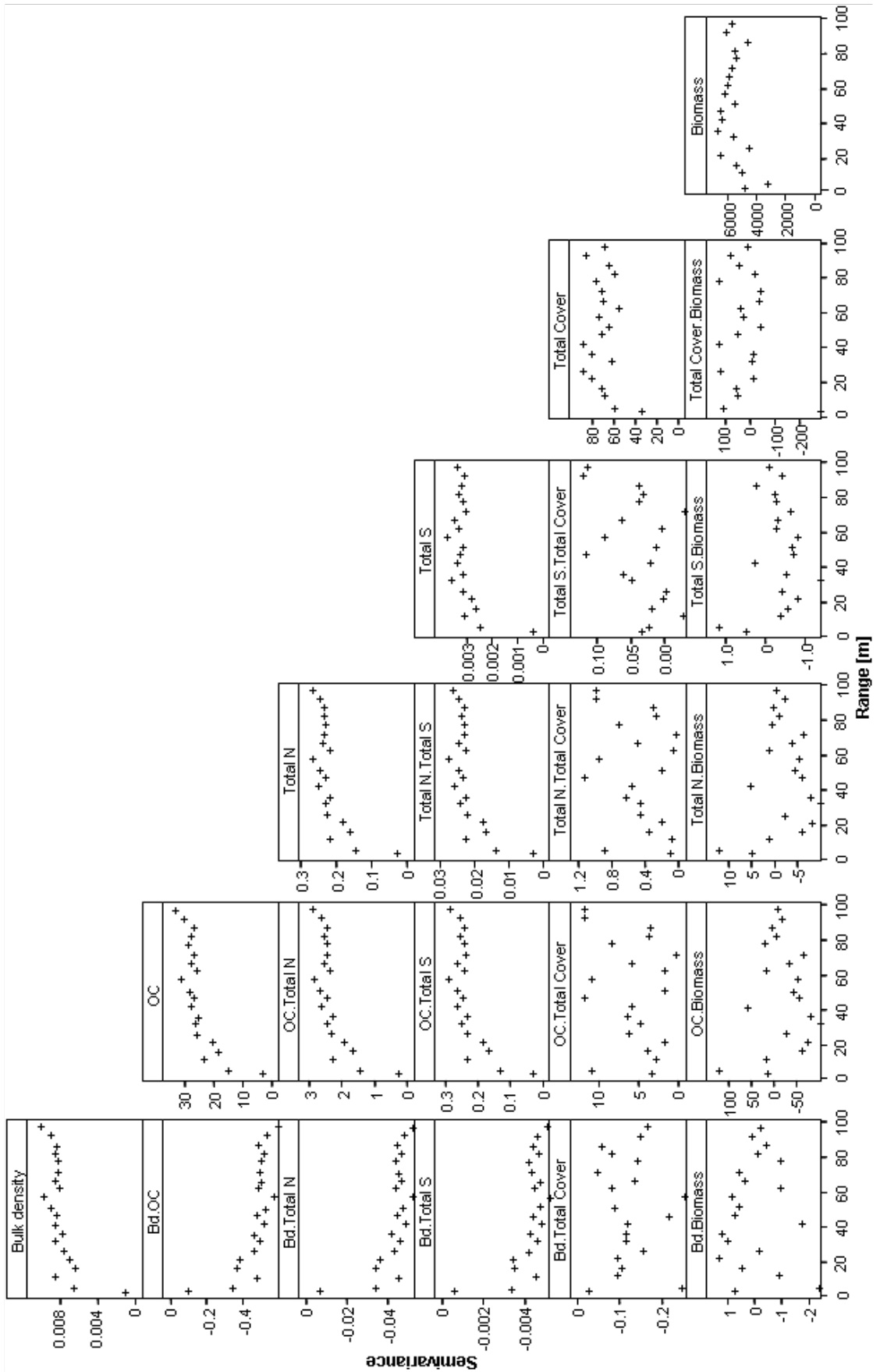


Figure 22: Omni-directional crossvariograms of bulk density, OC, total N and total S concentration (Group 1), vegetation cover and aboveground biomass (Group 2) in Ug79.

Crossvariograms of OC, total N and total S concentrations revealed a close positive spatial behaviour in all plots (Figure 22). All three elemental concentrations showed a close negative spatial behaviour for all plots when spatially correlated with bulk density. Aboveground biomass and vegetation cover showed positive crossvariances, but no spatial structure was detected in Ug79 indicating a heterogeneous distribution of vegetation. OC, total N and total S were spatially positively correlated with vegetation cover, but showing no spatial structure in Ug79. Crossvariances of aboveground biomass and topsoil properties were positive for narrow distances (<20 m), but turned out negative for wider point pairs, revealing no spatial structure in Ug79. In contrary, Hg vegetation parameters (data not shown) showed a clear spatial structure with positive crossvariances for distances narrower than 40 m and increasing negative crossvariances for wider point pairs, indicating a homogeneous distribution of vegetation in large patches (40 m). Compared to Ug79, crossvariances of aboveground biomass and topsoil properties were positive for wider distances (<40 m), and turned out negative for wider point pairs similar to Ug79. This indicates that vegetation and topsoil properties form large uniform patches up to 40m in Hg and heterogeneously distributed small patches (<20 m) in Ug79.

5.1.2 Large grids

All data collectives on the large grids were normally distributed. Anisotropic behaviour, caused by a trend in direction of northeast (45° in directional variograms for distances >500 m), was found on Cg_{large} . It was not detrended, because the number of affected point pairs was low. Spatial behaviour of all properties in both plots was analysed using omnidirectional variograms. All experimental variograms except total S in Wg_{large} were fitted with spherical models (Table 11). Clear differences were found between both plots for all properties and groups (Table 10).

Topsoil properties in Group I (bulk density, OC, total N and total S concentration, $\delta^{13}C$) revealed higher values for variance and sill in Wg_{large} and higher values for nugget, $Nu/Nu+Si$ and wider ranges in Cg_{large} . Cg_{large} showed a mean range of 174 m (± 38 m) and a mean $Nu/Nu+Si$ of 72 % (± 3 %). Wg_{large} accounted for a mean range of 83 m (± 10 m) and a mean $Nu/Nu+Si$ of 41 % (± 6 %). Total S

concentration exhibited more than 30 % shorter ranges compared to the mean of all topsoil properties in Cg_{large} .

Table 11: Nugget, sill and range values derived from fitted variogram models of large grid sampling (Sph = spherical model; Wg_{large} = large grid winter grazing, Cg_{large} = large grid continuously grazed). Nu/Nu+Si gives the percental contribution of nugget to total variance (nugget + sill). Variance gives the calculated statistical variance of each parameter in each plot. Several parameters were merged in three conceptual groups, based on comparable range values (Group I, Group II and Group III).

Group	Parameter	Plot	Nugget	Sill	Range [m]	Variance	Nu/Nu+Si [%]	Method
Group I	Bulk density	Wg_{large}	0.0028	0.0027	87.7	0.006	50.2	Sph
		Cg_{large}	0.0033	0.0011	176.3	0.005	74.9	Sph
	OC	Wg_{large}	7.3	12.9	72.8	20.1	36.1	Sph
		Cg_{large}	12.2	5.1	201.7	17.1	70.7	Sph
	Total N	Wg_{large}	0.084	0.116	95.6	0.193	41.9	Sph
		Cg_{large}	0.121	0.040	183.9	0.160	75.2	Sph
	Total S	Wg_{large}	not fittable					
		Cg_{large}	0.0018	0.0007	147.6	0.002	73.3	Sph
$\delta^{13}C$	Wg_{large}	0.15	0.25	77.5	0.40	37.2	Sph	
	Cg_{large}	0.38	0.14	200.0	0.50	73.1	Sph	
Group II	Vegetation cover	Wg_{large}	90.0	60.0	70.0	155.4	60.0	Sph
		Cg_{large}	50.7	227.1	194.0	248.4	18.3	Sph
	Aboveground biomass	Wg_{large}	650.0	940.0	95.0	1552.7	40.9	Sph
		Cg_{large}	1835.3	3513.1	246.5	4672.6	34.3	Sph
Group III	Ah	Wg_{large}	250.0	230.0	132.0	453.0	52.1	Sph
		Cg_{large}	240.0	210.0	380.0	456.6	53.3	Sph
	pH	Wg_{large}	0.043	0.043	132.0	0.082	50.3	Sph
		Cg_{large}	0.063	0.080	390.0	0.123	44.0	Sph

The vegetation properties in Group II (vegetation cover, aboveground biomass) showed only slight differences in spatial distribution compared to the topsoil properties. Compared to Wg_{large} , Cg_{large} had higher values in all variables except for the nugget of vegetation cover and Nu/Nu+Si. The mean range value in Cg_{large} was higher ($234 \text{ m} \pm 23 \text{ m}$) and the mean Nu/Nu+Si was lower ($26\% \pm 0.1 \%$). Values in Wg_{large} were comparable to Group I with a mean range of $83 \text{ m} (\pm 18 \text{ m})$ and a mean Nu/Nu+Si of $50\% (\pm 14\%)$.

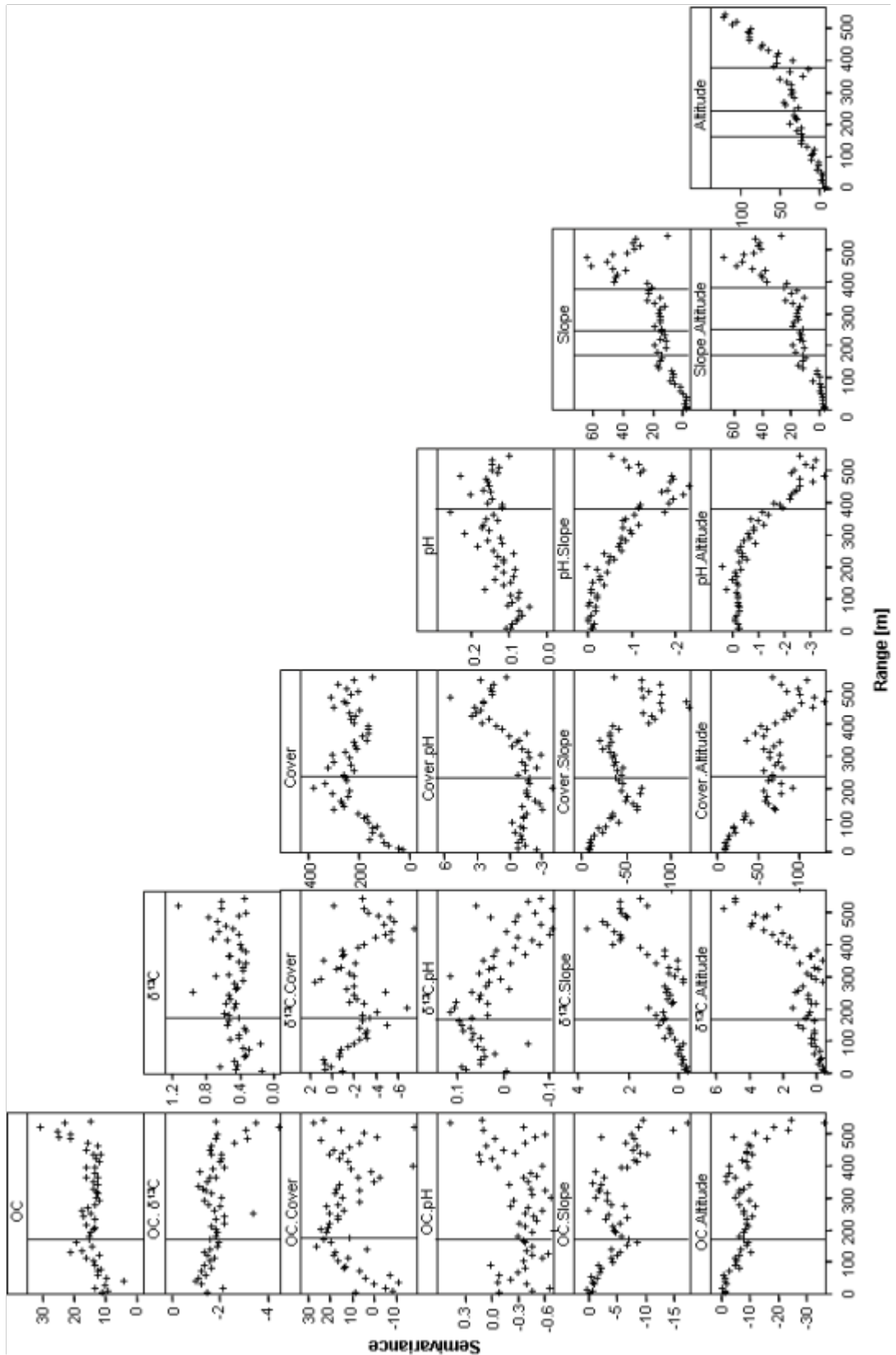


Figure 23: Omni-directional crossvariograms of OC concentration and $\delta^{13}\text{C}$ (representing Group 1), vegetation cover (representing Group 2), pH (representing Group 3), slope angle and altitude in Cg_{large} .

Group III consists of pH and Ah thickness and also exhibited different spatial distributions. Both plots showed similar data and differed only in range values. Cg_{large} had a mean range of 385 m (± 7 m) and a mean Nu/Nu+Si of 49% ($\pm 7\%$). Wg_{large} accounted for a range of 132 m (± 1.3 m) and a comparable mean Nu/Nu+Si of 51% ($\pm 1.3\%$).

All cross variograms within the groups showed strong positive spatial correlations (Figure 23). Only bulk density and $\delta^{13}C$ covaried negatively with OC, total N and total S concentration. Low positive spatial correlations were also detected between the properties in Group I and Group II. Group III showed different spatial distributions. All properties in Cg_{large} and Wg_{large} showed strong spatial correlations to the topographic properties slope angle and altitude (Figure 23).

5.2 Discussion

5.2.1 Small-scale heterogeneity of topsoils following grazing exclusion

Grazing changed the spatial distributions of topsoil and vegetation properties on the small scale (Table 9, Figure 21). A heterogeneous mosaic of small patches was found in the ungrazed plot Ug79 and mainly large homogeneous patches were found in the grazed plots Cg and Hg. The ungrazed plot Ug99 was characterised as a transition between grazed and long-term ungrazed states. Topsoil and vegetation properties showed similar semivariograms, but no clear spatial structure in ungrazed plots (Figure 22). It is assumed that this is the result of three intertwined, grazing-induced process complexes - direct physical impacts of grazing sheep on topsoils, disturbance effects of grazing on vegetation and wind erosion.

The physical impact of grazing animals changes the microtopography in flat areas. Small mounds around plants are removed and depressions are filled by a combination of hoof action and reduction of vegetation cover. This results in increased and spatially homogenised bulk densities in grazed areas (Gibson, 1988; MartinezTuranzas *et al.*, 1997; Nash *et al.*, 2004). These assumptions are in accordance with Zhao *et al.* (2007), who reported reduced soil water content in the studied grazed plots as a consequence of soil compaction and reduced infiltration due to trampling. These processes may explain the findings of spatially more uniform

bulk densities and a more homogeneous distribution of elemental concentrations in Hg and Cg (Table 9, Figure 21).

Beside these physical effects of grazing animals on the spatial distribution of topsoils, continued grazing alters the habitus, species composition and spatial distribution of vegetation (Posse *et al.*, 2000). Herbivory reduces plant biomass and consequently reduces the input of organic matter to soils (Naeth *et al.*, 1991; Northup *et al.*, 1999; Neff *et al.*, 2005). Accordingly, elemental concentrations, potential for loosening topsoils (Steffens *et al.*, 2008) and protection of soils against animal trampling are also reduced (da Silva *et al.*, 2003). Confirmation for the loosening potential of organic matter, by increasing aggregation and reducing compaction, can be drawn from data, as bulk density and elemental concentration were not only statistically, but also spatially highly correlated (Figure 22). It is assumed that loosening of topsoils is the combined result of better root growth, higher litter inputs and loose deposition of fine material in ungrazed areas and especially around plants.

Long-term grazing changes the species composition, as grazing-sensitive species become less abundant or disappear and grazing-insensitive species increase and may dominate the ecosystem (Cheng *et al.*, 2004). Pronounced changes in species composition and plant functional groups due to increased grazing intensities were observed in the studied plots (Giese, 2007). Uniform grazing lawns, composed of several grazing-insensitive species, are characteristic for grazed areas (Milchunas *et al.*, 1989; Northup *et al.*, 2005). Adler and Lauenroth (2000) and Milchunas and Lauenroth (1989) observed more homogeneous small-scale distributions of above- and belowground biomass following grazing in a shortgrass steppe in Colorado. Homogeneous distributions of low aboveground biomass and vegetation cover were found in Hg and Cg and their formation was attributed to the high grazing intensity. Crossvariograms support the assumption of large homogeneous patches of topsoil and vegetation in Hg (data not shown). Low and spatially homogeneous inputs of organic matter from grazing lawns may explain the findings of homogeneously distributed low elemental concentrations and high bulk densities in the grazed plots.

Grazing in semiarid ecosystems is associated with decreasing standing biomass (Milchunas & Lauenroth, 1993) and significantly reduced vegetation height and vegetation cover (Golodets & Boeken, 2006). A direct consequence is an

increase in wind speed near the soil surface, leading to less deposition of nutrient-rich fine material, as deposition is controlled by vegetation height and vegetation cover (Li *et al.*, 2005; Hoffmann *et al.*, 2007). If the vegetation height in this ecosystem is reduced below a certain threshold of 9 to 4 cm, erosion of topsoils takes place (Hoffmann *et al.*, 2008).

Different spatial distributions in Ug79 showed that grazing cessation initiates the heterogenisation of topsoils and vegetation (Figure 22). The absence of trampling, the recovering vegetation and dust deposition around plants seem to be the responsible processes. As these processes take time to change the properties in a measurable way, transitions between the extremes have to be assumed. Spatial distributions of topsoils are comparable to grazed areas and distributions of vegetation are like ungrazed areas in the transition plot Ug99. Ug99 is the only plot where both vegetation properties show antipodal distributions - vegetation cover showed a more homogeneous, lawn-like distribution comparable to grazed plots, while aboveground biomass was heterogeneously distributed (pure nugget effect), similar to Ug79. This discrepancy can be explained by the regeneration of the grazing lawn vegetation. The spatial distribution of vegetation, as measured by vegetation cover, remains constant, but individual plants grew better and produce more biomass without browsing. As some species recover faster than others, this results in a more heterogeneously distributed biomass. Crossvariograms of biomass and topsoil properties support this assumption in Ug79, as crossvariances were spatially not structured and positive for short distances (<15 m) but negative for long distances (>15 m). For the studied plots a heterogeneous distribution of vegetation in small patches in ungrazed plots compared to large homogeneous patches in grazed plots are assumed. Ehrenfeld *et al.* (1997) found no accordance between spatial patterns of vegetation and soil variables. They attribute their findings to the different spatial behaviour of vegetation and soil properties in time causing these discrepancies. The findings of this thesis support the conservative behaviour of soils against changes that was reported for example by Reynolds *et al.* (1997) and show the vegetation to be an important factor initiating the recovery of ecosystems after disturbance.

5.2.2 Large-scale heterogeneity of topsoils follows geomorphology

All properties in Cg_{large} and Wg_{large} showed strong spatial correlations to the topographic properties slope angle and altitude (Figure 23). All properties in Cg_{large} reached a maximum in semivariance at a range >400 m. All semivariograms at distances >400 m compared measurements at sampling points in the flat area in the western part with points in the slope-summit area in the eastern part of the plot (Figure 13). High semivariograms for all properties showed that these areas are most different from each other (Figure 24).

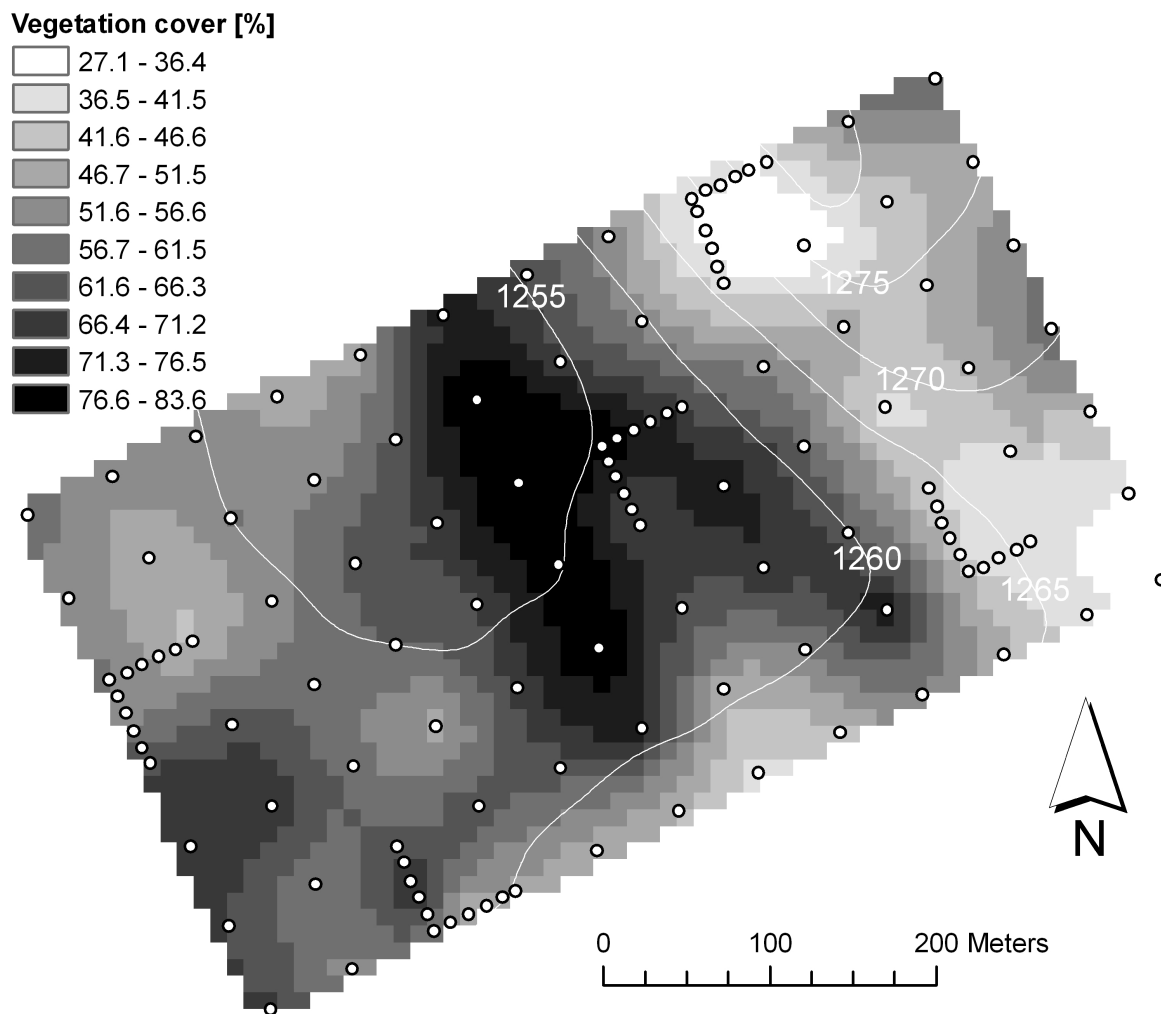


Figure 24: Map of vegetation cover in Cg_{large} (calculated using ordinary cokriging). Contour lines give the elevation in m above sea level.

This is ascribed to two interrelated processes. One process was the erosion of carbon-rich topsoils in grazed sites and especially at slope-summit positions, resulting in low elemental concentrations, low Ah thicknesses and, as a result of the

increased influence of the underlying acid rock, lower pH and higher bulk densities. The eroded carbon-rich, fine material was deposited in flat areas, leading to high elemental concentrations, high Ah thicknesses, high pH-values and low bulk densities. The other process resulted from the less favourable plant growing conditions (low nutrient and water availability) at slopes and summits, which could be seen in low vegetation cover and low living biomass in the data. Higher vegetation cover and higher living biomass were a result of better plant growing conditions in flat areas and especially depressions (Augustine, 2003). More evidence could be found in the positive spatial correlation between $\delta^{13}\text{C}$ and slope angle and altitude. $\delta^{13}\text{C}$ increased with increasing slope angle, probably as a consequence of a higher contribution of C4-plants on steeper slopes (Figure 23). This pointed towards lower water contents and less favourable growing conditions on slopes. Burke *et al.* (1999) and Hook and Burke (2000) also found the spatial variability of soil organic matter fractions to be strongly related to topography in a semiarid shortgrass steppe in Colorado and ascribed their findings to erosion and deposition and differences in texture as a consequence of these processes.

While Ah thickness and pH (Group III) differed only between the topographic extremes summit and depression, Group I (bulk density, OC, total N, total S concentration and $\delta^{13}\text{C}$) and Group II (vegetation cover, aboveground biomass) also differed between slope and summit and flat parts and depression. Group I and Group II depicted an additional maximum in semivariance at a range of 200 m, in contrast to Group III (pH and Ah thickness). This distance corresponded to the spatial extent of smaller units in Cg_{large} (Figure 13). The western part was divided into two flat areas by a longish depression. Each of the three units had a spatial extent of 200 m. And also the eastern part of Cg_{large} was divided in slope and summit, each with a spatial extent of 200 m. These smaller units differed as well in plant growing conditions and preferential accumulation of soil material in depressions, producing this spatial pattern. This difference was most notable for vegetation cover (Figure 24). High values of vegetation cover in the depression were attributed to high water and nutrient availability. Schimel *et al.* (1985) found topography-related differences in the total mass of C, N and P and ascribed this to different inputs of organic matter following different water and nutrient availabilities affecting the growth of vegetation.

Wg_{large} showed similar topography-related semivariograms for all properties. But the differences between depression, slope and summit were less pronounced, as vertical differences and slope angles in Wg_{large} were lower. The lower grazing intensity in Wg_{large} additionally masked the topographic differences.

To summarise, topography controlled the spatial distribution of topsoil and vegetation properties when samples were taken at large scales (>10 m sampling distance). It is further concluded that grazing intensified the topography-related patterns. This has to be considered when impacts of other factors are to be evaluated.

5.2.3 Detectability of spatial patterns is scale dependent

Different spatial distributions for vegetation and topsoil properties were observed in Cg and Cg_{large} (Table 9 and Table 11, Figure 25). Both grids showed similar values for variance and sill, but Cg_{large} accounted for clearly higher values of nugget, range and $Nu/Nu+Si$ for all analysed properties.

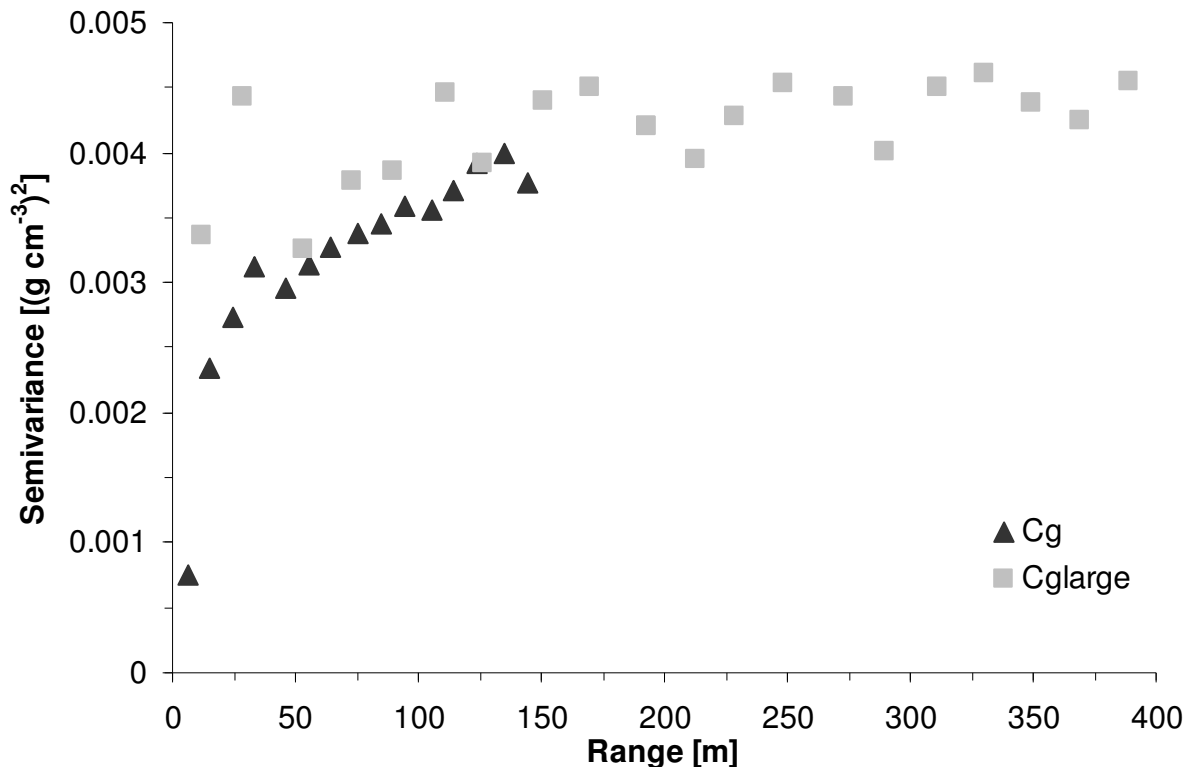


Figure 25: Spatial distribution as affected by sampling scale - omni-directional semivariograms of bulk density in Cg and Cg_{large} .

C_g exhibited spatial dependencies in the first 130 m, while $C_{g_{large}}$ was characterised by a high portion of nugget and no comparable spatial dependencies at small scales. The spatial behaviour of C_g seemed to explain the small-scale variabilities in $C_{g_{large}}$. As both grids were sampled in the same plot, these differences were the result of sampling at different scales. Similar results were reported by Qi and Wu (1996) for landscape pattern analysis of elevation and aboveground biomass using spatial autocorrelation indices. They found an overall decline in the degree of spatial autocorrelation with considered scale. Spatial patterns in grasslands varying across many scales were also reported elsewhere (Ehrenfeld *et al.*, 1997; Rietkerk *et al.*, 2000; Rietkerk *et al.*, 2004). Fuhlendorf and Smeins (1999) examined the influence of considered scales on the detectability of grazing-induced changes in vegetation in a semiarid grassland in Texas. They concluded that grazing can have positive, negative and no influences on spatial heterogeneity of vegetation, depending on the scale of observation. As $C_{g_{large}}$ was sampled with a minimum distance of 10 m and a standard distance of 50 m, small-scale effects, recognised with the small grid (minimum distance of 5 m, standard distance 15 m) and attributed to grazing impacts, were not detectable with the large grid.

Generally the findings of this thesis confirm the assumption that spatial heterogeneity decreases with increasing sampling distance (Wiens, 1989) and underline the demand of many authors to include different scales when analysing spatial impacts of grazing or cultivation on soil and vegetation properties (Hook *et al.*, 1991; Qi & Wu, 1996; Golluscio *et al.*, 2005; Maestre *et al.*, 2005; Northup *et al.*, 2005). While the large grids displayed impacts of topography and no aspects of grazing, the small grids showed different distributions correlated with grazing intensity and time since cessation. The results also support the statement that there is no correct or ideal sampling distance (Wu, 2004), as the ungrazed plots exhibited high portions of nugget. The reasons for this small-scale variability may be elucidated by applying smaller sampling distances than used in this study to clarify processes taking place at the scale of resource islands and individual plants. It is concluded that the choice of sampling scheme has a crucial influence on the results that will be obtained. The spatial extent as well as the sampling distance between individual points determine the quality of the study and the conclusions that will be drawn from it.

5.3 Conclusion

It was observed that the detectability of spatial patterns of topsoil (bulk density, OC, total N and total S concentration, $\delta^{13}\text{C}$, pH and Ah thickness) and vegetation properties (vegetation cover and aboveground biomass) in a semiarid steppe is scale-dependent. Topography controlled the spatial distribution of topsoil and vegetation properties on the large scale (sampling distance 50 m). Grazing intensified this topographic pattern, but did not change the spatial distribution. This is assumed to be the result of erosion and deposition and favourable or less favourable plant growing conditions. Grazing controlled the spatial distribution of topsoil and vegetation properties on the small scale (sampling distance 15 m). Grazed sites were characterised by a homogeneous distribution and ungrazed sites by a heterogeneous distribution of topsoil and vegetation properties. This is ascribed to the homogenising impacts of hoof action, formation of uniform grazing lawns and wind erosion in grazed areas. Recovery, observed as a heterogenisation of spatial distributions, already became evident after five years in vegetation properties, but not until 25 years after grazing cessation in topsoil properties. Recovering vegetation and higher deposition of windblown material around recovering plants are presumed to be the crucial processes initiating the recovery of grazing-degraded areas.

6. Alteration of soil organic matter pools and aggregation in topsoils as driven by OM input

6.1 Results

6.1.1 Physical fractionation

6.1.1.1 Mass, OC and C to N ratio

All aggregate size classes in the four plots were characterized by a sandy texture consisting of 65 to 73% coarse-silt and sand (Table 12). For the OC balance, these coarse particle size classes were negligible and contained in most cases <5% of the OC (data not shown). Mean bulk soil OC recovery across all plots was 95% (Cg: 91%, Wg: 97%, Ug99: 91%, Ug79: 101%).

OC concentrations of cSi differed between 3.5 and 13.0 mg OC g⁻¹ fraction, mSi between 9.5 and 21.8 mg OC g⁻¹ fraction, fSi revealed the highest concentrations between 60.8 and 78.7 mg OC g⁻¹ fraction, cC ranged between 59.8 and 73.0 mg OC g⁻¹ fraction and fC between 29.1 and 41.4 mg OC g⁻¹ fraction. C to N ratios generally narrowed with decreasing particle size class from 7.0 to 10.3 for mSi, 9.1 to 9.9 for fSi, 7.4 to 8.3 for cC and 6.4 to 7.6 for fC. Total amounts of OC in particle size fractions were comparable between plots and ASC. Highest amounts were found in cC (2.65 to 6.97 mg OC g⁻¹ soil) and fSi (2.09 to 3.19 mg OC g⁻¹ soil), followed by fC (1.00 to 2.54 mg OC g⁻¹ soil), mSi (0.74 to 1.61 mg OC g⁻¹ soil) and cSi (0.59 to 1.45 mg OC g⁻¹ soil). The differences between the plots are assumed to be the result of differences in texture (Table 13). The C loading of particles <20 µm (Hassink, 1997) was calculated to consider differences in texture and showed comparable C sequestration potentials of particles <20 µm (14.3 to 19.2 mg OC g⁻¹ soil) and comparable saturation levels between 49% and 76% (Table 12).

There were clear differences in mass and OC concentration, C to N ratio and total amount of OC for the three POM and between differently grazed plots. Between different ASC only fPOM differed. OC concentrations and C to N ratios of fPOM decreased with decreasing aggregate size. While fPOM in cASC ranged between

Table 12: Mass distribution, OC concentration and C/N of soil fractions and contribution of OC of a specific fraction to the bulk soil of three aggregate size classes (cASC = 2000-6300 µm, mASC = 630-2000 µm, fASC = <630 µm; Cg = continuously grazed, Wg = winter grazing, Ug99 = ungrazed since 1999, Ug79 = ungrazed since 1979). All numbers give the arithmetic mean and standard deviation of two replicates. Potential C loading of particles <20 µm was calculated using the empirical formula of Hassink (1997; Equation 7). Current C-loading is the sum of the measured OC concentrations of the fractions <20µm.

	cASC (2000-6300 µm)			mASC (630-2000 µm)			fASC (<630 µm)					
	Cg	Wg	Ug99	Cg	Wg	Ug99	Cg	Wg	Ug99			
>200 µm	74.35	106.51	99.59	273.78	99.26	168.90	149.59	461.32	64.28	81.74	66.14	162.45
63-200 µm	396.78	391.78	399.47	295.76	354.88	336.13	348.40	158.17	404.67	409.44	424.41	396.99
	197.35	192.41	189.47	131.60	193.49	169.29	173.42	89.48	214.23	198.82	225.67	168.50
cSi	3.6	3.6	3.9	5.9	3.7	3.5	3.7	13.0	3.7	4.6	3.9	8.6
(20-63 µm)	8.3	8.8	13.2	10.4	8.5	8.6	8.6	10.8	8.3	9.4	9.5	10.4
	0.71±0.0	0.69±0.0	0.74±0.0	0.77±0.3	0.72±0.2	0.59±0.1	0.64±0.1	1.17±0.3	0.78±0.1	0.91±0.1	0.89±0.1	1.45±0.4
OC [mg g ⁻¹ ASC]												
OC [mg g total soil ⁻¹]	0.09	0.11	0.10	0.05	0.07	0.07	0.08	0.11	0.60	0.67	0.66	1.18
Mass [mg g ⁻¹ soil]	92.63	83.31	76.47	72.49	84.46	71.93	80.73	55.27	85.57	85.01	79.27	79.66
OC [mg g fraction]	9.5	11.3	10.5	16.4	10.1	10.3	12.8	21.8	14.4	15.2	14.3	20.2
C/N	9.3	7.0	9.3	10.3	7.1	9.8	9.6	9.9	9.9	10.0	9.7	10.3
(6.3-20 µm)	0.88±0.0	0.94±0.0	0.80±0.0	1.19±0.2	0.85±0.1	0.74±0.0	1.04±0.1	1.20±0.0	1.23±0.2	1.29±0.2	1.13±0.1	1.61±0.2
OC [mg g ⁻¹ ASC]												
OC [mg g total soil ⁻¹]	0.12	0.15	0.10	0.07	0.08	0.08	0.13	0.11	0.95	0.95	0.84	1.31
Mass [mg g ⁻¹ soil]	44.34	45.08	44.47	34.89	44.21	41.01	42.44	26.56	48.61	46.61	48.36	40.37
OC [mg g fraction]	60.8	69.9	66.0	73.0	68.7	68.8	70.4	78.7	61.1	66.5	66.0	71.5
C/N	9.4	9.1	9.6	9.9	9.3	9.8	9.7	9.6	9.3	9.4	9.4	9.6
(2.0-6.3 µm)	2.70±0.1	3.15±0.1	2.93±0.2	2.55±0.1	3.04±0.0	2.82±0.0	2.99±0.2	2.09±0.2	2.97±0.1	3.10±0.0	3.19±0.1	2.89±0.1
OC [mg g ⁻¹ ASC]												
OC [mg g total soil ⁻¹]	0.36	0.48	0.38	0.16	0.29	0.31	0.38	0.20	2.30	2.28	2.37	2.35
Mass [mg g ⁻¹ soil]	96.98	95.40	97.45	71.14	94.21	92.84	95.34	42.89	110.94	90.37	97.39	85.07
OC [mg g fraction]	67.7	73.0	69.8	69.2	68.2	70.9	66.8	61.8	60.7	70.2	64.8	59.8
C/N	8.0	7.7	8.2	8.0	7.7	8.1	8.3	7.4	8.0	8.0	8.1	7.6
(0.2-2.0 µm)	6.56±0.5	6.97±0.0	6.80±0.2	4.92±0.1	6.42±0.0	6.59±0.0	6.37±0.0	2.65±0.3	6.74±0.2	6.34±0.1	6.32±0.1	5.09±0.4
OC [mg g ⁻¹ ASC]												
OC [mg g total soil ⁻¹]	0.87	1.07	0.88	0.30	0.61	0.73	0.82	0.25	5.21	4.66	4.69	4.14
Mass [mg g ⁻¹ soil]	76.58	65.73	54.92	42.52	57.59	64.27	42.68	24.14	55.08	74.07	37.80	47.67
OC [mg g fraction]	33.1	37.7	35.5	35.5	36.6	32.4	29.1	41.4	34.1	31.5	37.4	34.7
C/N	6.9	6.5	7.0	6.6	6.6	6.6	7.4	6.6	6.7	6.4	7.6	6.4
(<0.2 µm)	2.54±0.0	2.48±0.4	1.95±0.1	1.51±0.1	2.11±1.0	2.08±0.3	1.24±0.1	1.00±0.1	1.88±0.2	2.33±0.0	1.41±0.1	1.65±0.2
OC [mg g ⁻¹ ASC]												
OC [mg g total soil ⁻¹]	0.34	0.38	0.25	0.09	0.20	0.23	0.16	0.09	1.45	1.72	1.05	1.34
C-Saturation of particles <20µm (Hassink, 1997)	12.7	13.5	12.5	10.2	12.4	12.2	11.6	6.9	12.8	13.1	12.1	11.2
potential [mg g soil]	18.4	17.8	19.2	14.6	18.4	17.8	19.2	14.3	17.2	17.8	19.2	14.9
Saturation [%]	69	76	65	70	67	69	61	49	75	73	63	75
OC in mineral fractions	71	79	59	34	53	56	48	22	84	86	74	74

Table 12: continued

	cASC (2000-6300 μm)			mASC (630-2000 μm)			fASC (<630 μm)						
	Cg	Wg	Ug79	Cg	Wg	Ug99	Cg	Wg	Ug79				
fPOM	Mass [mg g^{-1} soil]	12.78	6.66	24.93	65.86	64.92	48.92	56.39	129.85	11.20	9.32	8.31	11.68
	OC [mg g^{-1} fraction]	241.9	140.4	233.1	273.3	150.6	165.4	182.6	218.7	117.6	114.4	148.7	177.6
	C/N	26.1	18.1	25.1	26.5	16.6	15.3	18.6	15.7	13.5	13.4	13.4	13.1
	OC [mg g^{-1} ASC]	3.09 \pm 0.1	0.94 \pm 0.0	5.81 \pm 0.4	18.00 \pm 3.0	9.78 \pm 2.3	8.09 \pm 0.3	10.30 \pm 0.1	28.40 \pm 3.9	1.32 \pm 0.0	1.07 \pm 0.0	1.24 \pm 0.1	2.07 \pm 0.2
	OC [mg g^{-1} total soil ¹]	0.41	0.14	0.75	1.10	0.93	0.90	1.32	2.68	1.02	0.78	0.92	1.69
oPOM	Mass [mg g^{-1} soil]	5.65	6.28	6.57	8.69	5.16	4.53	7.40	6.24	3.73	3.07	7.89	5.88
	OC [mg g^{-1} fraction]	330.6	340.2	341.5	371.9	336.7	337.6	353.0	376.6	283.6	279.8	318.2	366.9
	C/N	16.1	17.1	17.9	17.2	15.8	18.2	15.2	15.4	14.9	15.0	13.6	14.3
	OC [mg g^{-1} ASC]	1.87 \pm 0.0	2.14 \pm 0.3	2.24 \pm 0.3	3.23 \pm 0.7	1.74 \pm 0.2	1.53 \pm 0.3	2.61 \pm 0.3	2.35 \pm 0.4	1.06 \pm 0.1	0.86 \pm 0.2	2.51 \pm 0.2	2.16 \pm 0.4
	OC [mg g^{-1} total soil ¹]	0.25	0.33	0.29	0.20	0.16	0.17	0.33	0.22	0.82	0.63	1.86	1.75
oPOM _{small}	Mass [mg g^{-1} soil]	2.54	6.85	6.64	3.27	1.82	2.18	3.62	6.08	1.69	1.55	4.76	1.73
	OC [mg g^{-1} fraction]	221.1	126.9	201.7	185.6	197.1	214.1	201.6	158.0	205.0	204.8	210.2	173.8
	C/N	11.6	10.5	11.5	9.4	11.2	12.3	11.1	10.7	11.7	12.9	10.8	9.3
	OC [mg g^{-1} ASC]	0.56	0.87	1.34	0.61	0.36	0.47	0.73	0.96	0.35	0.32	1.00	0.30
	OC [mg g^{-1} total soil ¹]	0.07	0.13	0.17	0.04	0.03	0.05	0.09	0.09	0.27	0.23	0.74	0.25
OC in POM fractions	29	21	41	66	47	44	52	78	16	14	26	26	

Table 13: Soil and vegetation characteristics of upper 10 cm (ANPP = Above-ground net primary productivity, BNPP = Below-ground net primary productivity, Gao, 2007; Cg = continuously grazed, Wg = winter grazing, Ug99 = ungrazed since 1999, Ug79 = ungrazed since 1979) given as arithmetic means and standard deviations of three representative soil pits. Letters give significant differences ($p=0.05$).

Plot	Grazing intensity [sheep units ha^{-1} yr^{-1}]	ANPP [g m^{-2}]	BNPP [g m^{-2}]	Sand [g g^{-1}]	Silt [mg g^{-1}]	Clay [mg g^{-1}]	OC [mg g^{-1}]	Total N [mg g^{-1}]	¹⁴ C concentration [pMC]	pH (CaCl_2)
Cg	1.2	114.0 \pm 23.7 a	n.d.	560 \pm 8 ab	200 \pm 5 a	240 \pm 3 ab	16.7 \pm 3.8 a	1.84 \pm 0.5 a	105.08	6.9
Wg	0.5	126.3 \pm 4.3 a	191.0 \pm 76.7a	500 \pm 4 ab	230 \pm 4 a	270 \pm 1 b	21.5 \pm 3.0 a	2.18 \pm 0.2 a	99.95	6.8
Ug99	0	128.0 \pm 15.8 a	n.d.	450 \pm 4 b	290 \pm 4 a	260 \pm 0 b	22.8 \pm 3.0 a	2.34 \pm 0.3 a	109.16	7.1
Ug79	0	175.5 \pm 14.0 b	380.0 \pm 153.4 b	600 \pm 4 a	180 \pm 4 a	220 \pm 1 a	21.3 \pm 1.8 a	2.06 \pm 0.1 a	112.16	6.8

140.4 to 273.3 mg OC g⁻¹ fraction and revealed a C to N ratio of 18.1 to 26.5, the range decreased to 117.6 to 177.6 mg OC g⁻¹ fraction and a C to N ratio of 13.1 to 13.5 in fASC. In contrast to fPOM, OC concentrations and C to N ratios of oPOM varied between 283.6 and 376.6 mg OC g⁻¹ fraction and 13.6 and 18.2 across all plots and ASC. The smaller fraction oPOM_{small} had lower OC concentrations between 126.9 and 221.1 mg OC g⁻¹ fraction and narrower C to N ratios between 9.3 and 12.9. Generally, mass concentration and total amount of OC increased in the order Cg/Wg < Ug99 < Ug79. This trend increased from oPOM_{small} to oPOM and fPOM and was stronger in mASC and cASC. The largest total OC amounts were found in Ug79 for the fPOM of the two coarse ASC. These findings are in good accordance with significantly greater organic matter inputs, measured as above- and belowground net primary productivity, in Ug79 compared to Ug99, Wg and Cg (Table 13; Gao, 2007).

To summarise, ungrazed areas showed higher contributions of POM and especially fPOM in mASC and cASC. Particle size fractions revealed comparable mass and C distributions between all plots and across all ASC. The C saturation level of particles <20 µm was comparable between the four plots.

6.1.1.2 Chemical composition of POM and particle size fractions in three ASC

¹³C CPMAS-NMR spectra revealed a high contribution of alkyl C and O-alkyl C in all analyzed fractions (Figure 26). Across three ASC and four plots carbonyl C and alkyl C increased and aryl and O-alkyl C decreased with decreasing particle size. Alkyl C to O-alkyl C ratios (A/O-A; Baldock *et al.*, 1997) increased in the order fPOM < oPOM < fSi < cC < mSi < oPOM_{small} < fC (Figure 27). This sequence remained constant across the three ASC, but A/O-A increased with decreasing aggregate size for all fractions. Differences between individual fractions were pronounced for the fPOM and oPOM, but smaller for the oPOM_{small} and particle size fractions. oPOM_{small} had large values between 0.6 and 0.8 that were comparable to particle size fractions, while fPOM and oPOM exhibited lower values between 0.2 and 0.6. Across the majority of analysed fractions, Ug79 showed a slightly wider A/O-A compared to Ug99, Wg and Cg. Notable was that fPOM in fASC showed similar values to oPOM in mASC and fPOM of mASC similar values to oPOM in cASC.

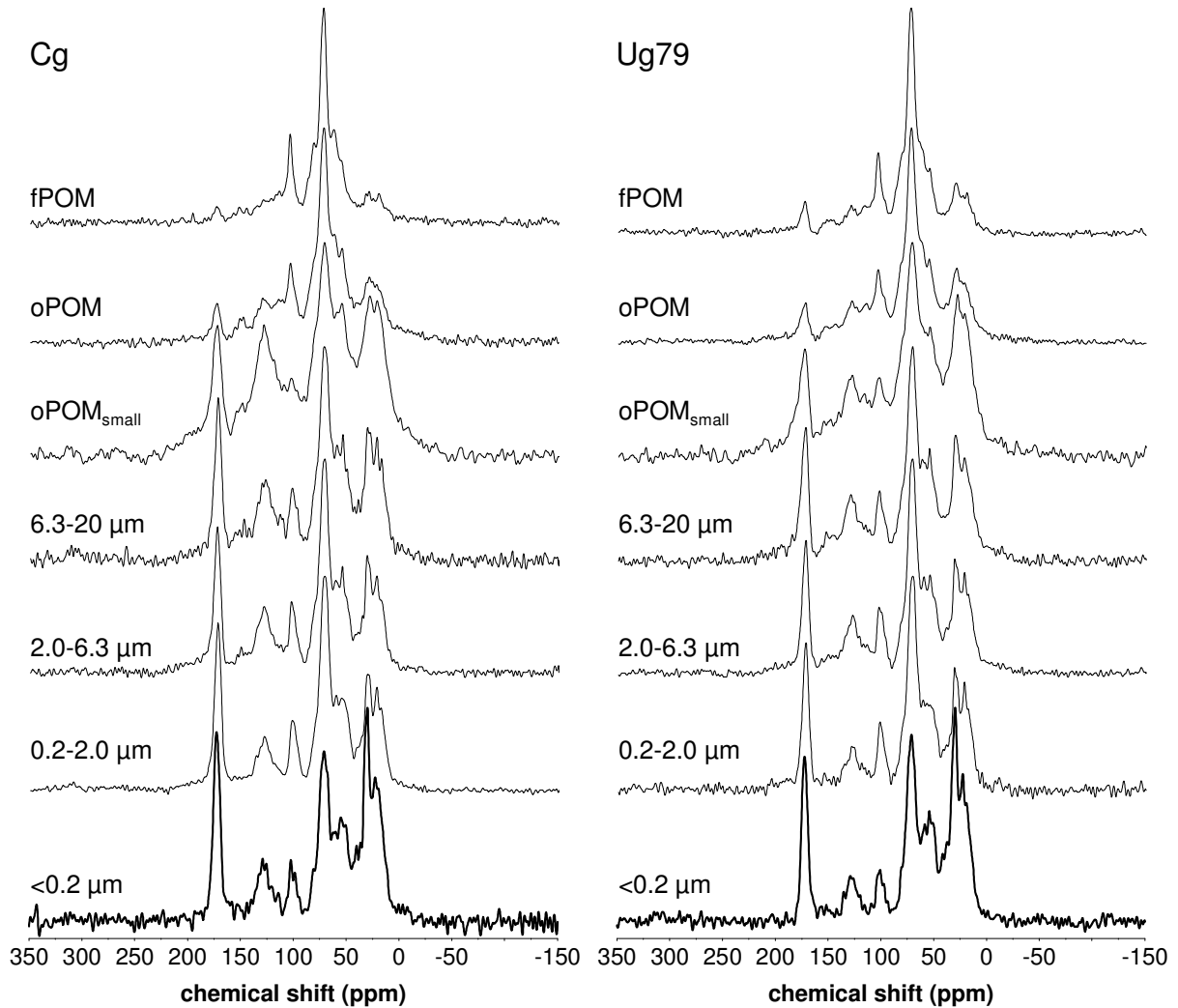


Figure 26: ^{13}C CPMAS NMR spectra of POM and selected particle size fractions of cASC in Cg and Ug79 (Cg = continuously grazed, Ug79 = ungrazed since 1979; cASC = 2000-6300 μm). A maximal line broadening of 10 Hz was applied.

Clearly different radiocarbon concentrations between all four plots, but no effects of aggregate size were found (Table 13 and Figure 28). Across all fractions, Ug79 had clearly larger radiocarbon concentrations compared with Cg. In both plots, oPOM was younger than oPOM_{small} and radiocarbon concentrations of particle size fractions decreased with decreasing particle sizes. Radiocarbon concentrations of the fractions ranged from 95.47 to 118.99 pMC (corresponding to radiocarbon ages from 375 ± 20 to modern). The fractions oPOM_{small} in mASC and fASC, cC and fC in Cg were older than 1954 with pre-bomb radiocarbon concentrations of less than 100 pMC.

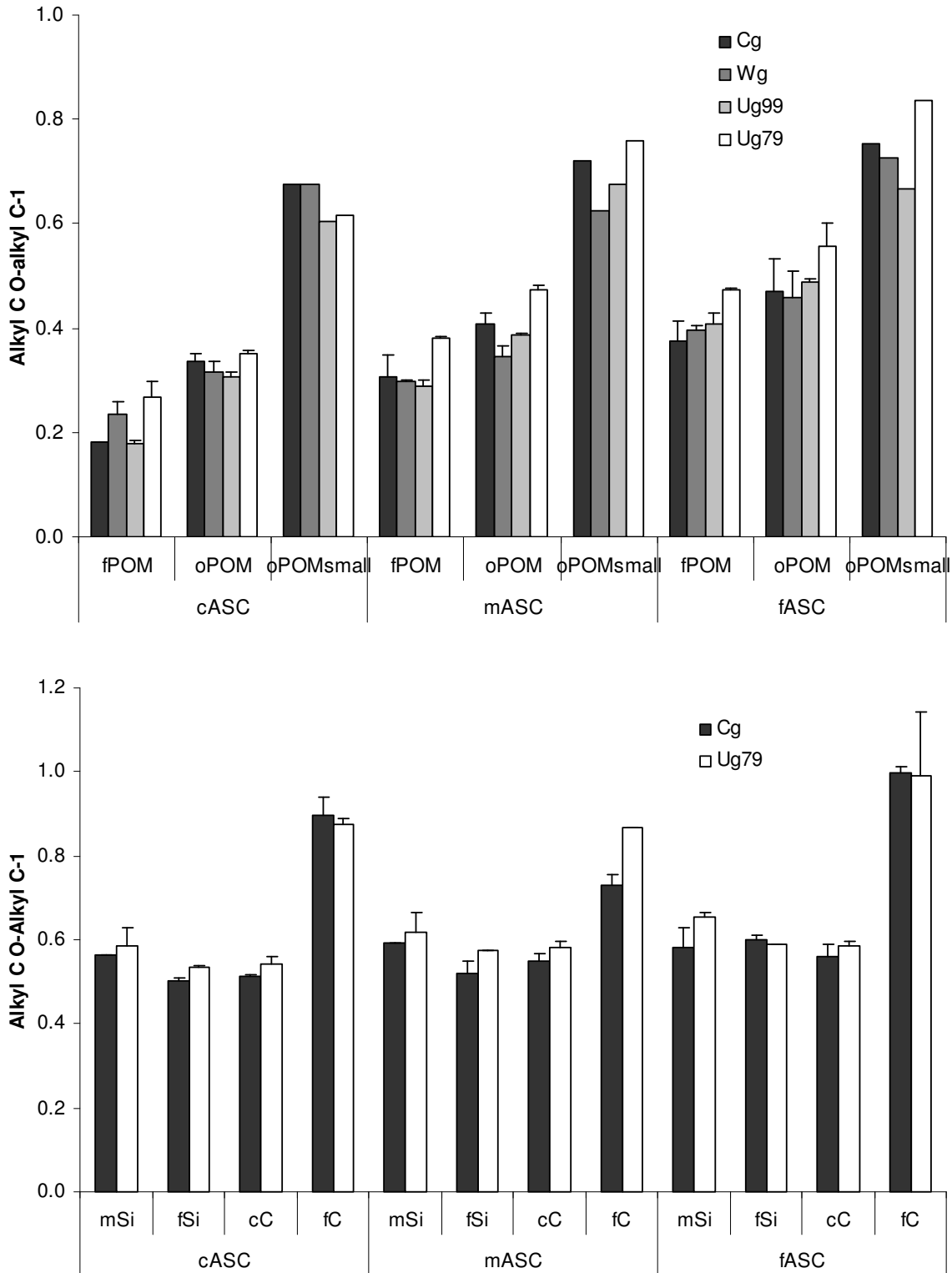


Figure 27: Chemical composition of POM and selected particle size fractions of three ASC as analysed by ^{13}C CPMAS NMR spectroscopy (Cg = continuously grazed, Wg = winter grazing, Ug99 = ungrazed since 1999, Ug79 = ungrazed since 1979; cASC = 2000-6300 μm , mASC = 630-2000 μm , fASC = <630 μm). All results are given as alkyl C to O-alkyl C ratios (Baldock *et al.*, 1997) and arithmetic means of two replicates; error bars give the standard deviation (no standard deviations were calculated for oPOM_{small}).

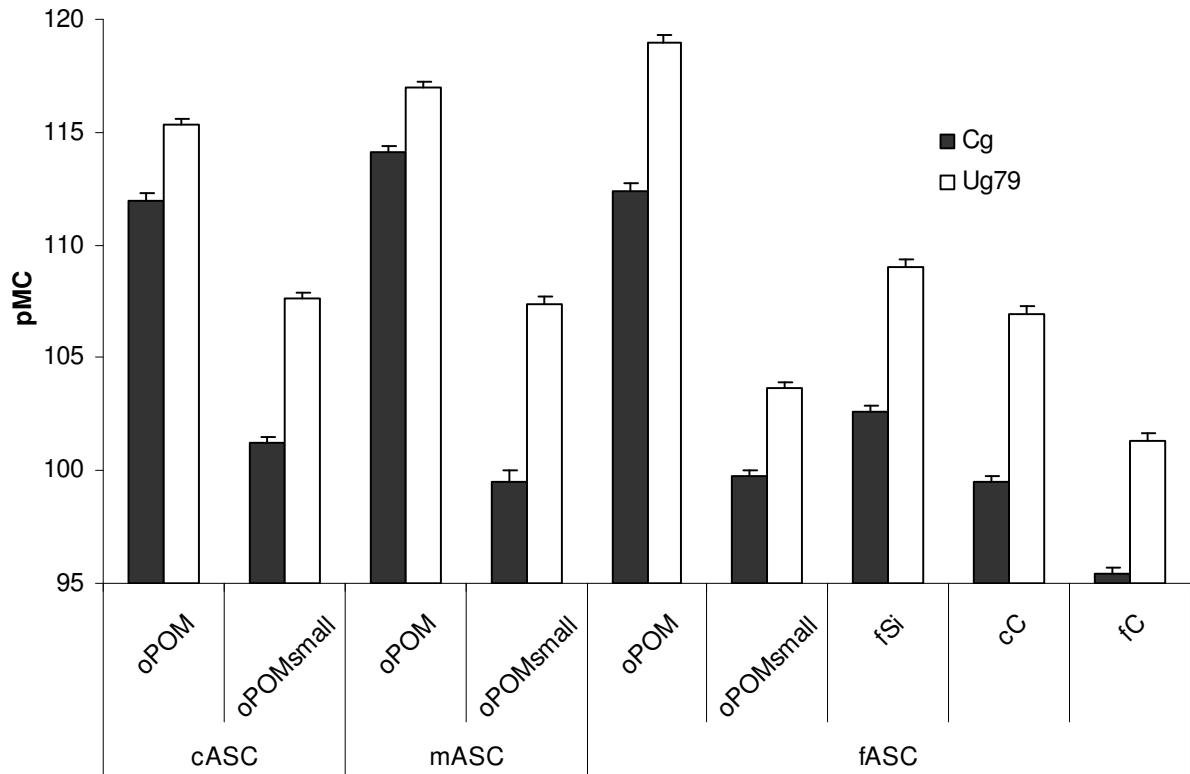


Figure 28: Radiocarbon concentrations of selected POM and particle size fractions of three ASC in Cg and Ug79 (Cg = continuously grazed, Ug79 = ungrazed since 1979; cASC = 2000-6300 μm , mASC = 630-2000 μm , fASC = <630 μm). Radiocarbon concentrations of mSi were not determined. Error bars give the 1 σ measurement uncertainty.

Neutral sugars contributed between 21% and 32% to ASC SOM. The quantity and composition of seven neutral sugars (rhamnose, fucose, arabinose, xylose, mannose, galactose and glucose) were different between Cg and Ug79, between different ASC and between POM and particle size fractions (Figure 29). Low concentrations of rhamnose and fucose (<5% of total neutral sugars) were found across all fractions. The mainly plant-derived neutral sugars arabinose and xylose, and the mainly microbial-derived neutral sugars galactose and mannose showed a diametrical behaviour across all fractions. High contributions of galactose and mannose were associated with low contributions of arabinose and xylose and vice versa. Therefore, all further results are given as (galactose + mannose)/(arabinose + xylose) ratios (GM/AX; Oades, 1984). GM/AX of POM varied between 0.3 and 1.3 and increased from fPOM to oPOM and with decreasing ASC. Particle size fractions had higher GM/AX values between 2.2 and 4.5 and decreased in the order mSi > cC > fSi > fC. Ug79 revealed slightly higher GM/AX values in seven of ten analyzed fractions.

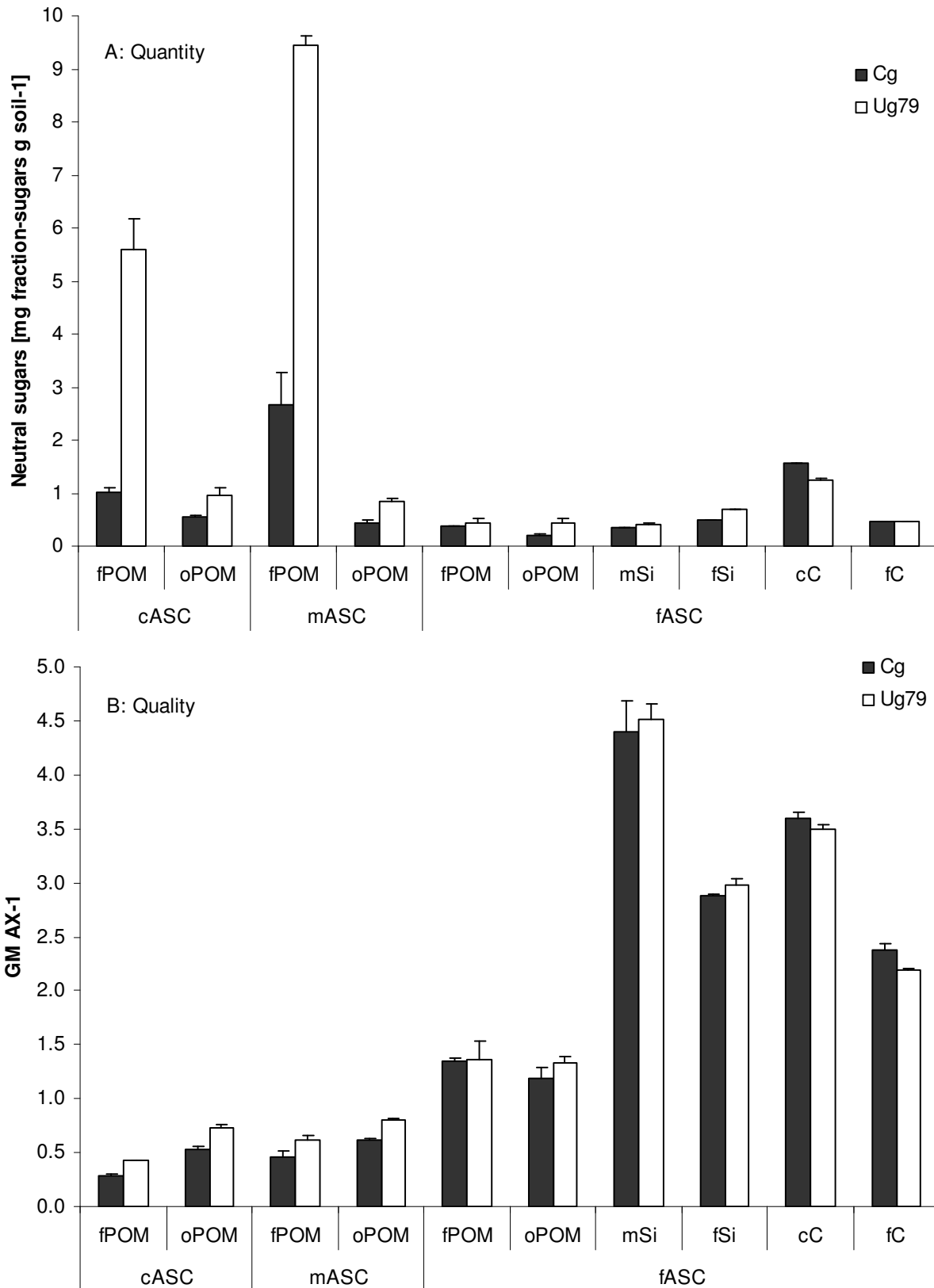
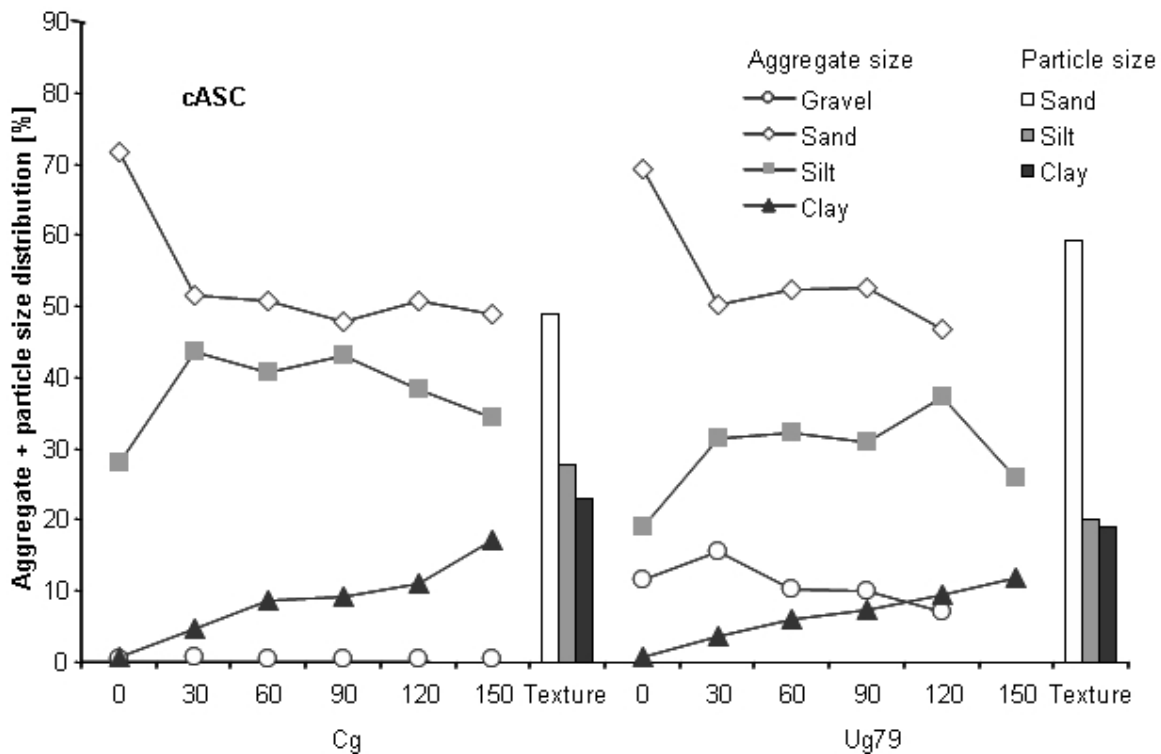


Figure 29: Quantity and quality of neutral sugars in selected POM and particle size fractions of three ASC in Cg and Ug79 (Cg = continuously grazed, Ug79 = ungrazed since 1979; cASC = 2000-6300 μm , mASC = 630-2000 μm , fASC = <630 μm). Qualitative results are given as galactose+mannose)/(arabinose+xylose) ratios (Oades, 1984) and mean values of four replicates (error bars represent the standard deviation).

6.1.2 Aggregate stability

Aggregate stability was different between Ug79 and Cg and between the three ASC (Figure 30). If no ultrasonic energy was applied, the particle size distribution of all six ASC was similar; the contribution of gravel- and sand-sized particles was greater, that of clay-sized particles smaller and that of silt-sized particles similar to particle size analyses. If 30 J ml^{-1} were applied, the contribution of gravel- and sand-sized particles decreased and that of silt- and clay-sized particles increased. Further increases of sonication energy did not affect the contribution of sand-sized particles. In general, the contribution of silt-sized particles decreased and that of clay-sized particles increased with increased sonication energy. Coarse and medium aggregates in Ug79 showed a greater resistance to sonication compared with Cg. Gravel-sized aggregates were abundant in cASC of Ug79, while no particles of this size were present in Cg. In mASC, the contribution of clay-sized particles in Ug79 was small and increased when 150 J ml^{-1} were applied. The contribution of sand-sized particles in mASC of Ug79 exceeded particle size analysis even at an energy input of 150 J ml^{-1} . Aggregates in Ug79 were more stable than in Cg and differences in stability decreased with decreasing aggregate size.



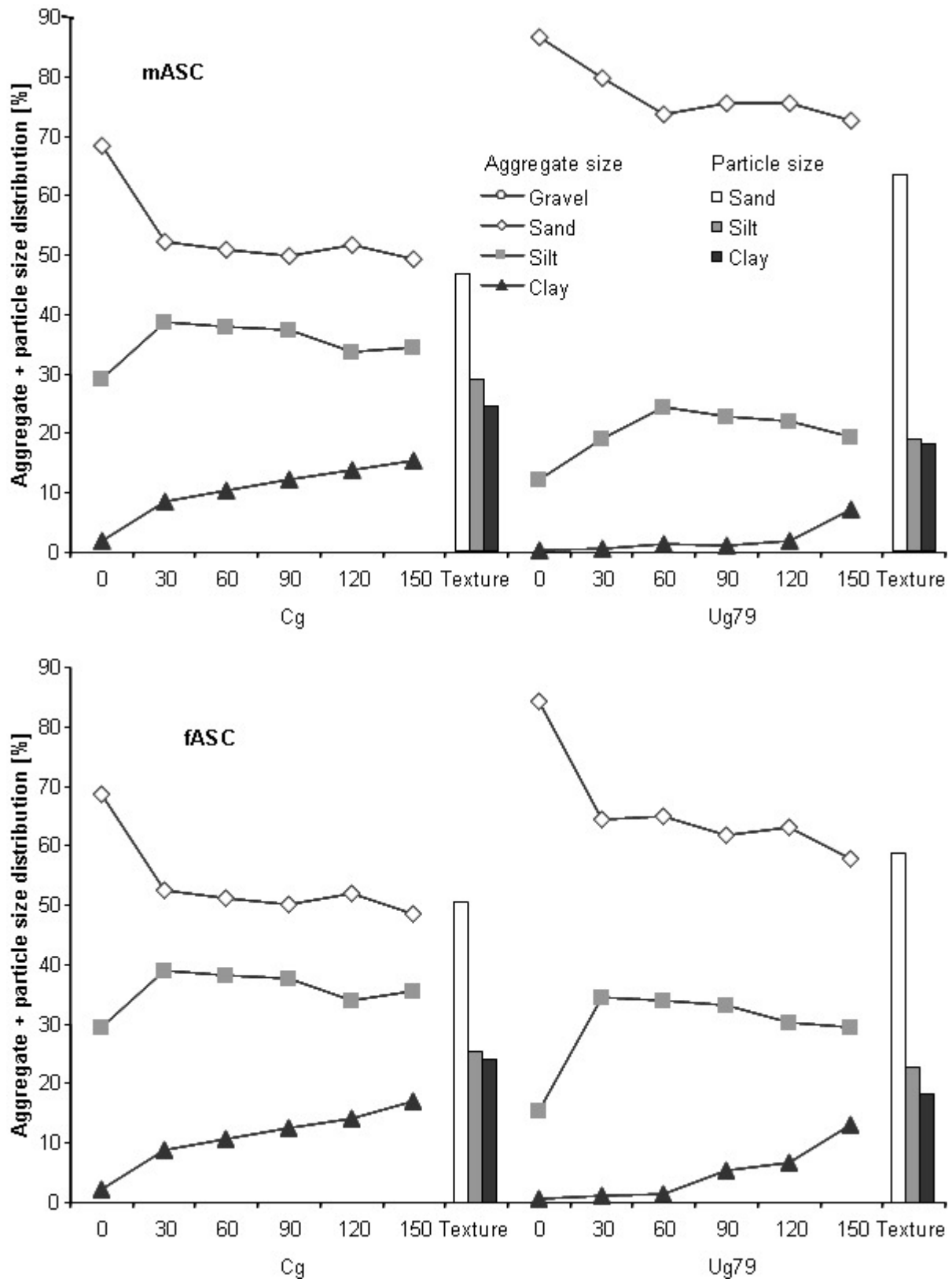


Figure 30: Aggregate stability of three ASC in topsoils of Cg and Ug79 as analysed by sonication (Cg = continuously grazed, Ug79 = ungrazed since 1979; cASC = 2000-6300 μm , mASC = 630-2000 μm , fASC = <630 μm). Amount of energy used was calculated using Equation 8.

6.2 Discussion

6.2.1 Impacts of grazing exclusion on topsoils

6.2.1.1 Quantity and distribution of SOM in POM and mineral fractions of steppe topsoils

Higher OM inputs as a consequence of grazing exclusion affected only OC amounts of POM (Table 12) and can be explained as a consequence of higher biomass production (Table 13), i.e. greater litter inputs. The increase was pronounced in cASC and mASC, with a larger contribution of POM OC to total SOC in Ug79 compared with Cg. Within the POMs, the effect decreased in the order fPOM > oPOM > oPOM_{small}. Many authors describe POMs as sensitive to management changes (Hassink *et al.*, 1997; Christensen, 2001), and especially the coarse POM pool reacts rapidly to management changes (Burke *et al.*, 1999; Tan *et al.*, 2007).

According to the empirical formula of Hassink & Whitmore (1997), these soils should have free capacities to sequester C in fine particle size fractions (Table 12). Despite this potential, no quantitative changes in mineral fractions were detected after 25 years of increased litter inputs. A mean carbon saturation of 68±8% was found for particles smaller than 20 µm in all four plots. This suggests that the C sequestration capacities of the mineral fraction <20 µm in these soils were saturated. Clay minerals in these soils consist predominantly of unweathered illite, which is characterized by a low surface area and low sorption capacities. It is assumed that these low surface clay minerals were not considered in the formula and the calculation overestimated the capacities. These findings support the assumption that organo-mineral associations can be saturated (Hassink & Whitmore, 1997; Baldock & Skjemstad, 2000).

To conclude, aggregate size fractionation followed by density and particle size fractionation produced fractions that were more sensitive to changing inputs after management changes than bulk soils. Higher litter input following grazing exclusion increased the OC amount in coarse POM. Total amounts and concentrations of SOM in particle size fractions were not affected by greater litter inputs from 25 years of grazing exclusion. This is ascribed to saturated C sequestration capacities of the mostly unweathered illite minerals.

6.2.1.2 SOM quality in POM and particle size fractions of steppe topsoils

Baldock *et al.* (1997) proposed the use of A/O-A ratios as a sensitive index of the extent of decomposition. Increasing alkyl C and decreasing O-alkyl C contributions with decreasing particle size were found across all grazing treatments, resulting in higher A/O-A ratios in smaller particle sizes (Figure 26 and Figure 27). Further evidence of successional decomposition “from coarse to fine particles” is found in neutral sugar concentrations, which contribute mainly to the O-alkyl region in ^{13}C CPMAS NMR spectra (Kögel-Knabner, 2002). Decreasing concentrations of neutral sugars from POM to particle size fractions were consistent with the decrease in the O-alkyl signal intensity (Figure 29). The decrease of neutral sugar concentrations is accompanied by an increase in GM/AX. According to Guggenberger *et al.* (1995) this can be seen as a consequence of a higher contribution of microbially derived neutral sugars with decreasing particle size. To summarise, both ^{13}C CPMAS NMR spectroscopy and neutral sugar analytics of all analyzed fractions show an increasing degree of decomposition with decreasing particle size, but no clear influence of grazing management (Figure 26, Figure 27, Figure 28, Figure 29).

Degrees of decomposition of POM increased in the order cASC < mASC < fASC (Figure 27). This is considered as a consequence of the predominant accrual of fresh OM in POM of coarse ASC. Greater litter inputs in ungrazed areas were predominantly incorporated in cASC and mASC (Table 12). POMs in cASC and mASC were more sensitive to management changes than particle size fractions. SOM quality was similar between differently grazed plots, but SOM quantity changed predominantly in coarse POM.

The most surprising result of this study is the higher post-bomb radiocarbon concentration of particle size fractions in Ug79 and especially the very young OM in fC in Ug79 (Figure 28). This fraction had a radiocarbon concentration of 101.3 ± 0.4 pMC, corresponding to a conventional age of less than 60 years, indicating a high contribution of young (post-bomb) OM. The same fraction in Cg has a radiocarbon concentration of 95.5 ± 0.2 pMC or a conventional age of 375 ± 20 years BP. Higher radiocarbon concentrations in Ug79 compared with Cg seem to be in contrast to generally higher A/O-A ratios in Ug79. Higher inputs of fresh OM (Table 13) are assumed to dilute the more decomposed fractions and decrease the A/O-A

ratio. This leads to the conclusion that despite similar decomposition processes, the turnover time in Ug79 was faster than in Cg. It is presumed that higher microbial activity in Ug79 stems from more favourable soil moisture and nutritional conditions in the ungrazed plot (Holt, 1997; Raiesi & Asadi, 2006).

To conclude, the qualitative analyses of SOM fractions corroborate the results regarding grazing effects on SOM quantity. Whereas particle size fractions were similar in OC amount and composition across all three ASC and between Cg and Ug79, POMs showed an increasing degree of decomposition with decreasing ASC. This is in line with the finding that inputs of OM are primarily incorporated in coarse ASC. Grazing cessation did not alter SOM forming processes, but affected the turnover of OC.

6.2.1.3 Stability of different aggregate size classes of steppe topsoils

Data shows strong effects of increased litter input due to grazing cessation on aggregate stability (Figure 30). While fASC showed comparable aggregate stabilities in Cg and Ug79, mASC and cASC were more stable in Ug79 compared with Cg. More evidences can be seen in a greater contribution of post-bomb radiocarbon in POM of Ug79 compared with Cg, pointing towards the protection of older material in more stable aggregates in the ungrazed plot (Figure 28). These findings are attributed to greater amounts of POM and neutral sugars in coarse ASC in Ug79 (Table 12 and Figure 29). In agreement with these findings, Pikul *et al.* (2007) found higher aggregate stabilities associated with high contributions of POM to SOM. POM quality was comparable in both plots and therefore seems not to affect aggregate formation. The A/O-A ratios of POMs increased with decreasing ASC (Figure 27). This is attributed to the predominant incorporation of undecomposed OM in coarse aggregates and faster turnover times of coarse aggregates. Similar results are described by John *et al.* (2005) and Christensen (2001) for temperate loamy soils under agricultural use. Further evidence can be seen in the fact that fPOM in fASC is chemically similar to oPOM in mASC, and fPOM of mASC has a comparable chemical quality to oPOM in cASC. Small aggregates are assumed to be stable and contain more decomposed POM. Higher litter inputs due to greater biomass production initiate the formation of coarse aggregates from the smaller aggregates. These coarse aggregates are less stable and have faster turnover times than small

aggregates, setting free formerly occluded and protected POM particles and small aggregates. Considering the concept of aggregate hierarchy, Tisdall & Oades (1982), Cambardella & Elliot (1993), Puget *et al.* (1995) and Six *et al.* (2004) showed that macroaggregates are predominantly affected by cultivation, while microaggregates are mostly unaffected. Grazing exclusion did not change the aggregate size distribution but POM quantities and aggregate stabilities of coarse ASC.

To summarise, coarse aggregates were less stable and had shorter turnover times than fine aggregates. Formation and stability of coarse aggregates was stimulated by high OM inputs after grazing cessation. Larger POM quantities resulting from grazing cessation are crucial for formation and stability of coarse aggregates.

6.2.2 Carbon sequestration in steppe topsoils - effects of grazing cessation

Cessation of overgrazing and implementation of moderate grazing intensity in grasslands are expected to increase C sequestration (Conant & Paustian, 2002). This study showed that higher biomass production and subsequent higher litter inputs from grazing cessation increased SOM quantities of certain fractions, especially in coarse POMs, but did not affect SOM quality (Table 12 and Figure 27). Grazing cessation did not only affect the amount of OM in POMs, which were used as sensitive indicators for forthcoming bulk soil OM changes, but also accelerated the turnover of the complete SOM system. It is assumed that the greater extent of decomposition (Figure 27), despite higher radiocarbon concentrations in Ug79 (Figure 28) is a consequence of faster turnover in ungrazed plots associated with greater microbial activity. Holst *et al.* (2008) found higher CO₂ production in Ug99 compared to Wg and related their findings to more favourable soil moisture conditions in the ungrazed plot. Holt (1997) described higher microbial and enzyme activities in ungrazed compared with grazed plots in semiarid Australia and attributed his findings to greater soil moisture and higher inputs of organic matter in ungrazed plots. Large radiocarbon concentrations revealed that increased litter inputs had already reached the fine clay fraction in Ug79, predominately in the form of microbial residues (GM/AX >2.0; Figure 29). Despite increasing radiocarbon concentrations, the OC quantity in these particle size fractions did not change. These results suggest

that the C sequestration limit of the particle size fractions in these soils was already reached. These results corroborate the theory of Hassink & Whitmore (1997) and Baldock & Skjemstad (2000), who claimed that pool of organo-mineral associations can be saturated.

Greater OM inputs from grazing cessation were mostly associated with increases in coarse POMs and triggered the formation and increased the stability of coarse aggregates. This OM pool is physically stabilised through spatial inaccessibility inside aggregates and contributes to the intermediate C sequestration potential of a soil (von Lützow *et al.*, 2006). Kölbl & Kögel-Knabner (2004) assumed a limitation of the POM pool occluded in aggregates. They attributed this to a limited capacity of soils to form aggregates. It is concluded that grazing cessation increased SOM amounts in Ug79, but a large portion was sequestered in the readily decomposable POM pool.

6.3 Conclusion

Physical fractionation is a useful tool to discriminate functional SOM pools. Clear differences between ASC were found and coarse aggregates (>630 µm) were identified as the ASC most sensitive to changes in OM input due to grazing management.

Grazing exclusion increased only the quantity of SOC stabilised in intermediate turnover POMs. Over 25 years no quantitative effects on smaller particle size fractions were found. Particle size fractions of these soils seem to be at the limit of their C sequestration capacity since higher inputs for 25 years did not change C saturation. The quality of SOM (¹³C CPMAS NMR spectroscopy, neutral sugars) was comparable across all fractions pointing towards similar mechanisms of SOM decomposition and alteration.

Grazing induced differences in aggregate stability were pronounced for coarse aggregates and were mainly driven by POM quantity. Effects of POM quality and particle size fractions were not verifiable.

Greater litter inputs after grazing cessation increased turnover rates. All pools were involved in C cycling, as can be seen in higher radiocarbon concentrations in

fine particle size fractions in ungrazed plots. SOM in the fine clay fraction was also involved in the increased C cycling.

Steppe ecosystems should not be referred to generally as C sinks. In this soil system, additional C was stored in intermediate but still relatively unstable POMs. When evaluating C sequestration potentials of soil systems, both quantity and quality of the particle size fractions play an important role and should be considered with caution.

7. Distribution of soil organic matter between fractions, aggregate size classes and horizons

7.1 Results

7.1.1 Mass, OC concentration and C-to-N ratio of POM and particle size fractions

Clear differences were found between the differently grazed plots for OC quantities across many physical fractions. These differences are mainly driven by different masses of fractions while OC concentrations were generally comparable between the four plots. Mean bulk soil OC recovery was $101\pm 23\%$ (Ah1: $96\pm 6\%$, Ah2: $92\pm 15\%$ and Ah3: $116\pm 34\%$) across all plots and ASC.

7.1.1.1 POM fractions

Clearly higher fPOM-OC amounts were found in ungrazed plots, arising from differences in mass, while OC concentration and C to N ratio were comparable between the different plots across all ASC and horizons (Table 14). Mean OC concentration of the fPOM varied between 180 ± 51 mg OC g⁻¹, 146 ± 29 mg OC g⁻¹ and 165 ± 13 mg OC g⁻¹ from Ah1 to Ah3. C to N ratios were significantly different between the ASC and narrowed from cASC to mASC to fASC in all three horizons. Mean C to N ratios of the horizons were similar and differed between 18.0 and 21.0. Total amounts of fPOM-OC in each ASC were highest in Ug79 and comparable between Ug99, Wg and Cg across all ASC and horizons. In each plot and horizon, total fPOM-OC amounts were highest in mASC, decreased to cASC and were lowest in fASC. Generally, total amount of fPOM-OC decreased from Ah1 to Ah3.

Total amounts of oPOM-OC were clearly higher in ungrazed plots as a result of different masses. OC concentrations were similar between all four plots across all ASC and the horizon mean decreased not significantly from 336 ± 31 mg OC g⁻¹ in Ah1 to 290 ± 71 mg OC g⁻¹ in Ah2 and to 241 ± 81 mg OC g⁻¹ in Ah3. C to N ratios of oPOM showed no differences between horizons but decreased from cASC to mASC to fASC (18 ± 2 to 16 ± 2 to 15 ± 2). Total amounts of oPOM-OC decreased in all plots from cASC to mASC and fASC and decreased from Ah1 to Ah2 to Ah3. The

Table 14: Mass distribution, OC concentration and C/N of soil fractions and contribution of OC of a specific fraction to the bulk soil of three aggregate size classes as affected by grazing intensity (Cg = continuously grazed, Wg = winter grazing, Ug99 = ungrazed since 1999, Ug79 = ungrazed since 1979; cASC = 2000-6300 μm , mASC = 630-2000 μm , fASC = <630 μm). All numbers give the arithmetic mean and standard deviation of two replicates. Potential C-loading of particles <20 μm was calculated using the empirical formula of Hassink (1997; Equation 7). Current C-loading is the sum of the measured OC concentrations of the fractions <20 μm .

Ah1		cASC (2000-6300 μm)				mASC (630-2000 μm)				fASC (<630 μm)			
		Cg	Wg	Ug99	Ug79	Cg	Wg	Ug99	Ug79	Cg	Wg	Ug99	Ug79
Soil	OC [mg g^{-1} soil]	17.7	17.5	19.7	20.8								
Aggregates	OC [mg g^{-1} soil]	19.1	18.4	23.0	33.2	25.4	23.2	26.3	40.5	16.5	16.5	18.1	17.7
	Contribution [%]	13.2	15.4	13.0	6.1	9.5	11.1	12.8	9.5	77.3	73.5	74.2	84.5
fPOM	Mass [mg g^{-1}]	12.8	6.7	24.9	65.9	64.9	48.9	56.4	129.8	11.2	9.3	8.3	11.7
	OC [mg g^{-1}]	241.9	140.4	233.1	273.3	150.6	165.4	182.6	218.7	117.6	114.4	148.7	177.6
	C/N	26.1	18.1	25.1	26.5	16.6	15.3	18.6	15.7	13.5	13.4	13.4	13.1
	OC [mg g^{-1} ASC]	3.1	0.9	5.8	18.0	9.8	8.1	10.3	28.4	1.3	1.1	1.2	2.1
	OC [mg g^{-1} total soil]	0.4	0.1	0.8	1.1	0.9	0.9	1.3	2.7	1.0	0.8	0.9	1.8
oPOM	Mass [mg g^{-1}]	5.7	6.3	6.6	8.7	5.2	4.5	7.4	6.2	3.7	3.1	7.9	5.9
	OC [mg g^{-1}]	330.6	340.2	341.5	371.9	336.7	337.6	353.0	376.6	283.6	279.8	318.2	366.9
	C/N	16.1	17.1	17.9	17.2	15.8	18.2	15.2	15.4	14.9	15.0	13.6	14.3
	OC [mg g^{-1} ASC]	1.9	2.1	2.2	3.2	1.7	1.5	2.6	2.3	1.1	0.9	2.5	2.2
	OC [mg g^{-1} total soil]	0.2	0.3	0.3	0.2	0.2	0.2	0.3	0.2	0.8	0.6	1.9	1.8
oPOM _{small}	Mass [mg g^{-1}]	2.5	6.8	6.6	3.3	1.8	2.2	3.6	6.1	1.7	1.5	4.8	1.7
	OC [mg g^{-1}]	221.1	126.9	201.7	185.6	197.1	214.1	201.6	158.0	205.0	204.8	210.2	173.8
	C/N	11.6	10.5	11.5	9.4	11.2	12.3	11.1	10.7	11.7	12.9	10.8	9.3
	OC [mg g^{-1} ASC]	0.6	0.9	1.3	0.6	0.4	0.5	0.7	1.0	0.3	0.3	1.0	0.3
	OC [mg g^{-1} total soil]	0.1	0.1	0.2	0.0	0.0	0.1	0.1	0.1	0.3	0.2	0.7	0.3
Sand	Mass [mg g^{-1}]	471.1	498.3	499.1	569.5	454.1	505.0	498.0	619.5	469.0	491.2	490.5	559.4
	OC [mg g^{-1}]	0.5	0.5	0.7	0.7	0.9	0.5	0.7	1.1	0.5	0.5	0.8	0.8
	C/N	5.9	6.6	8.3	9.3	7.0	4.7	6.3	9.0	5.2	5.3	7.6	7.5
	OC [mg g^{-1} ASC]	0.2	0.3	0.3	0.4	0.4	0.3	0.4	0.7	0.2	0.2	0.4	0.4
	OC [mg g^{-1} total soil]	0.0	0.0	0.0	0.0	0.0	0.0	0.0	0.1	0.2	0.2	0.3	0.4
Silt	Mass [mg g^{-1}]	334.3	320.8	310.4	239.0	322.2	282.2	296.6	171.3	348.4	330.4	353.3	288.5
	OC [mg g^{-1}]	12.8	14.9	14.4	18.9	14.3	14.7	15.7	26.0	14.3	16.0	14.7	20.6
	C/N	8.7	8.4	11.7	10.3	8.2	9.1	9.0	10.3	8.8	9.5	9.5	10.3
	OC [mg g^{-1} ASC]	4.3	4.8	4.5	4.5	4.6	4.2	4.7	4.5	5.0	5.3	5.2	5.9
	OC [mg g^{-1} total soil]	0.6	0.7	0.6	0.3	0.4	0.5	0.6	0.4	3.9	3.9	3.9	5.0
Clay	Mass [mg g^{-1}]	173.6	161.1	152.4	113.7	151.8	157.1	138.0	67.0	166.0	164.4	135.2	132.7
	OC [mg g^{-1}]	52.4	58.6	57.4	56.6	56.2	55.2	55.1	54.5	51.9	52.8	57.2	50.8
	C/N	7.5	7.2	7.8	7.5	7.3	7.5	8.0	7.1	7.6	7.3	7.9	7.1
	OC [mg g^{-1} ASC]	9.1	9.4	8.7	6.4	8.5	8.7	7.6	3.7	8.6	8.7	7.7	6.7
	OC [mg g^{-1} total soil]	1.2	1.5	1.1	0.4	0.8	1.0	1.0	0.3	6.7	6.4	5.7	5.7
C-loading of particles <20 μm (Hassink, 1997)	current [mg g soil^{-1}]	12.7	13.5	12.5	10.2	12.4	12.2	11.6	6.9	12.8	13.1	12.1	11.2
	potential [mg g soil^{-1}]	18.4	17.8	19.2	14.6	18.4	17.8	19.2	14.3	17.2	17.8	19.2	14.9
	Loading [%]	69	76	65	70	67	69	61	49	75	73	63	75
POM	[% of ASC OC]	29	21	41	66	47	44	52	78	16	14	26	26
Particle size	[% of ASC OC]	71	79	59	34	53	56	48	22	84	86	74	74
POM	[% of total OC]	22	19	33	39								
Particle size	[% of total OC]	78	81	67	61								

Table 14: continued

Ah2		cASC (2000-6300 µm)				mASC (630-2000 µm)				fASC (<630 µm)			
		Cg	Wg	Ug99	Ug79	Cg	Wg	Ug99	Ug79	Cg	Wg	Ug99	Ug79
Soil	OC [mg g ⁻¹ soil]	13.5	10.4	12.1	9.4								
Aggregates	OC [mg g ⁻¹ soil]	15.3	11.2	12.9	10.7	16.2	11.9	13.2	9.5	12.7	10.0	11.6	9.2
	Contribution [%]	17.1	16.7	19.8	9.6	10.4	10.7	12.5	9.8	72.5	72.6	67.8	80.6
fPOM	Mass [mg g ⁻¹]	12.4	3.7	10.2	22.6	37.8	13.9	15.2	30.7	2.8	2.2	2.0	3.8
	OC [mg g ⁻¹]	178.4	200.0	116.9	135.1	93.7	134.3	135.3	130.7	145.1	178.2	155.6	154.0
	C/N	28.7	23.6	33.7	36.1	14.4	20.3	17.8	21.1	15.3	15.1	13.8	12.3
	OC [mg g ⁻¹ ASC]	2.2	0.7	1.2	3.1	3.5	1.9	2.1	4.0	0.4	0.4	0.3	0.6
	OC [mg g ⁻¹ total soil]	0.4	0.1	0.2	0.3	0.4	0.2	0.3	0.4	0.3	0.3	0.2	0.5
oPOM	Mass [mg g ⁻¹]	3.6	2.0	2.1	4.0	3.5	1.5	2.4	2.6	1.5	0.8	1.5	3.7
	OC [mg g ⁻¹]	345.6	365.3	329.6	333.2	235.6	194.2	296.0	232.7	335.8	343.6	321.9	141.2
	C/N	18.5	18.3	18.3	23.2	16.9	17.9	14.8	18.3	16.4	15.2	13.8	13.3
	OC [mg g ⁻¹ ASC]	1.2	0.7	0.7	1.3	0.8	0.3	0.7	0.6	0.5	0.3	0.5	0.5
	OC [mg g ⁻¹ total soil]	0.2	0.1	0.1	0.1	0.1	0.0	0.1	0.1	0.4	0.2	0.3	0.4
oPOM _{small}	Mass [mg g ⁻¹]	5.7	5.2	4.3	0.5	3.2	3.0	3.3	0.8	2.7	5.1	1.7	0.8
	OC [mg g ⁻¹]	54.2	186.7	188.2	174.0	181.4	146.7	241.0	143.8	139.7	93.3	224.5	224.7
	C/N	12.7	12.1	11.6	12.2	13.2	12.4	11.0	12.7	13.8	12.6	11.0	11.3
	OC [mg g ⁻¹ ASC]	0.3	1.0	0.8	0.1	0.6	0.4	0.8	0.1	0.4	0.5	0.4	0.2
	OC [mg g ⁻¹ total soil]	0.1	0.2	0.2	0.0	0.1	0.0	0.1	0.0	0.3	0.3	0.3	0.1
Sand	Mass [mg g ⁻¹]	484.2	513.8	548.0	730.5	481.8	554.4	578.6	792.1	501.9	511.2	553.1	693.3
	OC [mg g ⁻¹]	0.4	0.3	0.4	0.2	0.4	1.9	0.4	0.2	0.4	0.3	0.4	0.2
	C/N	4.9	4.1	7.2	4.2	4.2	7.8	6.0	4.4	4.4	4.2	7.2	4.0
	OC [mg g ⁻¹ ASC]	0.2	0.1	0.2	0.2	0.2	1.0	0.2	0.2	0.2	0.1	0.2	0.1
	OC [mg g ⁻¹ total soil]	0.0	0.0	0.0	0.0	0.0	0.1	0.0	0.0	0.1	0.1	0.2	0.1
Silt	Mass [mg g ⁻¹]	323.3	303.3	288.3	156.5	310.2	273.0	267.8	108.6	318.4	311.2	296.1	187.4
	OC [mg g ⁻¹]	9.4	4.9	10.1	12.3	9.1	8.7	11.8	12.6	9.3	5.8	10.9	10.8
	C/N	7.3	4.8	12.3	8.9	6.8	7.3	9.5	8.8	7.5	5.8	11.4	7.4
	OC [mg g ⁻¹ ASC]	3.1	1.5	2.9	1.9	2.8	2.4	3.2	1.4	3.0	1.8	3.2	2.0
	OC [mg g ⁻¹ total soil]	0.5	0.2	0.6	0.2	0.3	0.3	0.4	0.1	2.2	1.3	2.2	1.6
Clay	Mass [mg g ⁻¹]	170.9	172.0	147.1	85.9	163.6	154.3	132.7	65.3	172.8	169.5	145.6	111.0
	OC [mg g ⁻¹]	48.7	41.5	47.9	48.8	50.3	38.4	46.6	50.0	48.1	40.8	47.8	51.9
	C/N	7.4	6.9	7.6	7.0	7.5	7.2	7.8	6.8	7.3	7.1	8.1	7.3
	OC [mg g ⁻¹ ASC]	8.3	7.1	7.1	4.2	8.2	5.9	6.2	3.3	8.3	6.9	7.0	5.8
	OC [mg g ⁻¹ total soil]	1.4	1.2	1.4	0.4	0.9	0.6	0.8	0.3	6.0	5.0	4.7	4.6
C-loading of particles <20 µm (Hassink, 1997)	current [mg g soil ⁻¹]	11.0	8.5	9.6	5.8	10.8	7.4	8.9	4.5	10.9	8.6	9.7	7.6
	potential [mg g soil ⁻¹]	17.0	17.4	15.9	11.7	17.0	17.4	15.9	11.7	17.0	17.4	15.9	11.7
	Loading [%]	65	49	60	50	64	42	56	38	64	49	61	65
POM	[% of ASC OC]	25	22	21	42	30	22	27	50	10	11	10	14
Particle size	[% of ASC OC]	75	78	79	58	70	78	73	50	90	89	90	86
POM	[% of total OC]	15	15	15	21								
Particle size	[% of total OC]	85	85	85	79								

Table 14: continued

Ah3		cASC (2000-6300 μm)				mASC (630-2000 μm)				fASC (<630 μm)			
		Cg	Wg	Ug99	Ug79	Cg	Wg	Ug99	Ug79	Cg	Wg	Ug99	Ug79
Soil	OC [mg g^{-1} soil]	9.3	9.0	10.4	5.3								
Aggregates	OC [mg g^{-1} soil]	9.5	9.3	10.6	8.6	10.2	9.5	10.3	6.6	9.2	8.9	10.3	4.8
	Contribution [%]	13.2	16.6	28.6	10.3	8.3	11.3	16.5	8.3	78.5	72.1	55.0	81.4
fPOM	Mass [mg g^{-1}]	3.4	4.4	3.9	13.9	11.4	8.8	7.6	18.1	1.6	1.4	2.5	1.9
	OC [mg g^{-1}]	139.7	173.2	182.1	176.8	148.7	161.1	163.6	171.7	150.1	179.0	164.1	165.9
	C/N	23.1	24.8	29.1	28.4	19.2	17.3	20.3	18.6	15.8	15.6	14.1	15.6
	OC [mg g^{-1} ASC]	0.5	0.8	0.7	2.5	1.7	1.4	1.2	3.1	0.2	0.3	0.4	0.3
	OC [mg g^{-1} total soil]	0.1	0.1	0.2	0.3	0.1	0.2	0.2	0.3	0.2	0.2	0.2	0.3
oPOM	Mass [mg g^{-1}]	1.2	1.5	3.0	10.6	0.7	0.7	2.7	2.1	0.7	0.6	8.0	0.5
	OC [mg g^{-1}]	316.7	294.6	175.5	188.4	298.2	360.7	139.4	238.5	268.1	289.6	78.8	238.3
	C/N	17.5	17.0	14.0	19.0	14.9	15.1	12.9	19.2	16.9	16.1	14.1	16.7
	OC [mg g^{-1} ASC]	0.4	0.4	0.5	2.0	0.2	0.2	0.4	0.5	0.2	0.2	0.6	0.1
	OC [mg g^{-1} total soil]	0.0	0.1	0.1	0.2	0.0	0.0	0.1	0.0	0.1	0.1	0.3	0.1
oPOM _{small}	Mass [mg g^{-1}]	18.0	7.5	1.8	3.0	23.6	13.9	1.9	0.2	19.7	10.4	2.6	0.4
	OC [mg g^{-1}]	42.5	126.1	260.5	106.6	35.4	66.3	265.8	281.7	44.1	71.1	196.5	222.4
	C/N	11.2	12.4	10.1	10.5	12.7	10.2	10.5	13.6	13.5	9.6	11.1	13.0
	OC [mg g^{-1} ASC]	0.8	0.9	0.5	0.3	0.8	0.9	0.5	0.1	0.9	0.7	0.5	0.1
	OC [mg g^{-1} total soil]	0.1	0.2	0.1	0.0	0.1	0.1	0.1	0.0	0.7	0.5	0.3	0.1
Sand	Mass [mg g^{-1}]	476.9	503.1	554.3	769.3	486.5	520.2	561.9	830.0	478.5	502.2	545.3	746.6
	OC [mg g^{-1}]	0.5	0.5	2.5	0.2	0.6	0.4	2.0	0.1	0.5	0.5	2.4	0.2
	C/N	7.3	8.4	39.1	4.1	8.0	6.7	36.8	3.2	7.9	8.2	39.6	3.4
	OC [mg g^{-1} ASC]	0.2	0.2	1.4	0.2	0.3	0.2	1.1	0.1	0.2	0.2	1.3	0.1
	OC [mg g^{-1} total soil]	0.0	0.0	0.4	0.0	0.0	0.0	0.2	0.0	0.2	0.2	0.7	0.1
Silt	Mass [mg g^{-1}]	337.5	324.1	312.0	128.9	324.0	302.5	295.8	92.4	336.7	326.7	312.3	155.7
	OC [mg g^{-1}]	6.3	5.3	10.7	6.8	6.1	5.6	10.0	6.6	6.1	6.0	10.2	5.5
	C/N	16.8	11.2	44.7	7.9	13.4	12.8	41.9	7.3	12.4	14.0	53.9	6.2
	OC [mg g^{-1} ASC]	2.1	1.7	3.3	0.9	2.0	1.7	3.0	0.6	2.0	2.0	3.2	0.9
	OC [mg g^{-1} total soil]	0.3	0.3	1.0	0.1	0.2	0.2	0.5	0.1	1.6	1.4	1.7	0.7
Clay	Mass [mg g^{-1}]	163.0	159.4	125.1	74.3	153.9	153.9	130.1	57.2	162.7	158.7	129.3	94.9
	OC [mg g^{-1}]	34.0	33.0	33.4	37.0	33.8	32.9	31.2	37.3	34.4	34.7	32.7	34.2
	C/N	7.9	8.5	7.7	6.6	8.3	8.4	7.7	6.5	8.4	8.3	7.4	6.2
	OC [mg g^{-1} ASC]	5.5	5.3	4.2	2.8	5.2	5.1	4.1	2.1	5.6	5.5	4.2	3.2
	OC [mg g^{-1} total soil]	0.7	0.9	1.2	0.3	0.4	0.6	0.7	0.2	4.4	4.0	2.3	2.6
C-loading of particles <20 μm (Hassink, 1997)	current [mg g soil^{-1}]	7.2	6.6	5.5	3.5	6.7	6.4	5.3	2.7	7.2	7.1	5.6	4.0
	potential [mg g soil^{-1}]	15.8	19.6	16.9	11.5	15.8	19.6	16.9	11.5	15.8	19.6	16.9	11.5
	Loading [%]	46	34	33	31	43	33	31	23	45	36	33	35
POM	[% of ASC OC]	17	23	16	56	27	27	21	56	14	13	15	11
Particle size	[% of ASC OC]	83	77	84	44	73	73	79	44	86	87	85	89
POM	[% of total OC]	16	17	16	23								
Particle size	[% of total OC]	84	83	84	77								

ungrazed plots had the highest total amounts of oPOM-OC in all ASC of Ah1. In Ah2 and Ah3, Ug99 was similar to the grazed plots while Ug79 had clearly higher total amounts. The difference between Ug79 and Ug99, Wg and Cg decreased with decreasing ASC.

Differently grazed plots showed no clear differences in total amount of oPOM_{small}-OC. OC concentrations were similar between the different ASC across all horizons and decreased not significantly from $192 \pm 27 \text{ mg OC g}^{-1}$ in Ah1 to $166 \pm 55 \text{ mg OC g}^{-1}$ in Ah2 and to $143 \pm 96 \text{ mg OC g}^{-1}$ in Ah3. High fluctuations of OC concentrations between the plots in Ah2 and Ah3 were balanced by diverging masses and resulted in comparable total amounts. C to N ratios of oPOM_{small} were similar between the different plots, ASC and horizons and varied between 9.3 and 13.8. Total amounts of oPOM_{small}-OC were not significantly different between plots and horizons, but decreased from cASC to mASC and were lowest in fASC. Ug79 showed clearly lower proportions of oPOM_{small}-OC in Ah2 and Ah3.

To summarise, ungrazed areas showed higher absolute and relative amounts of POM and especially fPOM in mASC and cASC in Ah1 when compared to the grazed plots Wg and Cg. Ug99 was similar to Wg and Cg in Ah2 and Ah3 and Ug79 became more similar to the other three plots with depth.

7.1.1.2 Particle size fractions

Subdivisions of organo-mineral particle size fractions (coarse, medium and fine) were comparable among each other with respect to OC concentration and C to N ratio and are shown as mean sand, silt and clay values (Table 14).

Sand fraction OC was quantitatively similar across differently grazed plots, ASC and horizons (Table 14). OC concentrations varied between $0.18 \text{ mg OC g}^{-1}$ and $1.88 \text{ mg OC g}^{-1}$, while C to N ratios differed between 3.2 and 9.3. Total amounts of sand-OC were also comparable across plots, ASC and horizons and highest values were found in the Ah1 of the ungrazed plots. The Ah3 sand fraction in Ug99 showed higher C concentrations (mean = 2.3 mg OC g^{-1}), wider C to N ratios in Ah3 (mean = 38.5) and higher total amounts of sand-OC as a consequence of carbonates (Table 2).

Silt fraction OC was quantitatively comparable between the different plots and ASC, but showed differences between the three horizons. OC concentration

decreased highly significant from 16.5 ± 3.7 mg OC g⁻¹ in Ah1 to 9.7 ± 2.4 mg OC g⁻¹ in Ah2 and was lowest in Ah3 with 7.1 ± 2.0 mg OC g⁻¹. Ug79 showed clearly higher OC concentrations in silt-OC of Ah1 and Ah2. C to N ratio of silt-OC was similar in Ah1 and Ah2 with 9.5 ± 1 and 8.2 ± 2 across all ASC and plots. In Ah3, Cg, Wg and especially Ug99 showed clearly wider C to N ratios between 11.2 and 53.9 due to the presence of carbonates (Table 2). Total amounts of silt-OC in ASC were comparable between the three ASC in each horizon, but generally decreased in the order Ah1>Ah2>Ah3. All plots had similar amounts in Ah1 (mean of Ah1: 4.8 ± 0.5 mg OC g soil⁻¹), but showed higher variation in Ah2 (2.4 ± 0.7 mg OC g soil⁻¹) and Ah3 (1.9 ± 0.9 mg OC g soil⁻¹). Ug79 had significantly lower total amounts of silt-OC in Ah3.

The clay fractions contributed most to the total OC of all particle size classes and across all plots, ASC and horizons. Clay fraction OC was quantitatively comparable between the different plots and ASC, but showed strong differences between the three horizons. OC concentration of the clay fractions decreased on the highest level of significance from 54.9 ± 2.5 mg OC g⁻¹ in Ah1 to 46.7 ± 4.2 mg OC g⁻¹ in Ah2 and to 34.1 ± 1.7 mg OC g⁻¹ in Ah3. C to N ratios remained constant across all horizons, ASC and plots at 7.5 ± 0.6 . Total amounts of clay-OC were similar between three ASC for all plots and decreased significantly from 7.8 mg OC g ASC⁻¹ in Ah1 to 6.5 mg OC g ASC⁻¹ in Ah2 and to 4.4 mg OC g ASC⁻¹ in Ah3. Cg, Wg and Ug99 showed comparable total amounts in ASC, while Ug79 had 12% to 53% lower amounts of clay-OC than each horizon mean. This difference between the plots is assumed to be the result of differences in texture. The C loading of particles <20 µm (Hassink, 1997) was calculated to consider differences in texture and produced different C sequestration potentials of particles <20 µm between 19.6 mg C g soil⁻¹ and 11.5 mg C g soil⁻¹. Despite diverging sequestration potentials, the current carbon saturation was in the same range between the plots and ASC for each horizon, but decreased highly significant from $68 \pm 8\%$ in Ah1 to $55 \pm 9\%$ in Ah2 and to $35 \pm 7\%$ in Ah3. This is in good accordance with decreasing OC concentrations and total amounts of OC in silt and clay fractions (Table 14).

To summarise, sand fraction revealed comparable C quantities between all plots and across all ASC and horizons, while silt fractions were different between the horizons. The clay fraction generally contained the highest amount of OC and

showed differences between the plots due to different textures. Despite diverging C sequestration potentials, current C saturation of particles <20 µm was comparable between the four plots, but decreased highly significant with depth.

7.1.1.3 Relative contribution of fractions to total OC

The relative contribution of total POM and particle size fractions to total OC showed clear effects of differently grazed plots, ASC and horizons (Table 15). Generally, the contribution of POM fractions to total OC decreased and of silt and clay fractions increased in the order mASC-cASC-fASC and Ah1-Ah2-Ah3. Cg and Wg showed similar proportions across all fractions, ASC and horizons while Ug79 had clearly higher POM and lower clay contributions. Ug99 showed comparable contributions as Ug79 in Ah1 and was equal to Cg/Wg in Ah2 and Ah3. No clear differences were found between Ug79 and the other plots for fASC in Ah2 and Ah3. In this ASC, all plots showed the same distribution of OC between the POM and particle size fractions. The sand fraction contained the lowest proportion of total OC with values between 1.1% and 2.9% and showed no effects of grazing intensity, ASC or horizon. Ug99 had clearly higher values in Ah3, where the sand fractions contributed 12.5% to total carbon as a consequence of carbonates.

Table 15: Relative percental contribution of POM-OC, sand-OC, silt-OC and clay-OC to ASC-OC and bulk-OC of three horizons (cASC = 2000-6300 µm, mASC = 630-2000 µm, fASC = <630 µm; Cg = continuously grazed, Wg = winter grazing, Ug99 = ungrazed since 1999, Ug79 = ungrazed since 1979).

Horizon	Fraction	Total soil				cASC				mASC				fASC			
		Cg	Wg	Ug99	Ug79	Cg	Wg	Ug99	Ug79	Cg	Wg	Ug99	Ug79	Cg	Wg	Ug99	Ug79
Ah1	POM	22	19	33	39	29	21	41	66	47	44	52	78	16	14	26	26
	Sand	1	1	2	2	1	1	1	1	2	1	1	2	1	1	2	3
	Silt	27	29	26	28	22	26	20	14	18	18	18	11	30	32	29	34
	Clay	49	50	40	31	48	51	38	19	34	37	29	9	52	53	43	38
Ah2	POM	15	15	15	21	25	22	21	42	30	22	27	50	10	11	10	14
	Sand	1	2	2	2	1	1	2	2	1	9	2	2	1	1	2	2
	Silt	22	17	26	21	20	13	23	18	17	20	24	14	23	18	28	22
	Clay	61	66	57	57	54	64	55	39	51	50	47	34	65	69	60	62
Ah3	POM	16	17	16	23	17	23	16	56	27	27	21	56	14	13	15	11
	Sand	3	3	12	3	2	2	13	2	3	2	11	2	3	3	13	3
	Silt	22	21	31	16	22	18	32	10	20	18	29	9	22	22	31	18
	Clay	60	60	40	58	58	56	40	32	51	53	39	33	61	62	41	68

7.1.2 Chemical composition of POM fractions

Chemical composition of POM fractions as analysed by ^{13}C -NMR spectroscopy was similar between the differently grazed plots but showed significant differences between different POM fractions, ASC and horizons.

The chemical composition of the fPOM fraction was different between the ASC and between the horizons (Table 16). The proportions of carboxylic C increased from coarse to medium to fine ASC in each horizon and from $7\pm 2\%$ in Ah1 to $8\pm 3\%$ in Ah2 and to $9\pm 2\%$ in Ah3. Aryl C was similar across the three ASC in each horizon, but increased from $16\pm 2\%$ in Ah1 to $17\pm 1\%$ in Ah2 and to $19\pm 1\%$ in Ah3. O-alkyl C contributed most to the fPOM spectra (between 65% and 50%) and decreased with decreasing ASC in all horizons and generally with depth. The decrease from Ah1 to Ah2 and Ah3 was not observed for mASC. Alkyl C behaved inversely to O-alkyl C and increased with decreasing ASC while it decreased from Ah1 to Ah2 and Ah3 for mASC and fASC. Alkyl to O-Alkyl ratios (A/O-A; Baldock *et al.*, 1997) showed no clear differences with depth, but increased from 0.2 ± 0.1 in cASC to 0.3 ± 0.0 in mASC and were highest in fASC with 0.4 ± 0.0 (mean values across all horizons). The contribution of alkyl C and O-alkyl C to the fPOM-spectra decreased from 79.4% in cASC of Ah1 with decreasing ASC and depth to 69.6% in fASC of Ah3.

Compared to fPOM, the oPOM generally contained more carboxyl C and alkyl C, less O-alkyl C and comparable proportions of aryl C. A/O-A ratios of oPOM fractions were wider than fPOM ratios and increased from 0.3 ± 0.1 in cASC to 0.4 ± 0.1 in mASC and were widest in fASC with 0.5 ± 0.1 (mean values across all horizons). Carboxyl C slightly increased with decreasing ASC and depth, ranging between 7.3 and 11.5%. Aryl C was comparable between the ASC or slightly increased with decreasing ASC and generally increased from $16\pm 2\%$ in Ah1 to $18\pm 2\%$ in Ah2 to $20\pm 2\%$ in Ah3. Relative proportion of O-alkyl C decreased with ASC and depth from 58.1% in cASC of Ah2 (57.2% in Ah1) to 43.8% in fASC of Ah3. Alkyl C behaved inversely to O-alkyl C and increased with decreasing ASC from $18.5\pm 2.3\%$ in cASC to $21.2\pm 2.0\%$ in mASC and to $23.5\pm 1.9\%$ in fASC, but showed no trend with depth. The contribution of alkyl C and O-alkyl C decreased with ASC and depth from 76.0% in cASC of Ah1 to 66.8% in fASC of Ah3.

Table 16: Chemical composition of POM fractions as analysed by solid state ^{13}C NMR spectroscopy (fPOM = free particulate organic matter, oPOM = occluded particulate organic matter, oPOM_{small} = occluded particulate organic matter <20 μm ; cASC = 2000-6300 μm , mASC = 630-2000 μm , fASC = <630 μm ; Cg = continuously grazed, Wg = winter grazing, Ug99 = ungrazed since 1999, Ug79 = ungrazed since 1979).

	cASC			mASC			fASC			
	Cg	Wg	Ug99	Cg	Wg	Ug99	Cg	Wg	Ug99	
A1h1										
220-160	3.2	0.1	6.1	0.7	5.6	0.0	5.7	0.1	7.6	0.8
160-110	14.0	0.3	16.2	0.4	18.8	0.2	12.8	0.2	16.9	1.0
110-45	70.1	0.4	62.9	2.0	64.1	0.3	64.2	1.5	57.8	0.5
45-10	12.7	0.0	14.8	1.0	11.4	0.4	17.2	1.6	17.7	2.3
Alkyl/O-Alkyl	0.2	0.0	0.2	0.0	0.2	0.0	0.3	0.0	0.3	0.0
220-160	5.9	0.6	8.4	0.5	8.3	0.6	6.5	0.1	7.3	0.8
160-110	15.7	0.1	18.5	0.2	18.3	0.5	14.5	0.4	15.3	0.9
110-45	58.6	0.2	55.5	1.1	56.2	0.5	58.4	0.0	55.0	0.3
45-10	19.8	0.8	17.5	0.8	17.3	0.5	20.5	0.3	22.4	1.3
Alkyl/O-Alkyl	0.3	0.0	0.3	0.0	0.3	0.0	0.4	0.0	0.4	0.0
220-160	12.9	14.5	13.7	12.3	11.0	15.9	11.9	11.9	12.8	11.0
160-110	20.6	20.8	23.1	16.1	23.5	22.4	14.0	14.0	19.2	23.5
110-45	39.7	38.6	39.4	44.3	40.3	36.8	42.1	42.1	39.5	40.3
45-10	26.8	26.1	23.8	27.3	25.2	24.9	32.0	32.0	28.5	25.2
Alkyl/O-Alkyl	0.7	0.7	0.6	0.6	0.6	0.7	0.8	0.8	0.7	0.7
A1h2										
220-160	3.4	0.9	8.1	0.1	5.7	1.1	4.9	0.9	6.3	0.9
160-110	14.2	2.1	17.8	0.0	18.5	0.7	15.5	1.2	16.5	0.6
110-45	67.7	3.3	56.6	9.1	64.4	2.3	62.3	3.7	61.4	1.1
45-10	16.2	1.8	17.5	9.2	11.4	0.5	17.3	1.6	15.7	0.4
Alkyl/O-Alkyl	0.2	0.0	0.3	0.2	0.2	0.0	0.3	0.0	0.3	0.0
220-160	5.5	0.6	9.4	0.5	10.4	1.6	5.5	0.3	6.0	0.6
160-110	15.0	0.0	17.6	0.0	20.0	0.5	15.4	0.4	15.3	0.7
110-45	61.9	1.4	55.1	1.6	51.1	0.9	64.1	0.9	58.7	0.0
45-10	17.5	0.8	17.9	1.1	18.5	0.1	14.9	0.2	20.0	1.2
Alkyl/O-Alkyl	0.3	0.0	0.3	0.0	0.4	0.0	0.2	0.0	0.3	0.0
220-160	10.8	15.4	16.7	12.3	19.0	19.5	10.1	10.1	10.4	19.0
160-110	22.8	29.3	23.5	24.0	32.4	21.5	20.2	20.2	22.6	32.4
110-45	40.6	30.8	34.2	40.5	26.6	33.3	41.1	41.1	40.6	26.6
45-10	25.8	24.4	25.5	23.0	22.0	25.7	28.5	28.5	26.3	22.0
Alkyl/O-Alkyl	0.6	0.8	0.7	0.6	0.8	0.8	0.7	0.7	0.6	0.8
A1h3										
220-160	7.0	0.9	9.3	1.8	4.3	0.7	7.1	1.1	7.8	0.9
160-110	18.6	0.7	17.5	1.5	18.9	2.0	19.3	0.4	18.8	0.1
110-45	60.7	0.1	61.1	1.8	68.1	4.2	55.7	3.8	60.8	1.9
45-10	13.7	1.5	12.1	1.5	8.7	1.4	17.9	2.3	12.5	0.9
Alkyl/O-Alkyl	0.2	0.0	0.2	0.0	0.1	0.0	0.3	0.1	0.2	0.0
220-160	15.0	10.9	0.5	8.4	0.9	8.8	0.6	0.6	14.2	0.0
160-110	18.5	18.5	0.4	18.6	0.3	19.1	0.5	19.4	19.7	18.2
110-45	42.6	51.1	0.4	54.9	1.0	55.7	0.0	41.4	49.0	46.8
45-10	23.9	19.5	0.3	18.1	0.2	16.3	1.1	24.9	20.5	22.2
Alkyl/O-Alkyl	0.6	0.4	0.0	0.3	0.0	0.3	0.0	0.6	0.4	0.0
220-160	18.1	16.7	16.1	16.3	18.3	15.8	11.8	11.8	19.1	18.3
160-110	28.3	30.9	21.2	23.4	33.0	20.9	25.5	25.5	29.5	33.0
110-45	25.6	28.6	37.9	36.3	25.4	37.7	38.6	38.6	26.5	25.4
45-10	27.9	23.9	24.8	24.0	23.3	25.6	24.0	24.0	24.9	23.3
Alkyl/O-Alkyl	1.1	0.8	0.7	0.7	0.9	0.7	0.6	0.6	0.9	0.9

Chemical quality of the oPOM_{small} fractions was significantly different to oPOM and fPOM fractions. This fraction contained more carboxyl C, aryl C and alkyl C, but showed lower proportions of O-alkyl C when compared to fPOM and oPOM. A/O-A ratios of oPOM_{small} fractions were wider compared to oPOM ratios, strongly increased with decreasing ASC (in Ah1 and Ah2) and slightly increased with depth from 0.7 ± 0.1 in Ah1, 0.7 ± 0.1 in Ah2 and 0.8 ± 0.2 in Ah3. Carboxyl C was similar across the ASC in each horizon and increased from $13\pm 2\%$ in Ah1 to $14\pm 4\%$ in Ah2 and $17\pm 2\%$ in Ah3. The proportion of aryl C was constant in Ah1 and Ah2 ($20\pm 4\%$ and $25\pm 4\%$) and increased in Ah3 from $26\pm 4\%$ in cASC to $27\pm 5\%$ in Ah2 and was highest in fASC with $29\pm 5\%$. O-alkyl C decreased with decreasing ASC and horizon from 40.5% in cASC of Ah1 to 30.7% in fASC of Ah3. Alkyl C increased with ASC but also decreased with depth. A/O-A widened with ASC and depth. Alkyl C and O-alkyl C contribution to oPOM_{small} spectra was constant across ASC in Ah1 and Ah2 ($67.1\pm 0.6\%$ and $60.8\pm 0.6\%$) but decreased from cASC to mASC and fASC in Ah3 (Ah3 mean value: $55.9\pm 1.8\%$).

To summarise, chemical composition of POM fractions was not different between grazing intensities. Degrees of decomposition increased with decreasing ASC and increasing depth as indicated by alkyl/O-alkyl ratios. Contribution of alkyl C and O-alkyl C both decreased with depth while carboxyl C and aryl C increased.

7.2 Discussion

7.2.1 Quantity and distribution of SOM in steppe soils as affected by grazing cessation

7.2.1.1 POM fractions

The results show clear differences in amount and distribution of OC between differently grazed plots (Table 14 and Table 15). Ug79 had higher absolute and relative contributions of POM OC across all horizons. Ug99 showed clearly higher relative and absolute proportions of POM-OC compared to Wg and Cg in Ah1 and was similar to the grazed plots in Ah2 and Ah3. These findings were amplified for fPOM and oPOM and in cASC and mASC, while all plots were similar for oPOM_{small} and in fASC. Higher belowground biomass production due to grazing cessation is

assumed to be the source for higher POM-OC amounts and contributions in ungrazed plots. Time effects of recovery of grasslands from grazing in terms of POM-OC accumulation are indicated by differences between Ug99 and Ug79, the latter showing higher contributions of POM-OC only in Ah1. The longer enclosure period at Ug79 resulted in a wider ramified rooting system and extended the rooting zone down to deeper soil horizons leading to higher absolute and relative POM amounts. In Ug79, species composition diversified, including deeper rooting species, while vegetation in Cg, Wg and Ug99 mainly consisted of shallow rooting grass species. Gao *et al.* (2008a) reported higher species richness, species diversity and aboveground net primary productivity in Ug79 compared to Wg. They also found different species compositions and functional groups, with especially higher abundances of deep rooting perennial forbs, shrubs and semishrubs in Ug79 (Gao *et al.*, 2008b). Gao (2007) found higher belowground biomass and cumulated root lengths in Ah1 of Ug99 and Ug79 and in Ah2 and Ah3 of Ug79 compared to Cg.

Higher absolute and relative POM amounts were found in coarse and medium aggregates compared to fine aggregates. It is assumed that cASC and mASC are more sensitive to landuse changes and possibly act as indicators for changing carbon cycling processes in soils. Similar findings are reported by Hassink *et al.* (1997) and Christensen (2001). Large aggregates have shorter turnover times and are built by smaller aggregates. Many authors (Tisdall & Oades, 1982; Cambardella & Elliot, 1993; Puget *et al.*, 1995; Six *et al.*, 2004) described smaller aggregates to be more stable and to be bound by coagulating agents as oxides, carbonates and OM to larger aggregates. During these forming processes free particulate OM can be included inside aggregates or aggregates form around OM, due to microbial excretion of coagulating non recalcitrant substances, and be stabilised temporarily. The data shows that these processes also take place in deeper soil layers. The fASC was similar between all plots and showed no effects of increased OM inputs while mASC and cASC contained large amounts of POM. The fASC is assumed either to take part in the C cycling but not increasing as the potential carbon sequestration of this fraction is reached or incorporation of fresh OM to take more time because of longer aggregate turnover times. Kölbl and Kögel-Knabner (2004) deduced an upper limit of soils to sequester OC in form of occluded POM. They attributed this to a limited capacity of soils to store POM in aggregates. Gulde *et al.* (2008) found

indications for a hierarchical carbon sequestration. Small aggregates saturated faster than large aggregates, which have not shown an upper limit of sequestration. But the authors assume this fraction to be also limited.

To conclude, grazing cessation increased the amount of OC in the POM fraction. This process predominately took place in coarse and medium ASC, started in the topsoil and reached deeper horizons after more than 5 years as a product of changes in species composition.

7.2.1.2 Mineral fractions

Higher absolute and relative amounts of OC were found in POM fractions of the ungrazed plots, but OC in mineral fractions was similar across the differently grazed plots. Moreover, Ug79 had significantly lower total OC contents in Ah2 and Ah3 compared to Ug99, Wg and Cg. The higher contributions of sand in Ah2 and Ah3 of Ug79 (Table 2) were considered by calculating the current carbon loading of particles <20 µm. Similar C loadings, OC concentrations and C to N ratios of particles <20 µm were found across all horizons and plots and the differences in texture are assumed to be responsible for the different levels of total carbon content. Nevertheless, 25 years of higher biomass production and input, proved by clearly higher POM contributions in Ug79, have not changed the amount of C in fine particle size classes, but clearly increased the relative and absolute amount of POM across all horizons. It is assumed that the particle size fractions are saturated and inputs above this sequestration limit are stored primarily in form of labile POM fractions, even in deeper soil layers. Chung *et al.* (2008) and Gulde *et al.* (2008) analysed the effects of increased OM inputs (higher plant inputs due to higher plant productivity following N application and manure application) on the OC contents of different fractions of topsoils. Both authors found higher C contents only in coarse particulate organic matter fractions and macroaggregates, but report fine particle size fractions to remain constant in C content. Carter *et al.* (2003) proposed that once the capacity level of particle size classes was saturated, further organic C and N accumulation was associated with the POM fraction.

According to the empirical formula of Hassink (1997), large capacities for C sequestration should be free in deeper soil layers (mean current carbon loading in Ah2: 55% and in Ah3: 35%; Table 14). But decreasing OC concentrations of silt and

clay fractions with depth across all plots and ASC and very low current carbon loadings were found in deeper soil horizons. Two different processes are assumed to be responsible for the saturated behaviour of fine particle size classes in deeper horizons despite free potential sequestration capacities. The first assumption is that the empirical formula overestimated the real carbon sequestration capacities. In contrast to Hassink, other groups assumed C sequestration in particle size classes not to be related to the amount of silt and clay but to be related to specific surface area (Mayer, 1994; Kiem & Kögel-Knabner, 2002) or quantity and quality of oxides (Eusterhues *et al.*, 2005; Kleber *et al.*, 2005). Clay mineralogy as a first indicator for surface area was comparable between the horizons or contributions of clay minerals with higher specific surface areas even increased with depth (Table 5). Iron quantity and quality was comparable between plots and horizons (Table 3) or iron contents even decreased with depth. The potential carbon sequestration of a certain soil is assumed to be the product of many parameters like texture, clay mineralogy, specific surface area and quality and quantity of oxides and is therefore too complex to be estimated with a general empirical formula. Therefore, the potential carbon sequestration is supposed to be overestimated. Further it is suggested that OM decomposition and incorporation in steppe soils is retarded by the dry and cold climate (Gregorich *et al.*, 2006; Liu *et al.*, 2006). Zhao Y. (personal communication) found clearly lower water contents in deeper soil horizons compared to the topsoil of the studied plots. It is proposed that this water deficiency in deeper soil layers slows the decomposition process and delays the incorporation of OM in fine particle size classes of deeper horizons. 25 years of grazing cessation may be too short a period to increase the OC concentrations of fine particle size fractions in deeper soil horizons - effects of land use changes take longer periods to change the carbon saturation of deeper horizons in semiarid steppe soils. Giese *et al.* (2008) studied the litter decomposition dynamics in the same plots using litterbags and found soil water content to be the best predictor of root litter decomposition. They found clearly higher amounts of remaining root litter in dry years compared to wetter years.

To summarise, particle size fractions showed no quantitative effects of higher OM inputs. Particle size fractions seem to be saturated and the potential carbon sequestration of deeper soil horizons was overestimated. Carbon sequestration potentials of deeper soil layers should be assessed with caution and not derived from

topsoils. There is a general lack in knowledge of carbon sequestration potentials and stabilisation processes of deeper soil layers.

7.2.2 Effects of grazing cessation on the quality of POM fractions in steppe soils

Higher OM inputs due to grazing cessation did not affect the chemical quality of POM fractions as analysed by solid-state ^{13}C NMR spectroscopy. No clear differences of chemical composition were found between differently grazed plots (Table 16). This is in line with Ganjegunte *et al.* (2005), who analysed the effect of reduced grazing intensity on the chemical composition of fulvic and humic acids with solid-state ^{13}C NMR spectroscopy and found no significant differences.

But the results show clear differences between POM fractions, ASC and horizons. O-alkyl C decreased while alkyl C, carboxyl C and aryl C increased in the order $\text{fPOM} < \text{oPOM} < \text{pPOM}_{\text{small}}$ and $\text{cASC} < \text{mASC} < \text{fASC}$. OM predominately enters the soil system in form of the coarse fPOM and is subsequently decomposed, occluded in aggregates and set free again when coarse aggregates deteriorate. Beside physical breakdown, chemical degradation reduces the proportion of readily decomposable substances as carbohydrates (mainly represented by O-alkyl C) and increases the proportion of recalcitrant structures (Figure 31; carboxyl C, aryl C and alkyl C). Using solid-state ^{13}C NMR spectroscopy, Golchin *et al.* (1994) and Kölbl and Kögel-Knabner (2004) found occluded light fraction and POM to contain more alkyl C and less O-alkyl C than the free light fraction and POM. They suggested that during the inclusion of occluded OM, there is a selective decomposition of carbohydrates and relative enrichment of more stable OM compounds compared with free OM. These findings corroborate the theory of aggregate hierarchy and of faster turnover times with coarse aggregates while smaller aggregates are more stable (Puget *et al.*, 1995; Christensen, 2001; John *et al.*, 2005). Gregorich *et al.* (1996) describe similar findings of hierarchical decomposition of litter inputs using solid-state ^{13}C NMR spectroscopy. Baldock *et al.* (1997) proposed the alkyl C/O-alkyl C ratio (A/O-A) as a sensitive index of the extent of decomposition. Simpson *et al.* (2008) corroborate these findings and evaluated the potential of CPMAS NMR for assessment of SOM degradation compared to specific SOM biomarkers. Following their results, A/O-A showed comparable degrees of decomposition as source-specific biomarkers and

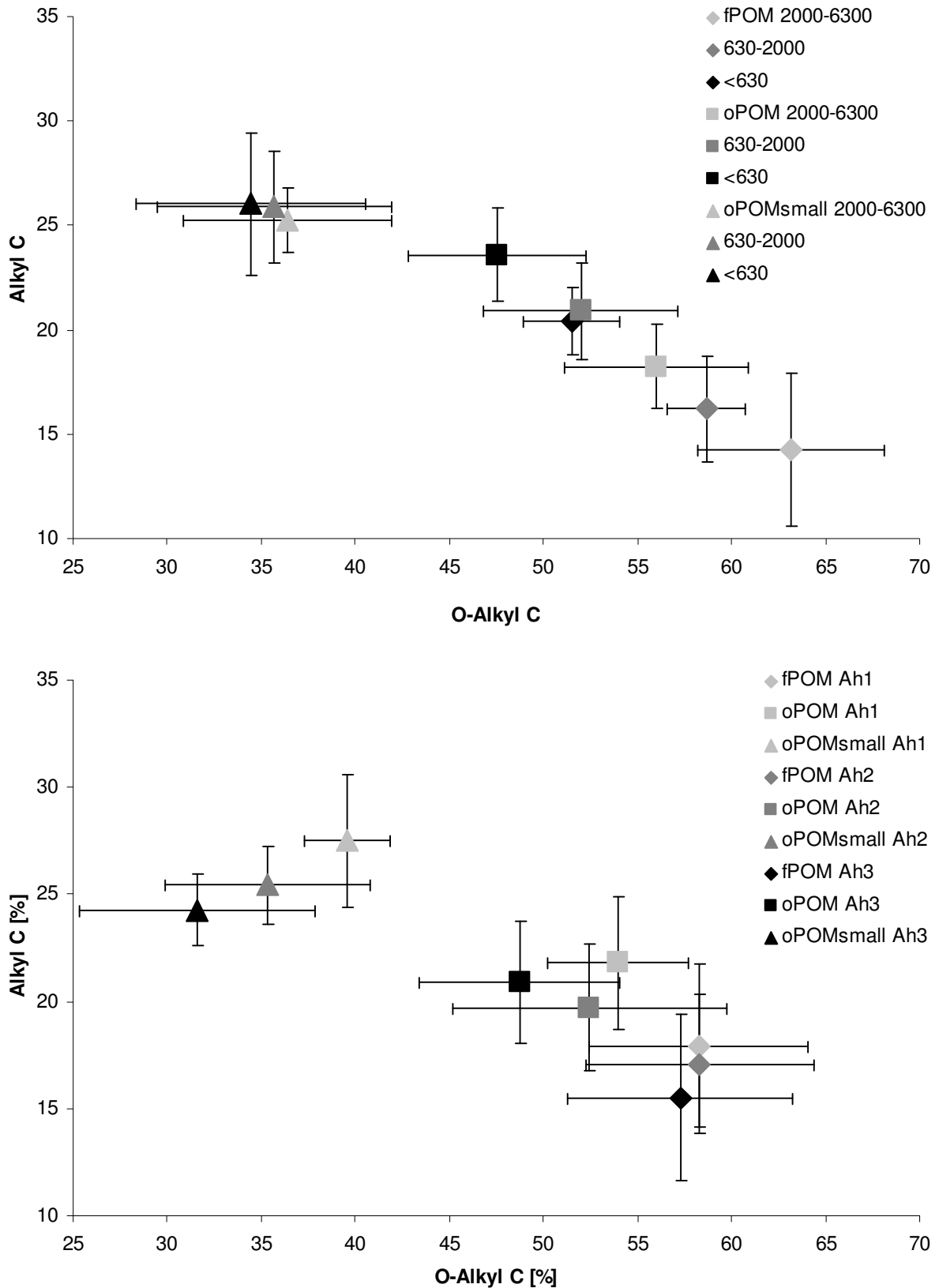


Figure 31: Chemical composition (solid state ^{13}C NMR spectroscopy) of POM fractions as affected by aggregate size (A) and sampling depths (B) (fPOM = free particulate organic matter, oPOM = occluded particulate organic matter, oPOM_{small} = occluded particulate organic matter <20 μm).

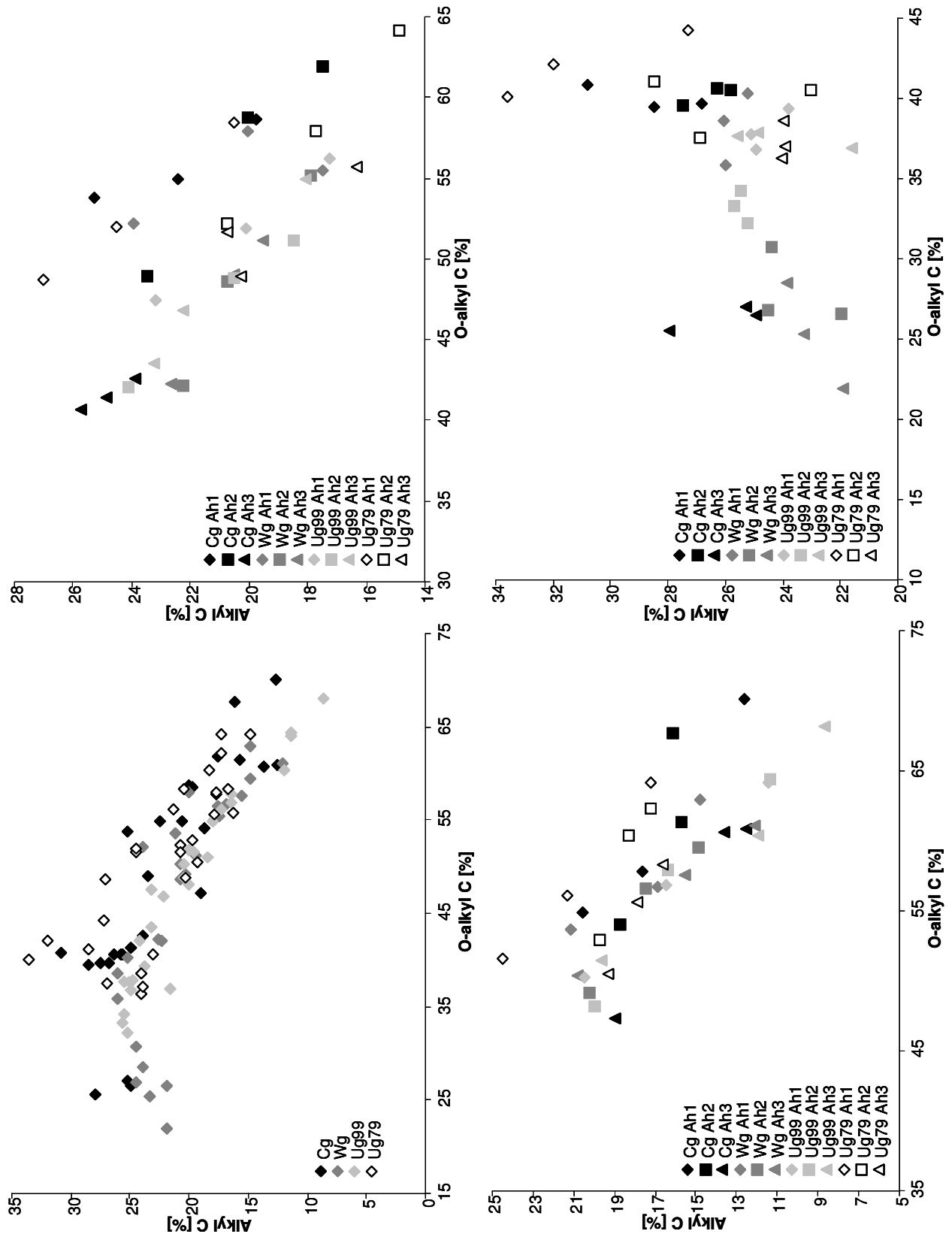


Figure 32: Chemical composition of POM fractions as analysed by solid state ^{13}C NMR spectroscopy (Cg = continuously grazed, Wg = winter grazing, Ug99 = ungrazed since 1999, Ug79 = ungrazed since 1979; fPOM = free particulate organic matter, oPOM = occluded particulate organic matter, oPOM_{small} = occluded particulate organic matter <20 μm).

were a useful tool for the assessment of the degradation stage of bulk SOM. Recalcitrant structures accumulated in the oPOM_{small} of the studied samples, with clearly higher percentages of alkyl C, aryl C and carboxyl C compared to fPOM and oPOM fractions and it is assumed that the oPOM_{small} is a preliminary endstage of OM decomposition.

Besides increasing stages of decomposition (A/O-A) with decreasing ASC and fraction, contributions of O-alkyl C and alkyl C decreased (from 75% in Ah1 to 51% in Ah3; Figure 31) and contributions of carboxyl C and aryl C increased with depth. Higher inputs of unaltered OM (fPOM) dilute the more decomposed SOM in Ah1 and Ah2, but in Ah3 only the more recalcitrant fractions were found (Figure 32). Higher contributions of O-alkyl C and alkyl C in oPOM_{small} of Ah2 and Ah3 of ungrazed plots were attributed to higher OM inputs in ungrazed plots due to grazing cessation (Figure 32). This is in good accordance with the findings of higher POM contributions (Table 14 and Table 15) and generally higher radiocarbon concentrations (Table 2) in deeper horizons of ungrazed plots. Moreover, it is assumed that higher inputs of root exudates following deeper rooting species led to higher contributions of O-alkyl C and alkyl C in deeper horizons of ungrazed plots. When using the A/O-A ratio, it should be taken into account that this ratio only considers two chemical shift regions, but the more recalcitrant fractions of aryl C and carboxyl C are disregarded. Comparable findings are not possible when just using A/O-A ratios.

To summarise, POM is decomposed hierarchically with ASC in steppe soils. POM decomposition is similar in different depths of steppe soils and no evidence were found for changing decomposition processes due to higher OM inputs following grazing cessation. Ungrazed plots had higher O-alkyl C and alkyl C contributions in deeper soil layers due to higher OM inputs through root litter and exudates.

7.2.3 Carbon sequestration in steppe soils

Our results showed higher relative and absolute amounts of POM in topsoils of ungrazed plots compared to grazed plots (Table 14 and Table 15). We ascribe this to higher inputs of OM following the recovery of vegetation after grazing cessation (Table 13). Higher POM amounts in subsoils predominate in the long-term ungrazed plot Ug79 and were ascribed to higher inputs of root-OM following a change in species composition towards deeper rooting plant species after long-term cessation

of grazing. These findings underline the importance of deeper soil layers for carbon sequestration - a topic that has not yet received much attention, but should be considered when sequestration potentials are to be assessed (Batjes, 1996; Jobbagy & Jackson, 2000; Rumpel *et al.*, 2002; Don *et al.*, 2008). This conclusion also corroborates the hypothesis of many authors who calculated carbon sequestration potentials and concluded that large amounts of OC can be stored in grazed steppe soils when grazing is abandoned or land-use management is improved (Conant & Paustian, 2002; Conant *et al.*, 2003; Derner & Schuman, 2007).

But in contrast to the POM fractions, the particle size fractions did not change quantitatively after 25 years of grazing cessation and higher litter inputs, neither in topsoils nor in subsoils. This is interesting as fine particle size fractions are of great importance for the long-term stabilisation of OM (von Lützow *et al.*, 2006) and may become even more important in deeper soil layers (Kaiser *et al.*, 2002). Our data showed decreasing current carbon loadings in subsoils and we assume these fine particle size fractions to be saturated. An upper limit of carbon sequestration in particle size fractions has been proposed by many authors (Hassink, 1997; Carter *et al.*, 2003; Kleber *et al.*, 2005; Stewart *et al.*, 2008). In deeper layers of our soils neither the empirical formula based on the quantity of fine particle size classes, nor the quantity and quality of iron oxides or clay mineralogy explained the overestimation of carbon sequestration capacities. We assume soil moisture and temperature to slow OM decomposition processes and to delay the incorporation of OM in particle size classes. Increased inputs of undecomposed OM due to grazing cessation are predominately stored in readily decomposable POM fractions. These results show that the assumption of increasing C sequestration following grazing cessation in grasslands is true for the total amount of C in the soil, but more emphasize has to be placed on the involved pools and stabilisation mechanisms. Overestimated C sequestration potentials in particle size classes together with the predominant stabilisation of fresh inputs in the readily decomposable POM pools will result in large sequestration capacities. But these capacities are not stable in the long-term and a climate change to wetter conditions or strong changes in management system may result in the relatively fast mobilisation of large amounts of C that was stored in the readily decomposable POM fraction. We conclude that

different pools and the related stabilisation mechanisms should be considered in all soil horizons separately when effects of land-use change are to be evaluated.

7.3 Conclusion

Grazing cessation led to increased amounts of coarse and medium POM in topsoils (<10 cm) already 5 years after grazing cessation. It is assumed that the recovering vegetation is responsible for greater OM inputs leading to higher amounts of POM in topsoils shortly after grazing cessation. Amounts of coarse and medium POM were elevated in subsoil horizons (>25 cm) after 25 years of grazing cessation, but not after 5 years. This was ascribed to higher root inputs of deeper rooting plant species becoming more abundant following a shifting plant community composition during long-term grazing cessation. OM in particle size fractions did not change quantitatively after grazing cessation in any horizon. The fine particle size fractions seem to be saturated or the incorporation of OM from fresh inputs into this fraction to take longer than 25 years. It can be concluded that greater OM inputs following grazing cessation were primarily stored in POM fractions. Chemical composition of POM fractions was analysed using ^{13}C CPMAS NMR spectroscopy and showed generally comparable results between all plots and horizons. The degree of decomposition increased with depth and predominately with decreasing aggregate size corroborating the theory of aggregate hierarchy. This study showed that semiarid steppe soils can sequester OC when grazing is abandoned and also subsoils may play an important role in the carbon sequestration of these ecosystems when management is improved in the long-term. But as a large proportion of the sequestered OM in top- as well as in subsoils is stored in the readily decomposable POM pool, the potential of semiarid steppe soils to act as carbon sinks has to be scrutinised.

8. Conclusion

The main focus of this dissertation was to understand how grazing and especially grazing cessation affect the quantity, quality and the distribution of SOM and its subsequent effects on soil aggregation in a semiarid steppe ecosystem. At first this study statistically confirmed the detrimental effects of heavy continued grazing on topsoils (0-4 cm) that lead to desertification in semiarid steppe ecosystems. It was shown that the recovery of degraded areas after grazing cessation started with the amelioration of vegetation. Individual plants act as nucleus of recovery by increasing the litter input and the accumulation of wind-blown materials. While the amelioration of chemical and physical topsoil properties was detected after 25 years of grazing cessation, the spatial distribution of vegetation showed first evidence of improvement already 5 years after grazing cessation. The subsequent larger litter inputs in ungrazed topsoils (0-10 cm) were predominately stored in the readily decomposable POM fractions. These higher POM amounts in ungrazed topsoils increased the abundance and the stability of coarse and medium aggregates in the ungrazed topsoils. Together with the higher soil cover by undisturbed vegetation this reduces the erodibility of topsoils and therefore reduces the erosion of fertile soil material and the formation of dust storms. In contrast to the POM fractions, particle size fractions in topsoils did not change quantitatively after grazing cessation. It is assumed that these fractions reached their carbon sequestration potential and were saturated. Despite this saturation, higher radiocarbon concentrations of these particle size fractions in Ug79 showed that the pool of organo-mineral associations is taking part in the carbon cycling faster than expected. This pool is generally taken as stable and to be slow-changing because of the intimate association of organic and inorganic matter. But this study gave evidence that this assumption has to be questioned and organo-mineral associations are not that stable and slow-changing. Deeper soil horizons were also affected by grazing cessation. Higher OM inputs in ungrazed plots have reached deeper soil horizons (>10 cm) after 25 years of grazing cessation and were predominately stored in the POM fractions. These findings are very interesting as the grazed steppe ecosystems are discussed as global carbon sinks that may sequester and more important stabilise large amounts of carbon also and especially in deeper soil layers. But as the reported higher inputs in deeper soil layers were also stored

predominately in the readily decomposable POM fractions, their long-term stabilisation has to be questioned.

The sampling design in combination with geostatistical analyses proved to be a suitable tool to detect impacts of grazing cessation on topsoil and vegetation parameters by assessing their spatial distribution. The large-scale sampling provided useful information on topographical effects, while small-scale sampling gave clear evidence for grazing-induced processes that would have not been detected without geostatistical analyses. Physical fractionation has been used previously to identify sensitive fractions and pools of the SOM. But in combination with an aggregate size separation the density and particle size fractionation provided a deeper insight into the carbon cycles and stabilisation mechanisms and into the formation and stabilisation of aggregates in this ecosystem.

Finally, this study showed that grazing reduction and especially grazing cessation can help mitigating the detrimental effects of heavy grazing on semiarid steppe soils when management is controlled for periods longer than 25 years. Higher abundance and stability of coarse and medium aggregates in ungrazed plots may also reduce the erodibility of topsoils and subsequently reduce the formation of dust storms. Grazed steppe soils may become a carbon sink in the long term by improving grazing management or completely stopping the grazing if the management is also controlled and the ecosystem protected from disturbance in the long-term.

9. References

- Abril, A. & Bucher, E.H. 1999. The effects of overgrazing on soil microbial community and fertility in the Chaco dry savannas of Argentina. *Applied Soil Ecology*, 12, 159-167.
- Adler, P.B. & Lauenroth, W.K. 2000. Livestock exclusion increases the spatial heterogeneity of vegetation in Colorado shortgrass steppe. *Applied Vegetation Science*, 3, 213-222.
- Amelung, W., Cheshire, M.V. & Guggenberger, G. 1996. Determination of neutral and acidic sugars in soil by capillary gas-liquid chromatography after trifluoroacetic acid hydrolysis. *Soil Biology and Biochemistry*, 28, 1631-1639.
- Ares, J., Del Valle, H. & Bisigato, A. 2003. Detection of process-related changes in plant patterns at extended spatial scales during early dryland desertification. *Global Change Biology*, 9, 1643-1659.
- Augustine, D.J. 2003. Spatial heterogeneity in the herbaceous layer of a semi-arid savanna ecosystem. *Plant Ecology*, 167, 319-332.
- Bai, Y.F., Han, X.G., Wu, J.G., Chen, Z.Z. & Li, L.H. 2004. Ecosystem stability and compensatory effects in the Inner Mongolia grassland. *Nature*, 431, 181-184.
- Baldock, J.A., Oades, J.M., Nelson, P.N., Skene, T.M., Golchin, A. & Clarke, P. 1997. Assessing the extent of decomposition of natural organic materials using solid-state C-13 NMR spectroscopy. *Australian Journal of Soil Research*, 35, 1061-1083.
- Baldock, J.A. & Skjemstad, J.O. 2000. Role of the soil matrix and minerals in protecting natural organic materials against biological attack. *Organic Geochemistry*, 31, 697-710.
- Balesdent, J., Chenu, C. & Balabane, M. 2000. Relationship of soil organic matter dynamics to physical protection and tillage. *Soil & Tillage Research*, 53, 215-230.
- Barger, N.N., Ojima, D.S., Belnap, J., Wang, S.P., Wang, Y.F. & Chen, Z.Z. 2004. Changes in plant functional groups, litter quality, and soil carbon and nitrogen

- mineralization with sheep grazing in an Inner Mongolian Grassland. *Journal of Range Management*, 57, 613-619.
- Batjes, N.H. 1996. Total carbon and nitrogen in the soils of the world. *European Journal of Soil Science*, 47, 151-163.
- Bauer, A., Cole, C.V. & Black, A.L. 1987. Soil property comparisons in virgin grasslands between grazed and nongrazed management-systems. *Soil Science Society of America Journal*, 51, 176-182.
- Berg, W.A., Bradford, J.A. & Sims, P.L. 1997. Long-term soil nitrogen and vegetation change on sandhill rangeland. *Journal of Range Management*, 50, 482-486.
- Bestelmeyer, B.T., Ward, J.P. & Havstad, K.M. 2006. Soil-geomorphic heterogeneity governs patchy vegetation dynamics at an arid ecotone. *Ecology*, 87, 963-973.
- Beukes, P.C. & Cowling, R.M. 2003. Non-selective grazing impacts on soil-properties of the Nama Karoo. *Journal of Range Management*, 56, 547-552.
- Binkley, D., Singer, F., Kaye, M. & Rochelle, R. 2003. Influence of elk grazing on soil properties in Rocky Mountain National Park. *Forest Ecology and Management*, 185, 239-247.
- Black, G.E. & Fox, A. 1996. Recent progress in the analysis of sugar monomers from complex matrices using chromatography in conjunction with mass spectrometry or stand-alone tandem mass spectrometry. *Journal of Chromatography A*, 720, 51-60.
- Braun-Blanquet, J. 1964. *Pflanzensoziologie - Grundzüge der Vegetationskunde*. Springer Verlag, Berlin, Wien, New York.
- Braunack, M.V. & Walker, J. 1985. Recovery of some surface soil properties of ecological interest after sheep grazing in a semiarid woodland. *Australian Journal of Ecology*, 10, 451-460.
- Brevik, E., Fenton, T. & Moran, L. 2002. Effect of soil compaction on organic carbon amounts and distribution, South-Central Iowa. *Environmental Pollution*, 116, S137-S141.
- Burke, I.C., Lauenroth, W.K., Riggle, R., Brannen, P., Madigan, B. & Beard, S. 1999. Spatial variability of soil properties in the shortgrass steppe: The relative

- importance of topography, grazing, microsite, and plant species in controlling spatial patterns. *Ecosystems*, 2, 422-438.
- Burke, I.C., Lauenroth, W.K., Vinton, M.A., Hook, P.B., Kelly, R.H., Epstein, H.E., Aguiar, M.R., Robles, M.D., Aguilera, M.O., Murphy, K.L. & Gill, R.A. 1998. Plant-soil interactions in temperate grasslands. *Biogeochemistry*, 42, 121-143.
- Cambardella, C.A. & Elliott, E.T. 1993. Carbon and Nitrogen Distribution in Aggregates from Cultivated and Native Grassland Soils. *Soil Science Society of America Journal*, 57, 1071-1076.
- Carter, M.R., Angers, D.A., Gregorich, E.G. & Bolinder, M.A. 2003. Characterizing organic matter retention for surface soils in eastern Canada using density and particle size fractions. *Canadian Journal of Soil Science*, 83, 11-23.
- Chen, B., Jahn, B.M., Wilde, S. & Xu, B. 2000. Two contrasting paleozoic magmatic belts in northern Inner Mongolia, China: petrogenesis and tectonic implications. *Tectonophysics*, 328, 157-182.
- Chen, Z. 1988. Topography and climate of Xilin river basin. In: *Research on Grassland Ecosystems* (ed. Station, I.M.G.E.R.), pp. 13–22. Science Press, Beijing.
- Cheng, X.L., An, S.Q., Liu, S.R. & Li, G.Q. 2004. Micro-scale spatial heterogeneity and the loss of carbon, nitrogen and phosphorus in degraded grassland in Ordos Plateau, northwestern China. *Plant and Soil*, 259, 29-37.
- Christensen, B.T. 2001. Physical fractionation of soil and structural and functional complexity in organic matter turnover. *European Journal of Soil Science*, 52, 345-353.
- Chung, H.G., Grove, J.H. & Six, J. 2008. Indications for soil carbon saturation in a temperate agroecosystem. *Soil Science Society of America Journal*, 72, 1132-1139.
- Conant, R.T. & Paustian, K. 2002. Potential soil carbon sequestration in overgrazed grassland ecosystems. *Global Biogeochemical Cycles*, 16, art. no. 1143.
- Conant, R.T., Paustian, K., Del Grosso, S.J. & Parton, W.J. 2005. Nitrogen pools and fluxes in grassland soils sequestering carbon. *Nutrient Cycling in Agroecosystems*, 71, 239-248.

- Conant, R.T., Paustian, K. & Elliott, E.T. 2001. Grassland management and conversion into grassland: Effects on soil carbon. *Ecological Applications*, 11, 343-355.
- Conant, R.T., Six, J. & Paustian, K. 2003. Land use effects on soil carbon fractions in the southeastern United States. I. Management-intensive versus extensive grazing. *Biology and Fertility of Soils*, 38, 386-392.
- Cressie, N. 1985. Fitting Variogram Models by Weighted Least-Squares. *Journal of the International Association for Mathematical Geology*, 17, 563-586.
- Cui, X.Y., Wang, Y.F., Niu, H.S., Wu, J., Wang, S.P., Schnug, E., Rogasik, J., Fleckenstein, J. & Tang, Y.H. 2005. Effect of long-term grazing on soil organic carbon content in semiarid steppes in Inner Mongolia. *Ecological Research*, 20, 519-527.
- da Silva, A.P., Imhoff, S. & Corsi, M. 2003. Evaluation of soil compaction in an irrigated short-duration grazing system. *Soil & Tillage Research*, 70, 83-90.
- Daniel, J.A., Potter, K., Altom, W., Aljoe, H. & Stevens, R. 2002. Long-term grazing density impacts on soil compaction. *Transactions of the Asae*, 45, 1911-1915.
- Deen, W. & Kataki, P.K. 2003. Carbon sequestration in a long-term conventional versus conservation tillage experiment. *Soil & Tillage Research*, 74, 143-150.
- Derner, J.D. & Schuman, G.E. 2007. Carbon sequestration and rangelands: A synthesis of land management and precipitation effects. *Journal of Soil and Water Conservation*, 62, 77-85.
- Don, A., Scholten, T. & Schulze, E.D. 2008. Conversion of cropland into grassland: Implications for soil organic-carbon stocks in two soils with different texture. *Journal of Plant Nutrition and Soil Science*.
- Dormaar, J.F. & Willms, W.D. 1998. Effect of forty-four years of grazing on fescue grassland soils. *Journal of Range Management*, 51, 122-126.
- Drewry, J.J. 2006. Natural recovery of soil physical properties from treading damage of pastoral soils in New Zealand and Australia: A review. *Agriculture Ecosystems & Environment*, 114, 159-169.

- Dubeux, J.C.B., Sollenberger, L.E., Comerford, N.B., Scholberg, J.M., Ruggieri, A.C., Vendramini, J.M.B., Interrante, S.M. & Portier, K.M. 2006. Management intensity affects density fractions of soil organic matter from grazed bahiagrass swards. *Soil Biology and Biochemistry*, 38, 2705-2711.
- Ehrenfeld, J.G., Han, X.G., Parsons, W.F.J. & Zhu, W.X. 1997. On the nature of environmental gradients: temporal and spatial variability of soils and vegetation in the New Jersey Pinelands. *Journal of Ecology*, 85, 785-798.
- Ellert, B.H. & Bettany, J.R. 1995. Calculation of organic matter and nutrients stored in soils under contrasting management regimes. *Canadian Journal of Soil Science*, 75, 529-538.
- Eusterhues, K., Rumpel, C. & Kögel-Knabner, I. 2005. Organo-mineral associations in sandy acid forest soils: importance of specific surface area, iron oxides and micropores. *European Journal of Soil Science*, 56, 753-763.
- Eusterhues, K., Rumpel, C. & Kögel-Knabner, I. 2007. Composition and radiocarbon age of HF-resistant soil organic matter in a Podzol and a Cambisol. *Organic Geochemistry*, 38, 1356-1372.
- Frank, A.B., Tanaka, D.L., Hofmann, L. & Follett, R.F. 1995. Soil carbon and nitrogen of northern Great-Plains grasslands as influenced by long-term grazing. *Journal of Range Management*, 48, 470-474.
- Franzluebbers, A.J., Wright, S.F. & Stuedemann, J.A. 2000. Soil aggregation and glomalin under pastures in the Southern Piedmont USA. *Soil Science Society of America Journal*, 64, 1018-1026.
- Fuhlendorf, S.D. & Smeins, F.E. 1999. Scaling effects of grazing in a semi-arid grassland. *Journal of Vegetation Science*, 10, 731-738.
- Ganjugunte, G.K., Vance, G.F., Preston, C.M., Schuman, G.E., Ingram, L.J., Stahl, P.D. & Welker, J.M. 2005. Soil organic carbon composition in a northern mixed-grass prairie: Effects of grazing. *Soil Science Society of America Journal*, 69, 1746-1756.
- Gao, Y. 2007. *Influences of different land use management on net primary productivity and belowground carbon allocation in a semi-arid Inner Mongolia Steppe*. PhD-Thesis, Christian-Albrecht-University of Kiel, Kiel.

- Gao, Y.Z., Giese, M., Han, X.G., Wang, D.L., Zhou, Z.Y., Brueck, H., Lin, S. & Taube, F. 2008a. Land use and drought interactively affect interspecific competition and species diversity at the local scale in a semiarid steppe ecosystem. *Ecological Research*.
- Gao, Y.Z., Giese, M., Lin, S., Sattelmacher, B., Zhao, Y. & Brueck, H. 2008b. Belowground net primary productivity and biomass allocation of a grassland in Inner Mongolia is affected by grazing intensity. *Plant and Soil*, 307, 41-50.
- Gernet, J. 1997. *Die chinesische Welt. Die Geschichte Chinas von den Anfängen bis zur Jetztzeit*. Suhrkamp, Frankfurt.
- Gibson, D.J. 1988. The Relationship of Sheep Grazing and Soil Heterogeneity to Plant Spatial Patterns in Dune Grassland. *Journal of Ecology*, 76, 233-252.
- Giese, K.M., Gao, Y., Zhao, Y., Pan, Q., Lin, S. & Brueck, H. 2008. Effects of grazing and rainfall variability on root and shoot decomposition in a semi-arid grassland. *Applied Soil Ecology*.
- Giese, M. 2007. *Nitrogen dynamics as affected by grazing in semi-arid grasslands of Inner Mongolia*. PhD thesis, Christian-Albrecht-University of Kiel, Kiel.
- Gifford, R.M. & Roderick, M.L. 2003. Soil carbon stocks and bulk density: spatial or cumulative mass coordinates as a basis of expression? *Global Change Biology*, 9, 1507-1514.
- Golchin, A., Oades, J.M., Skjemstad, J.O. & Clarke, P. 1994. Study of Free and Occluded Particulate Organic-Matter in Soils by Solid-State C-13 Cp/Mas Nmr-Spectroscopy and Scanning Electron-Microscopy. *Australian Journal of Soil Research*, 32, 285-309.
- Golluscio, R.A., Perez, J.A., Paruelo, J.M. & Ghera, C.M. 2005. Spatial heterogeneity at different grain sizes in grazed versus ungrazed sites of the Patagonian steppe. *Ecoscience*, 12, 103-109.
- Golodets, C. & Boeken, B. 2006. Moderate sheep grazing in semiarid shrubland alters small-scale soil surface structure and patch properties. *Catena*, 65, 285-291.

- Gregorich, E.G., Beare, M.H., McKim, U.F. & Skjemstad, J.O. 2006. Chemical and biological characteristics of physically uncomplexed organic matter. *Soil Science Society of America Journal*, 70, 975-985.
- Gregorich, E.G., Greer, K.J., Anderson, D.W. & Liang, B.C. 1998. Carbon distribution and losses: erosion and deposition effects. *Soil & Tillage Research*, 47, 291-302.
- Gregorich, E.G., Monreal, C.M., Schnitzer, M. & Schulten, H.R. 1996. Transformation of plant residues into soil organic matter: Chemical characterization of plant tissue, isolated soil fractions, and whole soils. *Soil Science*, 161, 680-693.
- Guggenberger, G., Zech, W., Haumaier, L. & Christensen, B.T. 1995. Land-Use Effects on the Composition of Organic-Matter in Particle-Size Separates of Soils .2. Cpmas and Solution C-13 Nmr Analysis. *European Journal of Soil Science*, 46, 147-158.
- Gulde, S., Chung, H., Amelung, W., Chang, C. & Six, J. 2008. Soil carbon saturation controls labile and stable carbon pool dynamics. *Soil Science Society of America Journal*, 72, 605-612.
- Hamza, M.A. & Anderson, W.K. 2005. Soil compaction in cropping systems - A review of the nature, causes and possible solutions. *Soil & Tillage Research*, 82, 121-145.
- Hartge, K.H. & Horn, R. 1992. *Die physikalische Untersuchung von Böden*. Enke Verlag, Stuttgart.
- Hassink, J. 1995. Decomposition Rate Constants of Size and Density Fractions of Soil Organic-Matter. *Soil Science Society of America Journal*, 59, 1631-1635.
- Hassink, J. 1997. The capacity of soils to preserve organic C and N by their association with clay and silt particles. *Plant and Soil*, 191, 77-87.
- Hassink, J. & Whitmore, A.P. 1997. A model of the physical protection of organic matter in soils. *Soil Science Society of America Journal*, 61, 131-139.
- Hassink, J., Whitmore, A.P. & Kubat, J. 1997. Size and density fractionation of soil organic matter and the physical capacity of soils to protect organic matter. *European Journal of Agronomy*, 7, 189-199.

- Hoffmann, C., Funk, R., Li, Y. & Sommer, M. 2008. Effect of grazing on wind driven carbon and nitrogen ratios in the grasslands of Inner Mongolia. *Catena*, 75, 182-190.
- Hoffmann, C., Funk, R., Wieland, R., Li, Y. & Sommer, M. 2007. Effects of grazing and topography on dust flux and deposition in the Xilingele grassland, Inner Mongolia. *Journal of Arid Environments*, doi: 10.1016/j.jaridenv.2007.09.004.
- Holst, J., Liu, C., Yao, Z., Brueggemann, N., Zheng, X., Giese, M. & Butterbach-Bahl, K. 2008. Fluxes of nitrous oxide, methane and carbon dioxide during freezing-thawing cycles in an Inner Mongolian steppe. *Plant and Soil*, 308, 105-117.
- Holst, J., Liu, C., Yao, Z., Bruggemann, N., Zheng, X., Han, X. & Butterbach-Bahl, K. 2007. Importance of point sources on regional nitrous oxide fluxes in semi-arid steppe of Inner Mongolia, China. *Plant and Soil*, 296, 209-226.
- Holt, J.A. 1997. Grazing pressure and soil carbon, microbial biomass and enzyme activities in semi-arid northeastern Australia. *Applied Soil Ecology*, 5, 143-149.
- Hong, D.W., Zhang, J.S., Wang, T., Wang, S.G. & Xie, X.L. 2004. Continental crustal growth and the supercontinental cycle: evidence from the Central Asian Orogenic Belt. *Journal of Asian Earth Sciences*, 23, 799-813.
- Hook, P.B. & Burke, I.C. 2000. Biogeochemistry in a shortgrass landscape: Control by topography, soil texture, and microclimate. *Ecology*, 81, 2686-2703.
- Hook, P.B., Burke, I.C. & Lauenroth, W.K. 1991. Heterogeneity of soil and plant N and C associated with individual plants and openings in north-american shortgrass steppe. *Plant and Soil*, 138, 247-256.
- Imhoff, S., da Silva, A.P. & Tormena, C.A. 2000. Spatial heterogeneity of soil properties in areas under elephant-grass short-duration grazing system. *Plant and Soil*, 219, 161-168.
- Ingram, L.J., Stahl, P.D., Schuman, G.E., Buyer, J.S., Vance, G.F., Ganjegunte, G.K., Welker, J.M. & Derner, J.D. 2008. Grazing impacts on soil carbon and microbial communities in a mixed-grass ecosystem. *Soil Science Society of America Journal*, 72, 939-948.

- Iqbal, J., Thomasson, J.A., Jenkins, J.N., Owens, P.R. & Whisler, F.D. 2005. Spatial variability analysis of soil physical properties of alluvial soils. *Soil Science Society of America Journal*, 69, 1338-1350.
- IUSS Working Group WRB. 2006. *World reference base for soil resources 2006*. FAO, Rome.
- Jahn, B.M., Wu, F.Y. & Chen, B. 2000. Granitoids of the Central Asian Orogenic Belt and continental growth in the Phanerozoic. *Transactions of the Royal Society of Edinburgh-Earth Sciences*, 91, 181-193.
- Jastrow, J.D., Amonette, J.E. & Bailey, V.L. 2007. Mechanisms controlling soil carbon turnover and their potential application for enhancing carbon sequestration. *Climatic Change*, 80, 5-23.
- Jastrow, J.D., Boutton, T.W. & Miller, R.M. 1996. Carbon dynamics of aggregate-associated organic matter estimated by carbon-13 natural abundance. *Soil Science Society of America Journal*, 60, 801-807.
- Jianguo, W. & Loucks, O. 1992. Xilingele. In: *Grasslands and Grassland Science in Northern China* (ed. Council, N.R.). The National Academies Press.
- Jobbagy, E.G. & Jackson, R.B. 2000. The vertical distribution of soil organic carbon and its relation to climate and vegetation. *Ecological Applications*, 10, 423-436.
- John, B., Yamashita, T., Ludwig, B. & Flessa, H. 2005. Storage of organic carbon in aggregate and density fractions of silty soils under different types of land use. *Geoderma*, 128, 63-79.
- Kadono, A., Funakawa, S. & Kosaki, T. 2008. Factors controlling mineralization of soil organic matter in the Eurasian steppe. *Soil Biology & Biochemistry*, 40, 947-955.
- Kaiser, K., Eusterhues, K., Rumpel, C., Guggenberger, G. & Kogel-Knabner, I. 2002. Stabilization of organic matter by soil minerals - investigations of density and particle-size fractions from two acid forest soils. *Journal of Plant Nutrition and Soil Science-Zeitschrift Fur Pflanzenernahrung Und Bodenkunde*, 165, 451-459.
- Kawamura, K., Akiyama, T., Yokota, H., Tsutsumi, M., Yasuda, T., Watanabe, O. & Wang, S.P. 2005. Quantifying grazing intensities using geographic information

- systems and satellite remote sensing in the Xilingol steppe region, Inner Mongolia, China. *Agriculture Ecosystems and Environment*, 107, 83-93.
- Kiem, R. & Kögel-Knabner, I. 2002. Refractory organic carbon in particle-size fractions of arable soils II: organic carbon in relation to mineral surface area and iron oxides in fractions < 6 μ m. *Organic Geochemistry*, 33, 1699-1713.
- Kleber, M., Mikutta, R., Torn, M.S. & Jahn, R. 2005. Poorly crystalline mineral phases protect organic matter in acid subsoil horizons. *European Journal of Soil Science*, 56, 717-725.
- Knicker, H., Gonzalez-Vila, F.J., Polvillo, O., Gonzalez, J.A. & Almendros, G. 2005. Fire-induced transformation of C- and N-forms in different organic soil fractions from a Dystric Cambisol under a Mediterranean pine forest (*Pinus pinaster*). *Soil Biology and Biochemistry*, 37, 701-718.
- Kögel-Knabner, I. 2002. The macromolecular organic composition of plant and microbial residues as inputs to soil organic matter. *Soil Biology and Biochemistry*, 34, 139-162.
- Kölbl, A. & Kögel-Knabner, I. 2004. Content and composition of free and occluded particulate organic matter in a differently textured arable Cambisol as revealed by solid-state C-13 NMR spectroscopy. *Journal of Plant Nutrition and Soil Science*, 167, 45-53.
- Kusky, T.M., Windley, B.F. & Zhai, M.G. 2007. Tectonic evolution of the North China Block: from orogen to craton to orogen. In: *Mesozoic Sub-Continental Lithospheric Thinning Under Eastern Asia* (eds. Zhai, M.G., Windley, B.F., Kusky, T.M. & Meng, Q.R.), pp. 1-34. Geological Society, Special Publications, London.
- Lavee, H., Sarah, P. & Imeson, A.C. 1996. Aggregate stability dynamics as affected by soil temperature and moisture regimes. *Geografiska Annaler Series a-Physical Geography*, 78A, 73-82.
- Lavrenko, E.M. & Karamysheva, Z.V. 1993. Steppes of the former Soviet Union and Mongolia. In: *Natural grasslands. Eastern hemisphere and résumé* (ed. Coupland, R.T.), pp. 3-59. Elsevier, Amsterdam, London, New York, Tokyo.

- Li, F.R., Kang, L.F., Zhang, H., Zhao, L.Y., Shirato, Y. & Taniyama, I. 2005. Changes in intensity of wind erosion at different stages of degradation development in grasslands of Inner Mongolia, China. *Journal of Arid Environments*, 62, 567-585.
- Li, F.R., Zhao, L.Y., Zhang, H., Zhang, T.H. & Shirato, Y. 2004. Wind erosion and airborne dust deposition in farmland during spring in the Horqin Sandy Land of eastern Inner Mongolia, China. *Soil & Tillage Research*, 75, 121-130.
- Li, R., Zheng, L. & Zhu, G. 1990. *Lakes and Environment in the Neimenggu Plateau*. Beijing Normal University Press, Beijing.
- Li, S.G., Harazono, Y., Oikawa, T., Zhao, H.L., He, Z.Y. & Chang, X.L. 2000. Grassland desertification by grazing and the resulting micrometeorological changes in Inner Mongolia. *Agricultural and Forest Meteorology*, 102, 125-137.
- Liang, E.Y., Vennetier, M., Lin, J.X. & Shao, X.M. 2003. Relationships between tree increment, climate and above-ground biomass of grass: a case study in the typical steppe, north China. *Acta Oecologica-International Journal of Ecology*, 24, 87-94.
- Liu, H.Y., Xu, L.H. & Cui, H.T. 2002. Holocene history of desertification along the woodland-steppe border in northern China. *Quaternary Research*, 57, 259-270.
- Liu, P., Huang, J.H., Han, X.G., Sun, O.J. & Zhou, Z. 2006. Differential responses of litter decomposition to increased soil nutrients and water between two contrasting grassland plant species of Inner Mongolia, China. *Applied Soil Ecology*, 34, 266-275.
- Liu, W., Siebel, W., Li, X.J. & Pan, X.F. 2005. Petrogenesis of the Linxi granitoids, northern Inner Mongolia of China: Constraints on basaltic underplating. *Chemical Geology*, 219, 5-35.
- Lobe, I., Amelung, W. & Du Preez, C.C. 2001. Losses of carbon and nitrogen with prolonged arable cropping from sandy soils of the South African Highveld. *European Journal of Soil Science*, 52, 93-101.
- Loveland, P. & Webb, J. 2003. Is there a critical level of organic matter in the agricultural soils of temperate regions: a review. *Soil & Tillage Research*, 70, 1-18.

- Maestre, F.T., Rodriguez, F., Bautista, S., Cortina, J. & Bellot, J. 2005. Spatial associations and patterns of perennial vegetation in a semi-arid steppe: a multivariate geostatistics approach. *Plant Ecology*, 179, 133-147.
- Malhi, S.S., Harapiak, J.T., Nyborg, M., Gill, K.S. & Flore, N.A. 2002. Autumn and spring applications of ammonium nitrate and urea to bromegrass influence total and light fraction organic C and N in a thin Black Chernozem. *Canadian Journal of Soil Science*, 82, 211-217.
- MartinezTuranzas, G.A., Coffin, D.P. & Burke, I.C. 1997. Development of microtopography in a semi-arid grassland: Effects of disturbance size and soil texture. *Plant and Soil*, 191, 163-171.
- Mayer, L.M. 1994. Relationship between mineral surfaces and organic-carbon concentrations in soils and sediments. *Chemical Geology*, 114, 347-363.
- McLaren, R.G. & Swift, R.S. 1977. Changes in soil organic sulfur fractions due to long-term cultivation of soils. *Journal of Soil Science*, 28, 445-453.
- Mehra, O.P. & Jackson, M.L. 1960. Iron oxide removal from soils and clays by a dithionite-citrate system buffered with sodium bicarbonate. In: *7th National Conference on Clays and Clay Minerals* (ed. Ingerson, E.), pp. 317-327. Pergamon Press, London.
- Meng, Q.R. 2003. What drove late Mesozoic extension of the northern China-Mongolia tract? *Tectonophysics*, 369, 155-174.
- Meng, Q.R., Hu, J.M., Jin, J.Q., Zhang, Y. & Xu, D.F. 2003. Tectonics of the late Mesozoic wide extensional basin system in the China-Mongolia border region. *Basin Research*, 15, 397-415.
- Mikhailova, E.A., Bryant, R.B., Cherney, D.J.R., Post, C.J. & Vassenev, II. 2000. Botanical composition, soil and forage quality under different management regimes in Russian grasslands. *Agriculture Ecosystems & Environment*, 80, 213-226.
- Milchunas, D.G. & Lauenroth, W.K. 1989. 3-Dimensional Distribution of Plant Biomass in Relation to Grazing and Topography in the Shortgrass Steppe. *Oikos*, 55, 82-86.

- Milchunas, D.G. & Lauenroth, W.K. 1993. Quantitative effects of grazing on vegetation and soils over a global range of environments. *Ecological Monographs*, 63, 327-366.
- Milchunas, D.G. & Lauenroth, W.K. 2001. Belowground primary production by carbon isotope decay and longterm root biomass dynamics. *Ecosystems*, 4, 139-150.
- Milchunas, D.G., Lauenroth, W.K., Chapman, P.L. & Kazempour, M.K. 1989. Effects of Grazing, Topography, and Precipitation on the Structure of a Semiarid Grassland. *Vegetatio*, 80, 11-23.
- Moore, D.M. & Reynolds, R.C. 1989. *X-ray diffraction and the Identification and Analysis of Clay Minerals*. Oxford University Press, London.
- Naeth, M.A., Bailey, A.W., Pluth, D.J., Chanasyk, D.S. & Hardin, R.T. 1991. Grazing impacts on litter and soil organic-matter in mixed prairie and fescue grassland ecosystems of Alberta. *Journal of Range Management*, 44, 7-12.
- Nash, M.S., Jackson, E. & Whitford, W.G. 2004. Effects of intense, short-duration grazing on microtopography in a Chihuahuan Desert grassland. *Journal of Arid Environments*, 56, 383-393.
- Neff, J.C., Reynolds, R.L., Belnap, J. & Lamothe, P. 2005. Multi-decadal impacts of grazing on soil physical and biogeochemical properties in southeast Utah. *Ecological Applications*, 15, 87-95.
- Neupert, R.F. 1999. Population, Nomadic Pastoralism and the Environment in the Mongolian Plateau. *Population and Environment: A Journal of Interdisciplinary Studies*, 20, 413-441.
- North, P.F. 1976. Towards an Absolute Measurement of Soil Structural Stability Using Ultrasound. *Journal of Soil Science*, 27, 451-459.
- Northup, B.K., Brown, J.R. & Ash, A.J. 2005. Grazing impacts on spatial distribution of soil and herbaceous characteristics in an Australian tropical woodland. *Agroforestry Systems*, 65, 137-150.
- Northup, B.K., Brown, J.R. & Holt, J.A. 1999. Grazing impacts on the spatial distribution of soil microbial biomass around tussock grasses in a tropical grassland. *Applied Soil Ecology*, 13, 259-270.

- Oades, J.M. 1984. Soil Organic-Matter and Structural Stability - Mechanisms and Implications for Management. *Plant and Soil*, 76, 319-337.
- Orr, H.K. 1975. Recovery from soil compaction on bluegrass range in Black Hills. *Transactions of the Asae*, 18, 1076-1081.
- Osher, L.J., Matson, P.A. & Amundson, R. 2003. Effect of land use change on soil carbon in Hawaii. *Biogeochemistry*, 65, 213-232.
- Pebesma, E.J. 2004. Multivariable geostatistics in S: the gstat package. *Computers & Geosciences*, 30, 683-691.
- Pebesma, E.J. & Wesseling, C.G. 1998. Gstat: A program for geostatistical modelling, prediction and simulation. *Computers & Geosciences*, 24, 17-31.
- Pikul, J.L., Osborne, S., Ellsbury, M. & Riedell, W. 2007. Particulate organic matter and water-stable aggregation of soil under contrasting management. *Soil Science Society of America Journal*, 71, 766-776.
- Posse, G., Anchorena, J. & Collantes, M.B. 2000. Spatial micro-patterns in the steppe of Tierra del Fuego induced by sheep grazing. *Journal of Vegetation Science*, 11, 43-50.
- Priewe, S. 2007. Herrscher aus der Steppe. *Abenteuer Archäologie*, 07, 14-20.
- Puget, P., Chenu, C. & Balesdent, J. 1995. Total and Young Organic-Matter Distributions in Aggregates of Silty Cultivated Soils. *European Journal of Soil Science*, 46, 449-459.
- Purtauf, T., Thies, C., Ekschmitt, K., Wolters, V. & Dauber, J. 2005. Scaling properties of multivariate landscape structure. *Ecological Indicators*, 5, 295-304.
- Qi, Y. & Wu, J.G. 1996. Effects of changing spatial resolution on the results of landscape pattern analysis using spatial autocorrelation indices. *Landscape Ecology*, 11, 39-49.
- Raiesi, F. & Asadi, E. 2006. Soil microbial activity and litter turnover in native grazed and ungrazed rangelands in a semiarid ecosystem. *Biology and Fertility of Soils*, 43, 76-82.
- RDevelopmentCoreTeam. 2004. R: A language and environment for statistical computing. R Foundation for Statistical Computing, Vienna, Austria.

- Reeder, J.D. & Schuman, G.E. 2002. Influence of livestock grazing on C sequestration in semi-arid mixed-grass and short-grass rangelands. *Environmental Pollution*, 116, 457-463.
- Ren, J., Li, S., Jiao, G. & Chen, P. 1998. Extensional tectonic system of Erlian fault basin group and its deep background. *Journal of China University of Geosciences*, 8, 40-44.
- Ren, J.Y., Tamaki, K., Li, S.T. & Junxia, Z. 2002. Late Mesozoic and Cenozoic rifting and its dynamic setting in Eastern China and adjacent areas. *Tectonophysics*, 344, 175-205.
- Reynolds, H.L., Hungate, B.A., Chapin, F.S. & Dantonio, C.M. 1997. Soil heterogeneity and plant competition in an annual grassland. *Ecology*, 78, 2076-2090.
- Rietkerk, M., Boerlijst, M.C., van Langevelde, F., HilleRisLambers, R., van de Koppel, J., Kumar, L., Prins, H.H.T. & de Roos, A.M. 2002. Self-organization of vegetation in arid ecosystems. *American Naturalist*, 160, 524-530.
- Rietkerk, M., Dekker, S.C., de Ruiter, P.C. & van de Koppel, J. 2004. Self-organized patchiness and catastrophic shifts in ecosystems. *Science*, 305, 1926-1929.
- Rietkerk, M., Ketner, P., Burger, J., Hoorens, B. & Olf, H. 2000. Multiscale soil and vegetation patchiness along a gradient of herbivore impact in a semi-arid grazing system in West Africa. *Plant Ecology*, 148, 207-224.
- Ripley, E.A. 1992. Grassland climate. In: *Natural grasslands: Introduction and western hemisphere (Ecosystems of the world)* (ed. Coupland, R.T.), pp. 7-24. Elsevier, Amsterdam, London, New York, Tokyo.
- Robinson, P.T., Zhou, M.F., Hu, X.F., Reynolds, P., Wenji, B. & Yang, J.S. 1999. Geochemical constraints on the origin of the Hegenshan Ophiolite, Inner Mongolia, China. *Journal of Asian Earth Sciences*, 17, 423-442.
- Rumpel, C. & Dignac, M.F. 2006. Chromatographic analysis of monosaccharides in a forest soil profile: Analysis by gas chromatography after trifluoroacetic acid hydrolysis and reduction-acetylation. *Soil Biology and Biochemistry*, 38, 1478-1481.

- Rumpel, C., Kogel-Knabner, I. & Bruhn, F. 2002. Vertical distribution, age, and chemical composition of organic carbon in two forest soils of different pedogenesis. *Organic Geochemistry*, 33, 1131-1142.
- Schimel, D., Stillwell, M.A. & Woodmansee, R.G. 1985. Biogeochemistry of C, N, and P in a Soil Catena of the Shortgrass Steppe. *Ecology*, 66, 276-282.
- Schlesinger, W.H., Raikes, J.A., Hartley, A.E. & Cross, A.E. 1996. On the spatial pattern of soil nutrients in desert ecosystems. *Ecology*, 77, 364-374.
- Schmidt, M.W.I., Rumpel, C. & Kögel-Knabner, I. 1999. Evaluation of an ultrasonic dispersion procedure to isolate primary organomineral complexes from soils. *European Journal of Soil Science*, 50, 87-94.
- Schuman, G.E., Reeder, J.D., Manley, J.T., Hart, R.H. & Manley, W.A. 1999. Impact of grazing management on the carbon and nitrogen balance of a mixed-grass rangeland. *Ecological Applications*, 9, 65-71.
- Schwertmann, U. 1964. Differenzierung der Eisenoxide des Bodens durch Extraktion mit Ammoniumoxalat-Lösung. *Zeitschrift für Pflanzenernährung, Düngung und Bodenkunde*, 105, 194-202.
- Sengör, A.M.C. & Natal'in, B.A. 1996. Paleotectonics of Asia: fragments of a synthesis. In: *The Tectonic Evolution of Asia* (eds. Yin, A. & Harrison, M.), p. 666. Press Syndicate of the University of Cambridge, Cambridge.
- Shi, G.H., Liu, D.Y., Zhang, F.Q., Jian, P., Miao, L.C., Shi, Y.R. & Tao, H. 2003. SHRIMP U-Pb zircon geochronology and its implications on the Xilin Gol Complex, Inner Mongolia, China. *Chinese Science Bulletin*, 48, 2742-2748.
- Shi, G.H., Miao, L.C., Zhang, F.Q., Jian, P., Fan, W.M. & Liu, D.Y. 2004. Emplacement age and tectonic implications of the Xilinhote A-type granite in Inner Mongolia, China. *Chinese Science Bulletin*, 49, 723-729.
- Simpson, M.J., Otto, A. & Feng, X.J. 2008. Comparison of solid-state carbon-13 nuclear magnetic resonance and organic matter biomarkers for assessing soil organic matter degradation. *Soil Science Society of America Journal*, 72, 268-276.

- Six, J., Bossuyt, H., Degryze, S. & Denef, K. 2004. A history of research on the link between (micro)aggregates, soil biota, and soil organic matter dynamics. *Soil & Tillage Research*, 79, 7-31.
- Smith, P. 2004. How long before a change in soil organic carbon can be detected? *Global Change Biology*, 10, 1878-1883.
- Soane, B.D. 1990. The role of organic-matter in soil compactibility - a review of some practical aspects. *Soil & Tillage Research*, 16, 179-201.
- Solomon, D., Lehmann, J., Lobe, I., Martinez, C.E., Tveitnes, S., Du Preez, C.C. & Amelung, W. 2005. Sulphur speciation and biogeochemical cycling in long-term arable cropping of subtropical soils: evidence from wet-chemical reduction and SK-edge XANES spectroscopy. *European Journal of Soil Science*, 56, 621-634.
- Soussana, J.F., Loiseau, P., Vuichard, N., Ceschia, E., Balesdent, J., Chevallier, T. & Arrouays, D. 2004. Carbon cycling and sequestration opportunities in temperate grasslands. *Soil Use and Management*, 20, 219-230.
- Spielvogel, S., Prietzel, J. & Kögel-Knabner, I. 2007. Changes of lignin phenols and neutral sugars in different soil types of a high-elevation forest ecosystem 25 years after forest dieback. *Soil Biology and Biochemistry*, 39, 655-668.
- Steffens, M., Kölbl, A., Giese, M., Hoffmann, C., Totsche, K.U., Breuer, L. & Kögel-Knabner, I. 2009a. Spatial variability of topsoil and vegetation in a grazed steppe ecosystem in Inner Mongolia (P.R. China). *Journal of Plant Nutrition and Soil Science*, 172.
- Steffens, M., Kölbl, A. & Kögel-Knabner, I. 2009b. Alteration of soil organic matter pools and aggregation in semi-arid steppe topsoils as driven by organic matter input. *European Journal of Soil Science*, 60.
- Steffens, M., Kölbl, A., Totsche, K.U. & Kögel-Knabner, I. 2008. Grazing effects on soil chemical and physical properties in a semiarid steppe of Inner Mongolia (P.R. China). *Geoderma*, 143, 63-72.
- Stewart, C.E., Plante, A.F., Paustian, K., Conant, R.T. & Six, J. 2008. Soil carbon saturation: Linking concept and measurable carbon pools. *Soil Science Society of America Journal*, 72, 379-392.

- Stuiver, M. & Polach, H.A. 1977. Reporting of C-14 Data - Discussion. *Radiocarbon*, 19, 355-363.
- Su, Y.Z., Li, Y.L., Cui, H.Y. & Zhao, W.Z. 2005. Influences of continuous grazing and livestock exclusion on soil properties in a degraded sandy grassland, Inner Mongolia, northern China. *Catena*, 59, 267-278.
- Su, Y.Z., Li, Y.L. & Zhao, H.L. 2006. Soil properties and their spatial pattern in a degraded sandy grassland under post-grazing restoration, Inner Mongolia, northern China. *Biogeochemistry*, 79, 297-314.
- Su, Y.Z., Zhao, H.L., Zhang, T.H. & Zhao, X.Y. 2004. Soil properties following cultivation and non-grazing of a semi-arid sandy grassland in northern China. *Soil & Tillage Research*, 75, 27-36.
- Sutie, J.M., Reynolds, S.G. & Batello, C. eds. 2005. *Grasslands of the World*. FAO, Rome.
- Tan, Z., Lal, R., Owens, L. & Izaurralde, R.C. 2007. Distribution of light and heavy fractions of soil organic carbon as related to land use and tillage practice. *Soil and Tillage Research*, 92, 53-59.
- Tang, K.D. & Yan, Z.Y. 1993. Regional Metamorphism and Tectonic Evolution of the Inner Mongolian Suture Zone. *Journal of Metamorphic Geology*, 11, 511-522.
- Tisdall, J.M. & Oades, J.M. 1982. Organic-Matter and Water-Stable Aggregates in Soils. *Journal of Soil Science*, 33, 141-163.
- Tong, C., Wu, J., Yong, S., Yang, J. & Yong, W. 2004. A landscape-scale assessment of steppe degradation in the Xilin River Basin, Inner Mongolia, China. *Journal of Arid Environments*, 59, 133-149.
- VandenBygaart, A.J. & Kay, B.D. 2004. Persistence of soil organic carbon after plowing a long-term no-till field in southern ontario, Canada. *Soil Science Society of America Journal*, 68, 1394-1402.
- Veldkamp, E. 1994. Organic-carbon turnover in 3 tropical soils under pasture after deforestation. *Soil Science Society of America Journal*, 58, 175-180.
- von Lützow, M., Kögel-Knabner, I., Ekschmitt, K., Matzner, E., Guggenberger, G., Marschner, B. & Flessa, H. 2006. Stabilization of organic matter in temperate

- soils: mechanisms and their relevance under different soil conditions - a review. *European Journal of Soil Science*, 57, 426-445.
- Wackernagel, H. 1998. *Multivariate geostatistics*. Springer, Berlin.
- Wang, C.Y., Wang, P. & Li, W.G. 2004a. Conodonts from the Permian Jisu Honguer (Zhesi) formation of inner Mongolia, China. *Geobios*, 37, 471-480.
- Wang, H.Y., Liu, H.Y., Cui, H.T. & Abrahamsen, N. 2001a. Terminal Pleistocene/Holocene palaeoenvironmental changes revealed by mineral-magnetism measurements of lake sediments for Dali Nor area, southeastern Inner Mongolia Plateau, China. *Palaeogeography Palaeoclimatology Palaeoecology*, 170, 115-132.
- Wang, H.Y., Liu, H.Y., Liu, Y.H. & Cui, H.T. 2004b. Mineral magnetism of lacustrine sediments and Holocene palaeoenvironmental changes in Dali Nor area, southeast Inner Mongolia Plateau, China. *Palaeogeography Palaeoclimatology Palaeoecology*, 208, 175-193.
- Wang, H.Z. & Mo, X.X. 1995. An Outline of the Tectonic Evolution of China. *Episodes*, 18, 6-16.
- Wang, R.Z. 2004. Responses of *Leymus chinensis* (Poaceae) to long-term grazing disturbance in the Songnen grasslands of north-eastern China. *Grass and Forage Science*, 59, 191-195.
- Wang, R.Z. & Ripley, E.A. 1997. Effects of grazing on a *Leymus chinensis* grassland on the Songnen plain of north-eastern China. *Journal of Arid Environments*, 36, 307-318.
- Wang, S.P., Wang, Y.F., Chen, Z.Z., Schnug, E. & Haneklaus, S. 2001b. Sulphur concentration of soils and plants and its requirement for ruminants in the inner Mongolia steppe of China. *Grass and Forage Science*, 56, 418-422.
- Wang, T., Zheng, Y.D., Li, T.B. & Gao, Y.J. 2004c. Mesozoic granitic magmatism in extensional tectonics near the Mongolian border in China and its implications for crustal growth. *Journal of Asian Earth Sciences*, 23, 715-729.
- Wang, X., Wang, T., Dong, Z., Liu, X. & Qian, G. 2006. Nebkha development and its significance to wind erosion and land degradation in semi-arid northern China. *Journal of Arid Environments*, 65, 129-141.

- Wang, X.M., Qiu, Z.D. & Opdyke, N.D. 2003. Litho-, Bio-, and Magnetostratigraphy and paleoenvironment of Tunggur Formation (Middle Miocene) in Central Inner Mongolia, China. *American Museum Novitates*, 1-31.
- Webster, R. & Oliver, M.A. 2001. *Geostatistics for Environmental Scientists*. Wiley, Chichester.
- Wiens, J.A. 1989. Spatial Scaling in Ecology. *Functional Ecology*, 3, 385-397.
- Wijesinghe, D.K., John, E.A. & Hutchings, M.J. 2005. Does pattern of soil resource heterogeneity determine plant community structure? An experimental investigation. *Journal of Ecology*, 93, 99-112.
- Willatt, S.T. & Pullar, D.M. 1984. Changes in soil physical-properties under grazed pastures. *Australian Journal of Soil Research*, 22, 343-348.
- Windley, B.F., Alexeiev, D., Xiao, W.J., Kroner, A. & Badarch, G. 2007. Tectonic models for accretion of the Central Asian Orogenic Belt. *Journal of the Geological Society*, 164, 31-47.
- Woods, L.E. 1989. Active organic-matter distribution in the surface 15 cm of undisturbed and cultivated soil. *Biology and Fertility of Soils*, 8, 271-278.
- Wu, H.B., Guo, Z.T. & Peng, C.H. 2003. Land use induced changes of organic carbon storage in soils of China. *Global Change Biology*, 9, 305-315.
- Wu, J.G. 2004. Effects of changing scale on landscape pattern analysis: scaling relations. *Landscape Ecology*, 19, 125-138.
- Wu, L., He, N., Wang, Y. & Han, X. 2008. Storage and dynamics of carbon and nitrogen in soil after grazing exclusion in *Leymus chinensis* grasslands of northern China. *Journal of Environmental Quality*, 37, 663-668.
- Xiao, W.J., Windley, B.F., Hao, J. & Zhai, M.G. 2003. Accretion leading to collision and the Permian Solonker suture, Inner Mongolia, China: Termination of the central Asian orogenic belt. *Tectonics*, 22.
- Xiao, W.J., Zhang, L.C., Qin, K.Z., Sun, S. & Li, J.L. 2004. Paleozoic accretionary and collisional tectonics of the Eastern Tianshan (China): Implications for the continental growth of Central Asia. *American Journal of Science*, 304, 370-395.

- Xiao, X.M., Wang, Y.F., Jiang, S., Ojima, D.S. & Bonham, C.D. 1995. Interannual Variation in the Climate and Aboveground Biomass of *Leymus-Chinense* Steppe and *Stipa-Grandis* Steppe in the Xilin River Basin, Inner-Mongolia, China. *Journal of Arid Environments*, 31, 283-299.
- Yang, X.P., Rost, K.T., Lehmkuhl, F., Zhenda, Z. & Dodson, J. 2004. The evolution of dry lands in northern China and in the Republic of Mongolia since the Last Glacial Maximum. *Quaternary International*, 118, 69-85.
- Yang, Z. & Song, C. 1992. The formation and evolution of the Otindag Sandy Land (in Chinese). In: *Resource Exploitation and Environment Studies of North China* (ed. Department of Geography, I.o.E.S.a.B.N.U.), pp. 40–46. Ocean Press, Beijing.
- Zar, J.H. 1999. *Biostatistical Analysis*. Prentice-Hall, Inc., Upper Saddle River, N.J.
- Zhao, Y., Peth, S., Krummelbein, J., Horn, R., Wang, Z.Y., Steffens, M., Hoffmann, C. & Peng, X.H. 2007. Spatial variability of soil properties affected by grazing intensity in Inner Mongolia grassland. *Ecological Modelling*, 205, 241-254.
- Zheng, Z., Kono, M., Tsunakawa, H., Kimura, G., Wei, Q.Y., Zhu, X.Y. & Hao, T.Y. 1991. The Apparent Polar Wander Path for the North China Block since the Jurassic. *Geophysical Journal International*, 104, 29-40.
- Zheng, Z., Tanaka, H., Tatsumi, Y. & Kono, M. 2002. Basalt platforms in Inner Mongolia and Hebei Province, northeastern China: New K-Ar ages, geochemistries, and revision of palaeomagnetic results. *Geophysical Journal International*, 151, 654-662.
- Zhou, Z.Y., Sun, O.J., Huang, J.H., Li, L.H., Liu, P. & Han, X.G. 2007. Soil carbon and nitrogen stores and storage potential as affected by land-use in an agro-pastoral ecotone of northern China. *Biogeochemistry*, 82, 127-138.
- Zhu, T.C. 1993. Grasslands of China. In: *Natural grasslands: Eastern hemisphere and résumé (Ecosystems of the world)* (ed. Coupland, R.T.), pp. 61-82. Elsevier, Amsterdam, London, New York, Tokyo.

10. Danksagung/Acknowledgements

Zunächst möchte ich Frau Prof. Dr. Ingrid Kögel-Knabner ganz herzlich danken, daß Sie mir dieses Thema überlassen hat. Vielen Dank für Denkanstöße zur richtigen Zeit, Einzelbetreuung beim Publizieren, Freiraum in der Bearbeitung des Themas, Motivation und viele Möglichkeiten, die Welt kennen zu lernen. Bei Prof. Dr. Frede und Prof. Dr. Schnyder sowie Prof. Dr. Hülsbergen bedanke ich mich für die Übernahme der Zweitgutachten sowie des Vorsitzes der Prüfungskommission.

Der Deutschen Forschungsgemeinschaft danke ich für die Finanzierung.

Angelika Kölbl gilt mein größter Dank. Sie war meine ideale Betreuerin, indem Sie nicht nur geduldig jeden meiner geschriebenen Sätze ca. 3-mal gelesen hat und immer noch sinnvolle Verbesserungsvorschläge geben konnte, sondern auch mit umfassenden Fachwissen und dem nötigen Bauchgefühl Böden einschätzen kann. Außerdem ist Sie sehr begeisterungsfähig und kann aus jedem noch so vertrackten Datensatz schnell die passende Quintessenz ziehen und demotivierte Doktoranden sehr schnell wieder aufbauen. An erster Stelle ist Sie jedoch eine sehr angenehme Arbeits- und Zimmerkollegin und Freundin!

All participants of MAGIM are gratefully acknowledged for the nice atmosphere of international and interdisciplinary cooperation. Xingguo Han and the Institute of Botany (Chinese Academy of Science) are gratefully acknowledged for giving me the opportunity to work at IMGERS, Lin Qimei and Zheng Haixia (Chinese Agricultural University) for logistical help in China and Holger Brück for information and help on vegetation and plant nutrition. Sander Huisman danke ich für die Einführung in die Geostatistik.

The MAGIM-PhD-students Marc Giese, Anne Schiborra, Thomas Glindemann, Jirko Holst, Bettina Ketzner, Katrin Schneider, Julia Krümmelbein, Carsten Hoffmann, Zheng Haixia, Gao Yingzhe, Wan Hongwei, Wang Chengjie, Liu Chunyan, Lya Fan, Zhao Ying, Wang Zhungyan, our drivers Zuo Baoji and Jin Shitou, the heavy grazing-farmer Guo Shuping and all drivers and workers are gratefully acknowledged for having the best time in china one can imagine. I had a great time having barbecue, playing soccer and cross golf, eating Mongolian hotpot, thousand year old eggs, drinking pi jiu, bai jiu... I am looking forward to return!

Viele nette Leute am Lehrstuhl für Bodenkunde waren in erheblichem Masse an dieser Arbeit beteiligt und ich hoff', dat ich keene verjeisse: Elfriede Schörk hat nicht nur unermüdlich, präzise und kompetent Fraktion um Fraktion gewonnen, sondern auch

immer den Überblick über alle meine Fläschchen und Kartons behalten. Gabi Albrecht hat meine Zucker aufs Beste extrahiert und gemessen und war/ist immer für die gute Laune zuständig. Ulrike Maul danke ich für Ihre Hilfe im Labor mit Eisen und Textur. Florian Schmalzl danke ich besonders, da er mir des Öfteren und besonders während der letzten Tage der Diss schnell, kompetent und unbürokratisch bei Rechner- und vor allem Datenproblemen geholfen hat. Brigitte Eberle und Elfriede Schuhbauer danke ich ebenfalls für Ihre Hilfe in Bezug auf Computer und Posterdruck. Ohne die Hilfe der Diplomanden/Masteranden/Grosspraktikumstudenden Barbara Gschrey, Olivia Kreyling, Elisabeth Eder und Srirangam Vijay Kumar, sowie der Hiwis Gabi Kolb, Bernadette Meier und Heike Werner wäre die Arbeit in diesem Umfang nicht möglich gewesen - Danke! Josef Fischer (Bayerische Kultur, Sprache and Kreisligafußball und Nachrichten). Heike Knicker, Jörg Prietzel, Katja Heister, Karin Eusterhues und Peter Schad haben mir bei verschiedenen Methoden und Fragen jederzeit hilfsbereit und kompetent geholfen. Alle anderen Leute am Institut haben auch zum Gelingen dieser Arbeit beigetragen - sie haben dafür gesorgt, dass ich mich wohl gefühlt habe und immer gern ans Institut gekommen bin und immer noch komme. Bei meinen Mitdoktoranden Carsten Werner Müller, Steffen Jann, Atze Fritzsche, André Hilscher, Alex Dümig, Martin Wiesmaier, Britt Pagels, Pascale Naumann, Thomas Caspari, Ingo Schöning, Nora Tyufekchieva und Josefine Beck möchte ich mich ganz herzlich für die schöne gemeinsame Zeit im Institut und in Freising bedanken.

Thomas Selige (Lehrstuhl für Pflanzenernährung, TU München) danke ich für die Unterstützung bei der Geostatistik und Stephan Haug (Lehrstuhl für Statistik, TU München) für schnelle Hilfe bei der Auswertung multivariater Statistik. Mick Locke, Chris Johnson and Michael C. Dodd are gratefully acknowledged for improving my language and getting each of my papers through its review process.

Meine Eltern, mein Bruder Flo und meine ganze Familie - Ihr habt nicht nur zu jeder Zeit euer volles Vertrauen in mich gesetzt, sondern mich immer in allen Dingen und mit allem zur Verfügung stehendem unterstützt – vielen, vielen Dank!

Saskia - Danke für alles, daß du mich während meiner „Paperschreibkoller“ ertragen und mich immer wieder an die wichtigen Dinge erinnert hast!

Curriculum vitae

Persönliche Daten

Markus Steffens
geboren am 10.07.1978 in Mechernich
deutsch

Berufstätigkeit

Seit 08.2008 Wissenschaftlicher Mitarbeiter
Technische Universität München, Lehrstuhl für Bodenkunde

Promotion

Seit 05.2004 Wissenschaftlicher Mitarbeiter / Promotion
Technische Universität München, Lehrstuhl für Bodenkunde

Soils of a semiarid shortgrass steppe in Inner Mongolia: Organic matter composition and distribution as affected by sheep grazing

Studium

06.2003 - 04.2004 Diplomarbeit
Forschungszentrum Jülich (Institut für Chemie und Dynamik der Geosphäre IV (Agrosphäre))
Photoabbau von Sulfonamiden auf Bodenoberflächen - Studien an Sulfadiazin

10.1998 - 04.2004 Studium der Angewandten Umweltwissenschaften
Universität Trier
Abschluss als Diplom Umweltwissenschaftler

Hauptfächer: Bodenkunde, Geologie
Nebenfächer: Fernerkundung, Physische Geographie

Praxiserfahrung

04.2008 - 06.2008 Wissenschaftlicher Mitarbeiter
Geohumus International GmbH, Frankfurt

02.2008 - 04.2008 Wissenschaftliche Hilfskraft
Bayerische Landesanstalt für Wald und Forstwirtschaft, Freising

Schulabschluss

08.1988 - 07.1997 Allgemeine Hochschulreife
Hermann-Josef-Kolleg Steinfeld